UNIVERSITY OF MILANO-BICOCCA

DEPARTMENT OF STATISTICS AND QUANTITATIVE METHODS
DOCTORAL THESIS IN STATISTICS AND MATHEMATICS FOR FINANCE

Pricing of gas storage contracts using a temperature dependent gas price model

Author: Alberto Santangelo
Registration n. 787794

Supervisor: Prof. Gianluca Fusai

Academic year 2016/2017

Abstract. It is well known that gas price follows a mean reverting dynamics with jumps. It is less known that jumps can happen when the demand of gas is high and storage levels are low, which usually occurs during the winter period when the consumption for heating purposes, especially in the residential sector, necessarily increases. It is then reasonable to assume that gas price is influenced by the atmospheric temperature. [Mu, 2007] was the first to study the dependence between the Henry Hub futures price and the temperature measured in the United States. [Stoll and Wiebauer, 2010] performed a somehow similar analysis on the price quoted in the Title Transfer Facility trading hub and the temperature measured in Germany, and found that temperature has an impact on the value of a gas storage contract/facility.

In this work we propose to model the gas price as a mean reverting jump-diffusion process with temperature dependent stochastic jump intensity, in order to evaluate gas storage contracts/facilities in the US market. As first proposed by [Boogert and De Jong, 2008], we compute the no arbitrage value of the contract by a real options approach. The ensuing discrete time stochastic optimal control problem is solved by dynamic programming. We compute the continuation value of the dynamic programming algorithm by Fast Fourier Transform (FFT), generalizing the approach proposed by [Kiely et al., 2015].

A no arbitrage approach requires the specification of a no arbitrage pricing measure and a calibration procedure that make the model consistent with the observed market prices of liquid derivatives contracts at the valuation date. However, the low liquidity of the options market can make the classical calibration procedure of implied volatilities unreliable in practice. For this reason we first specify gas and temperature dynamics under the real world measure, and estimate them using the relative time series. Then we derive the no arbitrage dynamics for the gas price by a suitable change of measure, which introduces in the dynamics new parameters that can account for market prices of risk implicits in futures and option prices.

Finally, we present some numerical results about the calibration of the model and the valuation of a gas storage contract.

Contents

Introduction

Contrary to other commodities, such as electricity, natural gas is a storable commodity. Gas storage facilities are useful to ensure the regular supply of gas to the consumers, especially when the demand is high. The peak of demand is usually registered during the winter period, since natural gas is a primary energy resource for residential and commercial heating.

Storage facilities are managed by public utilities or private merchants for different purposes, among which we recall distribution and trading. Obviously, the owner of such a facility is interested to know its value. For this reason, in the last years researchers have focused their attentions on the valuation of facilities or virtual storage contracts.

The possibility for the owner of the storage facility/contract to trade the gas is a crucial driver of its value. Indeed, since gas price depends mainly on the consumer demand, the owner can take advantage of this fact by buying gas when its price is low, namely when the demand is weak, and sell it when the price is high, i.e. when the demand is strong. Furthermore, gas consumption display a seasonal pattern that is closely related to the seasonality of the atmospheric temperature, that somehow results in a seasonality of the price, making it more or less predictable. Unfortunately, like the price of a stock, gas price is also characterized by random fluctuations over the short term, that can be caused by many factors, like for example unexpected shifts in weather conditions.

A real options approach for the evaluation of natural resources has been proposed for the first time by [Brennan and Schwartz, 1985]. Applied to the gas storage case, this approach amounts to evaluate a storage facility/contract as a real option written on the gas price. Clearly, like for financial options, the main driver of the real option value is the volatility of its underlying.

This thesis aims at providing a framework for computing the value of gas storage facilities/contracts using a gas price model that explicitly depends on the temperature, where the latter can drive the shocks in gas price and ultimately affect the storage value itself.

Chapter 1

Stylized empirical facts of gas price and temperature in the US

In the next section we will describe the stylized empirical facts characterizing the behavior of the Henry Hub gas price and its most liquid derivatives instruments, namely futures and options on futures. In the following one we will do the same for the temperature, and we will try to unearth a relationship between gas price and temperature itself.

1.1 Henry Hub natural gas market

The Henry Hub is located in Louisiana and it is the most important trading hub of natural gas in the United States. Here we provide a succinct description of the stylized empirical facts of the Henry Hub (HH) gas price. For an overview on the natural gas market and relative financial products, including a thorough description of financial products related to the Henry Hub gas price, see [Roncoroni et al., 2015].

The historical path of the HH gas price[1] over the period February 2, 2001 - March 9, 2016 shows an inhomogenous behavior over time, probably due to the relevant changes in the natural gas market structure occured in that period. Generally speaking, by looking at the historical path of the gas price displayed in Figure 1.1 we notice that it features an overall weak mean reverting pattern, which strengthened in the last five years (see Figure 1.1b), and sudden large spikes.

Intuitively, the mean-reversion effect should be typical of a commodity market, as it should represent the consequence of the interaction between supply and demand. However, the historical pattern of the Henry Hub gas price from February 2001 to approximately the end of the 2009 does not seem to support this intuition. During that period the time series seems to alternate mean reverting and random walk behaviors. This is partially in agreement with the results obtained by [Geman, 2007], who performed an econometric analysis on the New York Mercantile Exchange (NYMEX) one-month futures contract (which proxies the Henry Hub spot price) that showed the statistical absence of mean-reversion during the period January 1999 - October 2004.

As described by [Henaff et al., 2013], spikes are mainly caused by: i) the excess demand of gas during the winter period, when temperature is low and possibly gas reserves are almost empty; ii) technical problems affecting the supply chain, possibly caused by

[1]The Henry Hub gas price is quoted in Dollars per millions of British Thermal Unit ($/MMBTU). A BTU is a unit of heat and is defined as the amount of heat required to raise the temperature of one pound of water by one degree Fahrenheit.

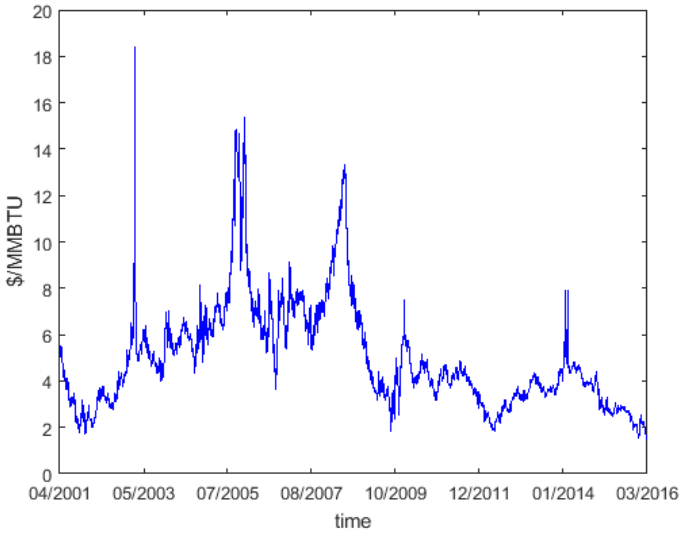

(a)

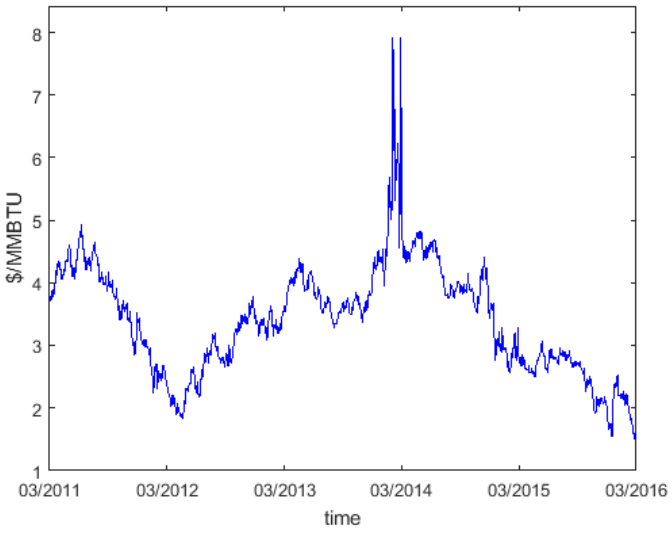

(b)

Figure 1.1: time series of the Henry Hub gas price over the period February 2, 2001 - March 9, 2016 (1.1a); time series of the Henry Hub gas price over the period March 2, 2011 - March 9, 2016 (1.1b) (source: Bloomberg).

extreme natural events. It is also possible that the gas price jumps due to an over-reaction of the market followed by the release of pessimistic temperature forecast after a colder than expected winter, as it actually occurred in March 2014 for the Henry Hub gas price (see Figure 1.1b).

It might be natural to suppose that the gas spot price displays a strong seasonal pattern, since consumption of energy usually does. However, as shown in Figures 1.1a-1.1b this is not the case for the Henry Hub gas price. On the other hand, seasonality characterizes the term structure of futures prices, as shown in Figure 1.2a. In fact, winter futures contracts trade at a premium with respect to summer futures contracts, reflecting the expectation of a higher demand of gas for heating purposes during the winter.

Even though the Henry Hub is a physical gas marketplace, organized electronic markets like the NYMEX and the Intercontinental Exchange (ICE) quote derivatives contracts written on its gas price. Other than futures, the most liquid derivatives are represented by options written on futures, whose prices can be represented through their implied volatilities[2], as shown in Figure 1.2b. Both futures and options convey different types of information about the behavior of the gas price. Futures prices, by definition, contain information about the expectation of the gas price, while options can explain its volatility.

1.2 Link between HH gas price and temperature

It seems sensible to assume that the temperature is a key driver of the consumption of gas, and ultimately its price. Gas consumption hits its maximum levels during the winter period, as a consequence of the high heating demand of residential, commercial and industrial consumers caused by low temperatures. Tables A.3-A.4-A.5 (see A.2 in the Appendix) contain the monthly consumption of bcf[3] of gas for type of consumer in the US during the period 2014-2016 (source: www.eia.gov/naturalgas/monthly), which show a higher consumption of gas during the winter period, especially by the residential sector. It is during the winter that gas reserves are depleted, while the summer represent the refilling season, as confirmed by the historical pattern of gas inventories in the US in Figure 1.3.

The historical path of the temperature in the US (similarly to the European case, see e.g. [Benth and Koekebakker, 2008]) displays at first sight some clearly distinguishable peculiarities, as shown in Figures 1.4a-1.4b. First, temperature features a strong seasonality pattern, accounting for low temperatures during the winter and high temperature during the summer. Second, it shows a strong mean reverting behavior, namely it tends to reverts to its sinusoidal mean level whenever it is far from it.

The dependence between gas and temperature has been already acknowledged and studied in the past by some researchers. [Mu, 2007] is to our knowledge the first (purely empirical) work focused on the study of the effect of temperature and storage on the HH spot gas price. In particular, the author proposes a GARCH model (see [Bollerslev, 1986]) with exogenous variables, including weather shocks and storage surprise factors that affect conditional mean and variance of gas futures price return. [Cartea and Williams, 2008] analyzed the UK gas market and acknowledged the fact that weather conditions drive the seasonality in the spot price, basically for the same reasons presented in this work. However, the model used by the authors to describe the spot price dynamics (the

[2]The implied volatilities are obtained by the so called "Black 76" option pricing formula [Black, 1976].
[3]Billion cubic feet.

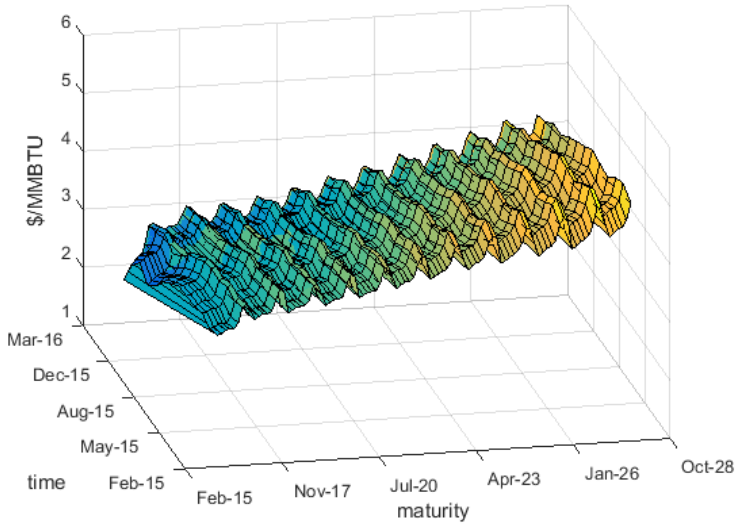

(a)

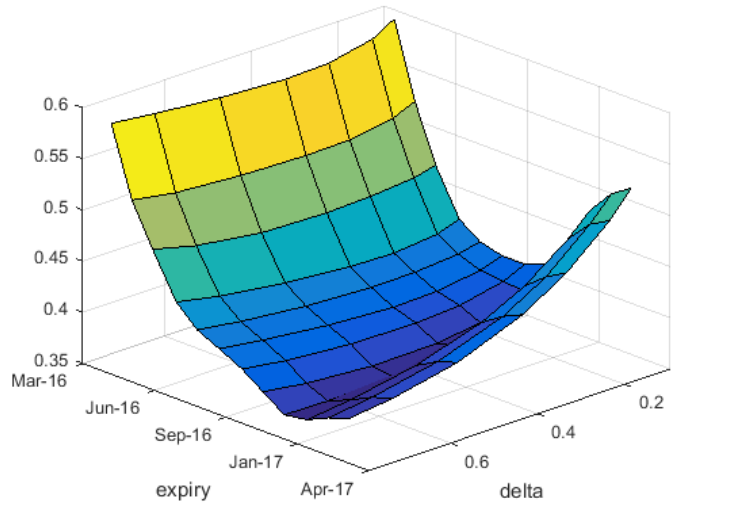

(b)

Figure 1.2: time series of the term structure of futures on the Henry Hub gas price over the period March 2, 2015 - March 9, 2016 (1.2a); Implied volatility surface of options on futures on March 9, 2016 (1.2b); (source: Bloomberg).

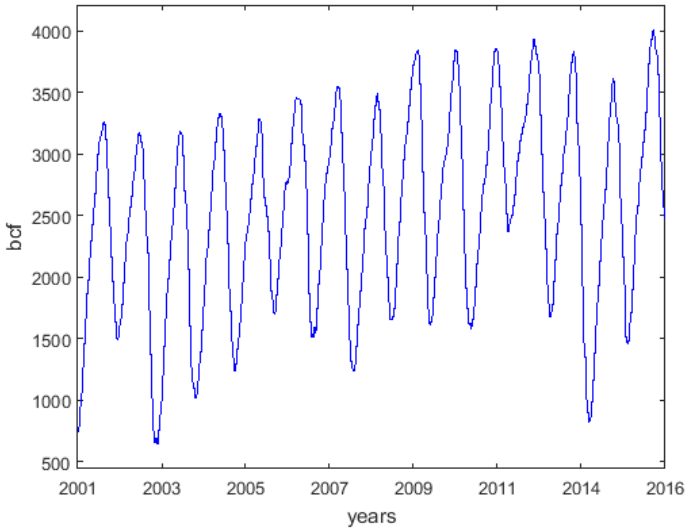

Figure 1.3: time series of gas storage inventories in the US over the period February 2, 2001 - March 9, 2016 (source: www.eia.gov).

Schwartz and Smith model, see [Schwartz and Smith, 2000]) does not explicitly include the temperature as a risk driver. [Stoll and Wiebauer, 2010] proposed a model where the gas price depends on a cumulative Heating Degree Days (HDD) index. A Heating Degree Day with respect to a reference threshold χ_1 (e.g. $\chi_1 = 15$ Celsius degrees) is defined as

$$HDD_t = (\chi_1 - T_t)^+, \, t = 1, \ldots, t^w,$$

where T_t is the average daily temperature[4] measured over a time period that lasts the whole winter, which conventionally starts on October 1 (time $t = 1$) and ends on March 31 (time $t = t^w$) of the subsequent year. Conversely, a Cooling Degree Day with respect to a reference threshold χ_2 (e.g. $\chi_2 = 15$ Celsius degrees) is defined as

$$CDD_t = (T_t - \chi_2)^+, \, t = t^w + 1, \ldots, t^s,$$

where T_t is the temperature measured over the summer, which usually start on April 1 (time $t = t^w + 1$) and ends on September 30 (time $t = t^s$) of the same year. In particular, the authors model the spot price by a discrete time linear factor model, where the normalized cumulative HHD represents an exogenous stochastic factor. The authors fitted the model on the time series of day ahead prices from the Title Transfer Facility (TTF) trading hub, which represents one of the most important trading hubs in the continental Europe, and the time series of the temperature recorded in Hannover by Germany's national meteorological service. Furthermore, they found that the temperature affects in a significant way the value of a gas storage facility. A work related to the previous one has been proposed by [Müller et al., 2015], who improved the original model by adding a oil dependent factor to the linear factor model for the spot price. [Baviera and Mainetti, 2016] instead propose a discrete time two factors model, where both gas price and temperature follows an AR(1)[5] dynamics with seasonality and dependent residuals.

[4]From now on we will use the term "temperature" instead of "mean daily temperature" for easy of explanation.

[5]Autoregressive of order one.

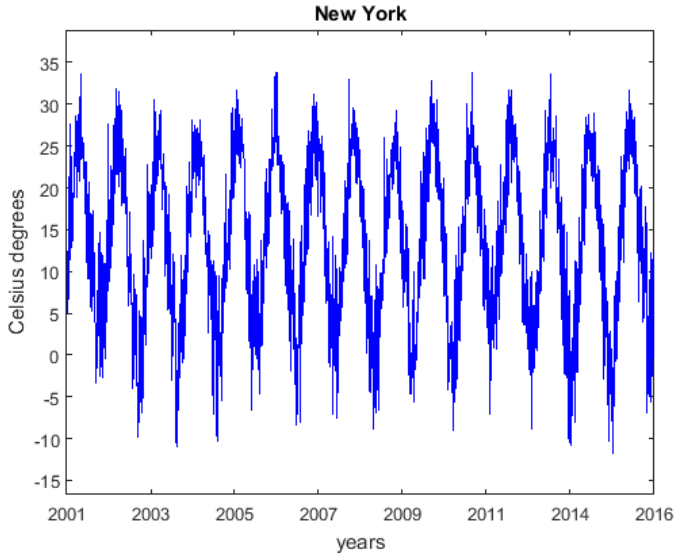

(a)

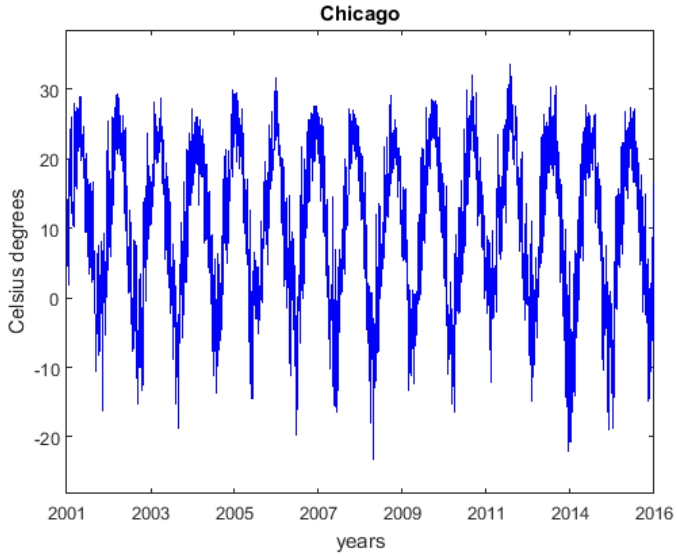

(b)

Figure 1.4: time series of the mean daily temperature recorded in New York over the period February 2, 2001 - March 9, 2016 (1.4a); time series of the mean daily temperature recorded in Chicago over the same period (1.4b); (source: academic.udayton.edu/kissock/http/Weather/citylistUS.htm.).

The deterministic function accounting for the dependence between the two dynamics incorporates what the authors called "delay parameter", which in principle can account for a dependence between gas price today and temperature today or at futures times. The authors found that there is a statistically significant "day ahead" dependence between the Henry Hub (HH) gas price and the temperature measured in the main cities of the US in terms of gas consumption (New York, Boston and Chicago), namely the gas price today depends on the temperature tomorrow. As a consequence, they conjecture that there is a dependence between one day ahead temperature forecast and gas price.

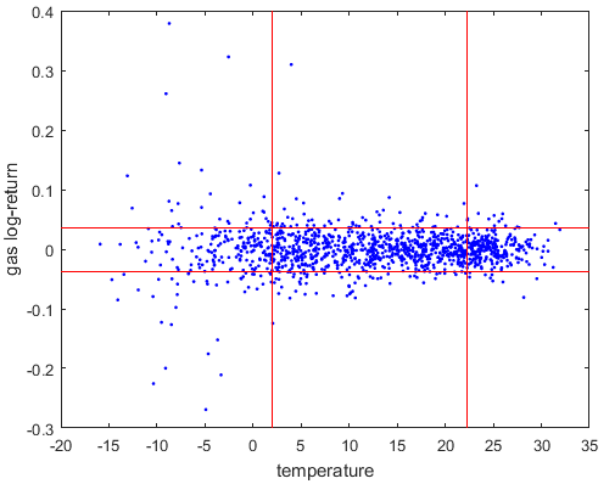

Figure 1.5: scatterplot of the HH gas log-return versus the arithmetic average of the mean daily temperature recorded in New York and Chicago over the period March 2, 2011 - March 9, 2016; the red bands represent the sample standard deviation around the sample mean of the historical samples of gas log-returns and temperature index; data for the HH gas price provided by Bloomberg; data for the temperature provided by the website academic.udayton.edu/kissock/http/Weather/citylistUS.htm.

In order to clarify the relationship between gas price and temperature in the US market, we make some heuristic observations based on the scatter-plot of the gas at the (log-) return level and the temperature index obtained as the arithmetic average of the temperatures measured in the most important areas of the US in terms of contribution to gas consumption, namely New York and Chicago. Indeed, these two cities are the most populous ones in their respective states, which in turns are the first contributors of gas consumption in the US for the residential sector (see http://www.eia.gov/naturalgas/monthly for all the historical data about gas consumption in the US). In Table 1.1 we report the mcf[6] of gas consumed by the residential sector during the period winter 2013/2014 - winter 2015/2016 in New York, Illinois and California states. To perform our analysis, we decided not to include the temperature measured in California, since the climate is warmer on average than the one in New York and, especially, Illinois, and this results in a lower consumption of gas during the colder months of the winter as shown in Table 1.1. It is worth noting that a more refined approach can be pursued to construct the temperature index, see e.g. [Mu, 2007].

From Figure 1.5 we notice that there is a surge in gas log-return volatility when the temperature index falls below 5 Celsius degrees, which usually occurs during the winter

[6]Million cubic feet.

	New York	Illinois	California
Oct 2013	16,869	22,739	28,241
Nov 2013	43,788	50,991	42,241
Dec 2013	69,857	80,459	75,364
Jan 2014	79,952	101,155	61,049
Feb 2014	74,901	84,515	49,235
Mar 2014	70,836	66,611	38,959
Oct 2014	16,260	22,380	21,140
Nov 2014	45,075	57,400	34,011
Dec 2014	62,632	62,983	57,876
Jan 2015	89,003	82,554	60,216
Feb 2015	91,104	85,540	40,902
Mar 2015	74,728	54,278	32,140
Oct 2015	20,673	18,138	19,235
Nov 2015	33,879	36,127	44,392
Dec 2015	44,300	50,976	73,056
Jan 2016	75,393	78,554	69,390
Feb 2016	67,663	62,368	43,489
Mar 2016	48,649	41,109	39,564

Table 1.1: monthly consumption of million cubic feet of gas for the residential sector in the states of New York, Illinois and California during the winter period of the seasons 2013/2014, 2014/2015, 2015/2016 (source: www.eia.gov/naturalgas/monthly).

period. Clearly, this is a non-linear dependence that cannot be captured by a correlation coefficient between two random variables. Furthermore, for normal or high levels of the temperature index we observe that gas return and temperature seems approximately independent. Therefore, we can distinguish two different regimes for gas log-returns, one regime characterized by high dispersion when the temperature is low, and another one characterized by low dispersion otherwise. This observations will guide us in the construction of the model for the evolution of the gas price, presented in the next section.

Before concluding, we stress that if the temperature is the crucial driver on the demand side, as suggested among others by [Brown and Yücel, 2008] and [Borovkova and Geman, 2006], gas inventory (see Figure 1.3) is an important driver for gas prices on the supply side, and thus in principle should be incorporated into a model for the evolution of the gas price. However, in this work we decided not to use the information content provided by such variable. Furthermore, an indirect way to account for the effect of exogenous variables (like temperature) on the dynamics of the gas price is represented by regime-switching models. Such models have been used for pricing gas storage contracts by [Chen and Forsyth, 2010] and [Bäuerle and Riess, 2016].

Chapter 2

Modelling gas and temperature

We propose a model that aims to explain in a parsimonious way the stylized empirical facts of the HH gas price time series and, in particular, that aims to account for sudden large deviations in gas price. Such deviations, which are concentrated mainly during winter periods, are modeled through a pure jump process with stochastic intensity driven by a suitable function of the temperature. The model used for describing the temperature (or a suitable "temperature index") process accounts for its typical seasonal behavior, namely high levels in the summer and low levels in the winter, through a suitable time dependent function.

On the other hand, to compute the value of a derivative contract written on the gas price, one can define a model that is consistent with the standard theory of no arbitrage pricing, and in particular that is able to replicate in a satisfactory way the gas price distribution implicit in quoted derivatives contract.

In order to satisfy both requirements, we follow a modelling approach that is common in the literature of commodity derivatives pricing (see e.g. [Cartea and Williams, 2008] for multiple interruptible supply contracts), and that consists in defining a suitable change of measure that allows one to pass from the real to the pricing measure (and viceversa).

We stress that our model will likely not be able to perfectly fit the actual distributions of the gas price under both real and pricing measures. However, since our primary focus is on pricing a gas storage contract, we will not perform a deep econometric analysis in order to reject or not the validity of our modelling assumptions.

2.1 Model setup

Let $(\Omega, \mathcal{F}, \mathbb{P})$ be a probability space equipped with a filtration $\mathbb{F} = \{\mathcal{F}_t, t \geq 0\}$, with $\mathcal{F}_t \subset \mathcal{F}$, satisfying the usual technical conditions. We refer to $\mathbb{P}$ as the real world probability measure of the gas price process $S = \{S_t,\ t \geq 0\}$. We assume that the numeraire is the bank account $M = \{M_t,\ t \geq 0\}$, which accrues at a continuously compounded risk-free rate $r \in \mathbb{R}$, i.e. $M_t = M_0 e^{rt}$, $M_0 = 1$.

2.2 Real world dynamics

2.2.1 Gas price dynamics

Based on the stylized empirical facts that we described in the previous sections, we model the HH gas price as a mean reverting, non stationary and non Gaussian Ornstein-Uhlenbeck process. For analytical tractability reasons that will become clear later on, we prefer not to model directly the gas price process $S = \{S_t,\, t \geq 0\}$ itself, but its natural logarithm. In particular, we assume that the $\mathbb{F}$-adapted gas log-price process $Y = \{Y_t = \ln S_t,\, t \geq 0\}$ satisfies the SDE

$$dY_t = \kappa(\mu - Y_t)dt + \sigma dB_t + dJ_t,\; Y_0 = \ln s_0, \tag{2.1}$$

where $s_0, \kappa, \sigma > 0$, $\mu \in \mathbb{R}$, $B = \{B_t, t \geq 0\}$ is a standard Brownian motion, $J = \{J_t,\, t \geq 0\}$ is a pure jump process defined as

$$J_t = \sum\nolimits_{i=0}^{N_t} G_i,\; J_0 = 0.$$

We assume that the i.i.d. jump sizes have a double exponential distribution [Kou, 2002] with density function

$$p_G(y) = \varsigma \upsilon_+ \exp(-\upsilon_+ y) \times 1_{\{y>0\}}(y) + (1-\varsigma)\upsilon_- \exp(-\upsilon_- |y|) \times 1_{\{y<0\}}(y), \tag{2.2}$$

where $\upsilon_- > 0, \upsilon_+ > 1$, $1 < \varsigma < 0$.

The counting process $N = \{N_t,\, t \geq 0\}$ is a Cox process [Cox and Isham, 1980] with an $\mathbb{F}$-predictable non-negative stochastic intensity process $\lambda = \{\lambda_t,\, t \geq 0\}$, which will be specified later on as a function of the temperature. By definition of Cox process, conditional on the sigma-algebra generated by the stochastic intensity process $\mathcal{F}_{\tilde{t}}^{\lambda} = \sigma(\{\lambda_t : t \leq \tilde{t}\}) \subset \mathcal{F}_{\tilde{t}}$, the probability between two times u and t, $u \leq t \leq \tilde{t}$, that $k \in \mathbb{N}$ jumps occur is

$$\mathbb{P}(N_t - N_u = k | \mathcal{F}_{\tilde{t}}^{\lambda}) = \frac{\left(\int_u^t \lambda_s ds\right)^k}{k!} \exp\left(-\int_u^t \lambda_s ds\right).$$

This fact implies that conditional on $\mathcal{F}_{\tilde{t}}^{\lambda}$, the jump process $\{J_t,\, t \leq \tilde{t}\}$ behaves as a compound Poisson process with time inhomogeneous deterministic intensity $\{\lambda_t : t \leq \tilde{t}\}$ and $\mathcal{F}_{\tilde{t}}^{\lambda}$-conditional characteristic function given by

$$\begin{aligned} \mathbb{E}[e^{i\omega J_t} | \mathcal{F}_{\tilde{t}}^{\lambda}] &= \exp\left((\phi_G(\omega) - 1)\int_0^t \lambda_s ds\right),\, t \leq \tilde{t}, \\ \phi_G(\omega) &= \frac{\varsigma \upsilon_+}{\upsilon_+ - i\omega} + \frac{(1-\varsigma)\upsilon_-}{\upsilon_- + i\omega},\, \omega \in \mathbb{R}, \end{aligned}$$

where $\phi_G(\cdot)$ is the characteristic function of each jump size G_i. Furthermore, as customary in the literature, we assume independence between the standard Brownian motion and the pure jump process, i.e. $B \perp J$, which is consistent with the empirically observed fact (see Figure 1.5) that temperature does not affect the "regular" variations of gas price.

The solution of the SDE (2.1) for $u \leq t$ is

$$Y_t = Y_u e^{-\kappa(t-u)} + \mu(1 - e^{-\kappa(t-u)}) + \sigma \int_u^t e^{-\kappa(t-s)} dB_s + \int_u^t e^{-\kappa(t-s)} dJ_s. \tag{2.3}$$

The model dynamics for the log-price (2.1) implies a mean reverting Ornstein-Uhlenbeck dynamics for the gas price process $S = \{S_t,\, t \geq 0\}$, satisfying the SDE

$$\frac{dS_t}{S_{t^-}} = \kappa \left(\mu + \frac{\sigma^2}{2\kappa} - \ln S_{t^-} \right) dt + \sigma dB_t + (\exp(G_{N_t}) - 1) dN_t,\, S_0 = s_0.$$

In order to gain intuition about the statistical properties of the model and the relationship between gas price and temperature, we observe that the log-gas price SDE (2.1) can be re-written as

$$dY_t = \kappa \left(\mu + \frac{\mu_G}{\kappa} \lambda_t - Y_t \right) dt + \sigma dB_t + d\bar{J}_t,\, Y_0 = \ln s_0, \tag{2.4}$$

with solution

$$Y_t = Y_u e^{-\kappa(t-u)} + \nu(u,t;\lambda_\cdot) + \sigma \int_u^t e^{-\kappa(t-s)} dB_s + \int_u^t e^{-\kappa(t-s)} d\bar{J}_s, \tag{2.5}$$

where

$$\nu(u,t;\lambda_\cdot) = \mu(1 - e^{-\kappa(t-u)}) + \mu_G \int_u^t e^{-\kappa(t-s)} \lambda_s ds$$

is the time dependent stochastic drift influenced by the temperature through the intensity process λ over the period $[u,t]$, and $\bar{J} = \{\bar{J}_t,\, t \geq 0\}$ is a compensated pure jump process with dynamics

$$\begin{aligned} d\bar{J}_t &= dJ_t - \mu_G \lambda_t dt \\ \mu_G &= \mathbb{E}[G_i] = \frac{\varsigma}{\upsilon_+} - \frac{(1-\varsigma)}{\upsilon_-}. \end{aligned}$$

It is now clear that through this modelling approach a seasonality effect induced by the temperature is introduced in the drift of the gas price dynamics.

Before concluding the description of the model, we remark that it is possible to replace the constant parameter μ in the drift of the gas price process with a time dependent function that accounts for the seasonality of the gas price. The choice of not including a seasonality function is motivated by the heuristic analysis of the stylized facts of the HH gas price time series we performed in the previous section.

2.2.2 Temperature dependent stochastic intensity

Temperature represents an exogenous source of risk with respect to the gas price. From a pricing perspective, it is a source of market incompleteness, since it cannot be directly traded. Nevertheless, the "temperature risk" can in principle be hedged by means of weather derivatives (see e.g. [Benth and Koekebakker, 2008]) if available.

There is a relatively limited literature on temperature modelling for the purpose of pricing temperature derivatives. [Alaton et al., 2002] proposed a non-stationary Ornstein-Uhlebenck process with time dependent drift and instantaneous volatility, in order to describe the temperature observed in Sweden. The time dependent drift is the sum of a constant long-term mean, a linear drift part and a seasonal component. The instantaneous volatility is a piecewise constant function of time, in that the temperature features a different empirical volatility over each month. An almost identical model was proposed also by [Dornier and Queruel, 2000] to describe the temperature in the US, with the only

difference of a constant instantaneous volatility parameter. [Benth and Šaltytė-Benth, 2005] generalized the previously cited models in order to account for non-zero skewness and semi-heavy tails, by modelling the shocks with a generalized hyperbolic Lévy process instead of a Brownian motion, which is better suited to describe the temperature in Norway. Other relevant, but somehow less interesting approaches from our point of view, for modelling the temperature have been proposed for example by [Brody et al., 2002] and [Campbell and Diebold, 2011].

We assume that the temperature (or a suitable temperature index) follows a $\mathbb{F}$-adapted mean reverting non stationary Ornstein-Uhlenbeck process $T = \{T_t,\, t \geq 0\}$ that satisfies the following SDE

$$dT_t = \left(\frac{dT_t^m}{dt} + a(T_t^m - T_t) \right) dt + \eta d\check{B}_t,\; T_0 = c_0, \tag{2.6}$$

where $a, \eta > 0$ and the drift depends on a time dependent function defined as

$$T_t^m = \delta + \beta t + \gamma \sin(\varrho + \vartheta t), \tag{2.7}$$

which accounts for long term level, linear drift and seasonal behavior of the temperature. We assume independence between the standard Brownian motion driving the gas price process and the one driving the temperature process, i.e. $\check{B} \perp B$. The solution of the SDE (2.6) for $u \leq t$ is

$$T_t = (T_u - T_u^m)e^{-a(t-u)} + T_t^m + \eta \int_u^t e^{-\kappa(t-s)} d\check{B}_s. \tag{2.8}$$

This model is a simplified version of the one proposed by [Alaton et al., 2002] and coincides with the model proposed by [Dornier and Queruel, 2000], in that here we assume constant instantaneous volatility.

The choice of the temperature model plays a key role in our modelling framework. Indeed, the pure jump process J depends on the temperature through the stochastic intensity process λ. In particular, consider the time interval $[0, \tau]$ and a finite partition

$$\mathcal{T} = \{t_0 = 0 < t_1 < \cdots < t_n < t_{n+1} < \cdots t_{\bar{n}} = \tau\}, \tag{2.9}$$

where $\tau < +\infty$ represents the final time of the contract or the storage facility. We assume that, for each $n = 0, \ldots, \bar{n}-1$, $\bar{n} \in \mathbb{N}$, the temperature revealed at time t_n of the partition affects the gas price over the interval $(t_n, t_{n+1}]$. Obviously, in order for the temperature to have a strong effect on the gas price, the partition (2.9) should be fine enough, and in particular we will assume from now on that the times $\{t_n\}_{n=0}^{\bar{n}}$ represent the days of the life of the contract/facility.

The temperature-dependent stochastic intensity process $\lambda = \{\lambda_t,\, t \geq 0\}$ is defined for $t_n < t \leq t_{n+1}$, $n = 0, \ldots, \bar{n} - 1$ as

$$\lambda_t = (\lambda^1 + \lambda^2(\alpha^1 - h(t, T_{t_n}))^+) \times 1_{\mathbb{H}}(t) + (\lambda^3 + \lambda^4(h(t, T_{t_n}) - \alpha^2)^+) \times 1_{\mathbb{C}}(t),\; \lambda_0 = 0, \tag{2.10}$$

where $(x)^+ = \max(x, 0)$, λ^1, λ^2, λ^3, $\lambda^4 \in \mathbb{R}_0^+$, α^1, $\alpha^2 \in \mathbb{R}$, and

$$1_{\mathbb{H}}(t) = \begin{cases} 1 & \text{if } t \in \text{ winter period} \\ 0 & \text{if } t \in \text{ summer period} \end{cases}$$

is the indicator function for the winter period, which according to a common convention in the literature starts on October 1 of the current year and ends on March 31 of the subsequent year, while $1_{\mathbb{C}}(\cdot) = 1 - 1_{\mathbb{H}}(\cdot)$ is the indicator function for the summer period. We choose the function $h(\cdot,\cdot)$ as the $\mathcal{F}_{t_n}$-conditional expectation of the temperature

$$h(t, c_n) = \mathbb{E}\left[T_t | T_{t_n} = c_n\right] = (c_n - T^m_{t_n})e^{-a(t-t_n)} + T^m_t,$$

i.e. the least-square best predictor of $T_{t_{n+1}}$ given T_{t_n}.

In this framework the temperature acts as a trigger of the pure jump process J: the larger the downward (upward) deviation of the temperature from the threshold α^1 (α^2), the higher the activity of the jump process, i.e. the higher is the probability of the gas price to jump.

Before proceeding in the discussion of the model, we want to spend a few words regarding the choice made to model the relationship between gas log-price and temperature. In particular, at first sight one may think that assuming that the temperature affects the price only on a discrete grid of times (2.9) is an artificial and simplistic assumption. However, as suggested by [Mu, 2007], the information about the temperature becomes available to the market on a discrete time basis (hourly, daily), and so its effect on the gas price is delayed. A delayed effect of temperature on consumption of energy has been already suggested by other researchers, see e.g. [Goia et al., 2010].

2.3 Some statistical properties of the model

In order to compute all the relevant statistical properties of the gas process (2.3), we need to know its (conditional and unconditional) distribution. Unfortunately, the expression for the density function of the gas log-price process (2.3) is not known in closed form, but the expressions for the conditional characteristic function for $t_n \leq u < t \leq t_{n+1}$, $n = 0, \ldots, \bar{n} - 1$,

$$\phi_{Y_t|\mathcal{F}_u}(\omega; Y_u, T_{t_n}) = \mathbb{E}[\exp(i\omega Y_t)|\,\mathcal{F}_u],\ \omega \in \mathbb{R},$$

the conditional log-characteristic function

$$\psi_{Y_t\mathcal{F}_u}(\omega; Y_u, T_{t_n}) = \ln \phi_{Y_t|\mathcal{F}_u}(\omega; Y_u, T_u),\ \omega \in \mathbb{R}, \tag{2.11}$$

and their unconditional counterparts can be recovered in (semi)-closed form. In particular, for $t_n \leq u < t \leq t_{n+1}$, $n = 0, \ldots, \bar{n} - 1$, the $\mathcal{F}_u$-conditional log-characteristic function is

$$\begin{aligned}
\psi_{Y_t|\mathcal{F}_u}(\omega; Y_u, T_{t_n}) &= \psi_{Y^D_t|\mathcal{F}_u}(\omega; Y_u) + \psi_{Y^J_t|\mathcal{F}_u}(\omega; T_{t_n}) \\
\psi_{Y^D_t|\mathcal{F}_u}(\omega; Y_u) &= i\omega e^{-\kappa(t-u)}Y_u + i\omega\mu(1 - e^{-\kappa(t-u)}) - \frac{\omega^2\sigma^2}{4\kappa}(1 - e^{-2\kappa(t-u)}) \\
\psi_{Y^J_t|\mathcal{F}_u}(\omega; T_{t_n}) &= \int_u^t (\phi_G(\omega e^{-\kappa(t-s)}) - 1)\lambda_s ds.
\end{aligned}$$

Notice that for the sake of clarity we split the log-characteristic function into a "diffusion part" and a "jump part". Furthermore, we stress that by construction of the model the intensity process (2.10) depends on T_{t_n} when $t \in (t_n, t_{n+1}]$, for $n = 0, \ldots, \bar{n} - 1$.

Instead, for $u < t$, the conditional log-characteristic function of the temperature process (2.8) simply reads

$$\psi_{T_t|\mathcal{F}_u}(\omega; T_u) = i\omega(T_u - T_u^m)e^{-a(t-u)} + i\omega T_t^m - \frac{\omega^2\eta^2}{4a}(1 - e^{-2a(t-u)}). \tag{2.12}$$

From the expression of the $\mathcal{F}_u$-conditional log-characteristic function it is immediate to recover the conditional expectation and variance for $t_n \leq u < t \leq t_{n+1}$, $n = 0, \ldots, \bar{n} - 1$,

$$\begin{aligned}
\mathbb{E}[Y_t|\mathcal{F}_u] = \quad & e^{-\kappa(t-u)}Y_u + \mu(1 - e^{-\kappa(t-u)}) + \\
& \frac{\partial}{\partial\omega}\int_u^t \left(\phi_G\left(\frac{\omega e^{-\kappa(t-s)}}{i}\right) - 1\right)\lambda_s ds\bigg|_{\omega=0} \\
\mathbb{V}ar[Y_t|\mathcal{F}_u] = \quad & \frac{\sigma^2}{2\kappa}(1 - e^{-2\kappa(t-u)}) + \\
& \frac{\partial^2}{\partial\omega^2}\int_u^t \left(\phi_G\left(\frac{\omega e^{-\kappa(t-s)}}{i^2}\right) - 1\right)\lambda_s ds\bigg|_{\omega=0},
\end{aligned}$$

which both depend on the jump part of the model (as well as higher moments if they exist) when the intensity process is above zero. Similarly, the expression for the first two conditional moments of the temperature process are for $u < t$

$$\begin{aligned}
\mathbb{E}[T_t|\mathcal{F}_u] &= (T_u - T_u^m)e^{-a(t-u)} + T_t^m, \\
\mathbb{V}ar[T_t|\mathcal{F}_u] &= \frac{\eta^2}{2a}(1 - e^{-2a(t-u)}).
\end{aligned}$$

While the unconditional log-characteristic function of the temperature process (2.8) is readily available from its conditional counterpart (2.12) in closed form, in order to recover the unconditional characteristic function of the gas log-price process we need to integrate

$$\begin{aligned}
\mathbb{E}[\exp(i\omega Y_t)|\mathcal{F}_t^\lambda] = \quad & \exp\Bigg(i\omega e^{-\kappa t}Y_0 + i\omega\mu(1 - e^{-\kappa t}) - \frac{\varpi^2\sigma^2}{4\kappa}(1 - e^{-2\kappa t}) + \\
& \int_0^t (\phi_G(\omega e^{-\kappa(t-s)}) - 1)\lambda_s ds\Bigg),
\end{aligned}$$

over the distribution generated by the trajectories of the temperature process (2.8) over the period $[0, t^*]$, where $t^* = \max\{t_n \in \mathcal{T} : t_n < t\}$, which can be done only numerically, e.g. by Monte Carlo integration.

Another interesting property of the model, that will be used later on, is the fact that for $t_n \leq u < t \leq t_{n+1}$, $n = 0, \ldots, \bar{n} - 1$, the two processes are $\mathcal{F}_u$-conditionally independent, namely

$$\psi_{Y_t,T_t|\mathcal{F}_u}(\omega; Y_u, T_{t_n}) = \psi_{Y_t|\mathcal{F}_u}(\omega; Y_u, T_{t_n}) + \psi_{T_t|\mathcal{F}_u}(\omega; T_{t_n}). \tag{2.13}$$

2.4 Maximum likelihood estimation

In order to calibrate the parameters of the gas price and the temperature processes under the real measure $\mathbb{P}$, we follow a discrete time maximum likelihood approach. We follow this approach for a practical reason: the time series of daily observations of the processes can be easily obtained, and we can compute the joint density of a discrete sample of the gas price with daily frequency as a product of the daily conditional distributions. Indeed,

from the conditional independence property (2.13) we deduce that the joint conditional probability can be factorized for $t_n < t_{n+1}$, $n = 0, \dots, \bar{n} - 1$, as

$$\mathbb{P}(Y_{t_{n+1}} \leq y, T_{t_{n+1}} < r | \mathcal{F}_{t_n}) = \mathbb{P}(Y_{t_{n+1}} \leq y | Y_{t_n} = x, T_{t_n} = c) \times \mathbb{P}(T_{t_{n+1}} \leq r | T_{t_n} = c).$$

Consider now the joint sample of gas log-price and temperature $\{(y_l, c_l)\}_{l=0}^{\bar{l}-1}$ of length $\bar{l} \in \mathbb{N}$. Given the set of parameters to be estimated $\Sigma = \{\mu, \kappa, \sigma, \lambda^1, \lambda^2, \lambda^3, \lambda^4, a, \eta\}$, the likelihood of the joint sample can be written as

$$\mathcal{L}(\Sigma | \{(y_l, c_l)\}_{l=0}^{\bar{l}-1}) = \prod_{l=1}^{\bar{l}-1} p_{Y_{t_l} | \mathcal{F}_{t_{l-1}}}(y_l | y_{l-1}, c_{l-1}) \times p_{T_{t_l} | \mathcal{F}_{t_{l-1}}}(c_l | c_{l-1}), \tag{2.14}$$

where the conditional density function of the temperature $p_{T_{t_l} | \mathcal{F}_{t_{l-1}}}(\cdot | c_{l-1})$ explicitly reads

$$p_{T_{t_l} | \mathcal{F}_{t_{l-1}}}(x|z) = \frac{1}{\sqrt{\frac{\eta^2}{2a}\left(1 - e^{-2a(t_l - t_{l-1})}\right)}} \times p_{\mathcal{N}(0,1)} \left(\frac{x - ((z - T^m_{t_{l-1}}) e^{-a(t_l - t_{l-1})} + T^m_{t_l})}{\sqrt{\frac{\eta^2}{2a}\left(1 - e^{-2a(t_l - t_{l-1})}\right)}} \right),$$

with $p_{\mathcal{N}(0,1)}(\cdot)$ denoting the standard normal density. Since $p_{Y_{t_l} | \mathcal{F}_{t_{l-1}}}(\cdot | y_{l-1}, c_{l-1})$ is not available in closed form, in order to implement the maximum likelihood estimation, we must resort to the FFT algorithm [Cooley and Tukey, 1965], which is feasible thanks to the availability of the closed form expression for the conditional characteristic function of the gas log-price (2.11). The parameters of the time dependent drift of the temperature $\Xi = \{\delta, \beta, \gamma, \varrho, \vartheta\}$ are estimated through a non-linear regression approach using the Matlab function `nlinfit`. A detailed exposition of the estimated parameters is given in Section 4.1.1.

Chapter 3

Pricing of gas storage contracts/facilities: a real options approach

There exists fundamentally two different kind of approaches to evaluate a gas storage contract/facility, namely the *intrinsic* and the *extrinsic* approach (see e.g. [De Jong, 2016], [Cartea et al., 2014], [Roncoroni et al., 2015]).

The intrinsic approach relies on computing the value of the contract/facility as the value of the optimal trading strategy that can be put in place at the valuation date by buying and selling futures contracts on gas with different maturities. In its simplest form, the strategy is static or "buy-and-hold", namely it exploits only the information contained in the current futures prices quoted on the market, and coincides with a classical calendar spread strategy on the futures curve, with the only difference of the presence of constraints on the gas that can be bought or sold. A more sophisticated approach, called *rolling intrinsic*, extends the classical intrinsic approach by allowing for the possibility of changing the strategy over time in order to exploit the random evolution of the futures curve.

From a modelling perspective, the intrinsic approach can be easily formulated as a deterministic optimization in the static case, that can be solved by linear programming.

The intrinsic approaches based on trading the futures curve do not permit to fully extract the extrinsic value, namely the optionality value, contained in a gas storage contract, which stems from the possibility for the owner of the contract/facility to buy gas when it is cheap and sell it when it is expensive. Indeed, the intrinsic approach does not account for the volatility of the spot gas price. In order to account for the extrinsic value, [Breslin et al., 2008] and [Eydeland and Wolyniec, 2003] among others suggests to evaluate a gas storage contract/facility as a long position in a basket of calendar spread options, possibly by means of a rolling strategy. Even though appealing from a hedging point of view, this approach is suboptimal from a valuation point of view, because it neglects the basic fact that buying or selling gas today can affect the ability to buy or sell gas at a future time. Furthermore, [Gray and Khandelwal, 2004] have shown that this approach does not yield substantially different results with respect to the basic rolling intrinsic approach.

As proposed for the first time by [Boogert and De Jong, 2008], in order to compute the value of the gas storage contract we will pursue a real option approach. Mathematically, this approach amounts to solve a stochastic optimal control problem.

Before exposing our approach, we proceed to give a review of the relevant literature about this and other modelling approaches for pricing gas storage contract/facilities.

3.1 Review of the relevant literature

The intrinsic approach is model free, in that it does not require a model for the evolution of the gas price or the futures curve. The rolling intrinsic approach, instead, requires a model to simulate the futures curve for each time of the contract/storage life, see e.g. [Gray and Khandelwal, 2004], [Breslin et al., 2009] for a study of the intrinsic rolling approach and a comparison between the basic approach based on trading the futures curve and the one based on trading spread options. A more recent work that extends the rolling intrinsic approach has been proposed by [Löhndorf and Wozabal, 2015].

Roughly speaking, the literature regarding the real option approach can be divided into two streams of research: one that deals with high-dimensional models for the evolution of the futures curve, and an alternative low-dimensional approach based on modelling the spot price dynamics.

In the first stream of literature, we recall the work of [Lai et al., 2010], who model the forward curve by means of a multivariate geometric Brownian motion, and obtain the value of a gas storage contract by solving an approximate dynamic programming problem. As noticed by [Löhndorf and Wozabal, 2015], the authors consider in the state space of the dynamic programming only the front month futures contract (other than the gas storage volume), thus greatly simplifying the optimization problem.

In the second stream of the literature, some relevant contributions have been proposed by [Bjerksund et al., 2008], [Boogert and De Jong, 2008], [Carmona and Ludkovski, 2010], [Chen and Forsyth, 2007], [Edoli and Vargiolu, 2013], [Felix and Weber, 2012], [Kiely et al., 2015] and [Thompson et al., 2009]. Roughly speaking, all these works have a common trait: they solve an optimal stochastic control problem in an approximate way.

Our approach classifies in the stream of low-dimensional spot pricing models. In particular, we obtain the value of the gas price contract/facility by numerically solving a stochastic optimal control problem via dynamic programming (see e.g. [Bertsekas et al., 1995]), where the state space includes both the gas price and the temperature. To do it, we define a suitable pricing measure, equivalent to the real one $\mathbb{P}$, for the gas price process S. The gas price model under the new pricing measure can be calibrated to the liquid derivatives on the Henry Hub gas price (futures, options) traded in the electronic markets, according to an approach that is typical of the literature on pricing financial derivatives.

3.2 Pricing dynamics

According to the standard theory of no arbitrage pricing (see e.g. [Björk, 2009]), in order to compute the fair value of a contingent claim we need a martingale measure such that the payoff of any tradable asset normalized by the numeraire is a martingale. In our setting, this would amount to pin down one of the infinite equivalent martingale measures $\mathbb{Q} \sim \mathbb{P}$, since the presence of jumps in the $\mathbb{P}$-dynamics of the gas price and its dependence on the temperature process are sources of market incompleteness.

Furthermore, as highlighted by [Benth and Koekebakker, 2008], even though gas is a storable and tradable commodity, costs and limitation to trading and the presence of

the *convenience yield* makes it difficult to derive the price of a futures contract on gas by replication, and so we will not require the discounted gas price process S_t/M_t to be a martingale under the pricing measure. For these reasons, we have the freedom to choose as a pricing measure $\mathbb{Q}$ any measure equivalent to the real one $\mathbb{P}$.

We choose to restrict our attention to the pricing measures generated by a particular Esscher transform, which we proceed to define. The choice is motivated by essentially two reasons. The first one is that it is analytically tractable, in that it does not dramatically change the statistical features of the model when passing from the real measure $\mathbb{P}$ to the pricing measure $\mathbb{Q}$. The second reason is that the Esscher transform introduces in the distribution of the gas and temperature process new parameters that can be interpreted as market prices of risk, which can be calibrated to the market data of liquid derivatives on natural gas.

3.2.1 Change of measure

The Esscher transform is a change of measure that has been originally proposed in an actuarial context by [Esscher, 1932]. [Gerber et al., 1994] extended its use to the class of Lévy processes, and used it in particular to generalize the Black-Scholes pricing formula [Black and Scholes, 1973], while [Kallsen and Shiryaev, 2002] further generalized it to semimartingale modelling. A special kind of Esscher transform called conditional Esscher transform has been proposed and studied by [Bühlmann et al., 1996]. In the specific context of commodity modelling, a relevant work is the one by [Benth and Sgarra, 2012], who used a Esscher transform for Lévy driven Ornstein-Uhlenbeck processes to model the risk premia in electricity markets. Here we propose an exponential tilting that closely resembles the Esscher transform, which for simplicity we shall call with abuse of terminology simply Esscher transform.

Consider the Esscher transform

$$Z_t^{\boldsymbol{\theta}} = \hat{Z}_t \times \tilde{Z}_t,\ t \geq 0, \tag{3.1}$$

parametrized by the bivariate $\mathbb{F}$-adapted process

$$\boldsymbol{\theta} = (\hat{\theta}, \tilde{\theta}) = \{(\hat{\theta}(t), \tilde{\theta}(t)),\ t \geq 0\}, \tag{3.2}$$

where

$$\begin{aligned}
\hat{Z}_t &= \exp\left(\int_0^t \hat{\theta}(u)dB_u - \frac{1}{2}\int_0^t \hat{\theta}^2(u)du\right) \\
\tilde{Z}_t &= \begin{cases} \exp\left(\int_{t_{n-1}}^t \tilde{\theta}(u)dJ_u - \psi_{\Delta J_t|\mathcal{F}_{t_{n-1}}}\left(-i\tilde{\theta}(\cdot); T_{t_{n-1}}\right)\right), \\ \text{for } t_0 < t \leq t_1, \quad n = 1 \\ \prod_{k=1}^{n-1} \Delta\tilde{Z}_{t_k} \times \exp\left(\int_{t_{n-1}}^t \tilde{\theta}(u)dJ_u - \psi_{\Delta J_t|\mathcal{F}_{t_{n-1}}}\left(-i\tilde{\theta}(\cdot); T_{t_{n-1}}\right)\right), \\ \text{for } t_{n-1} < t \leq t_n, \quad n = 2, \ldots, \bar{n} \end{cases} \\
\Delta\tilde{Z}_{t_k} &= \exp\left(\int_{t_{k-1}}^{t_k} \tilde{\theta}(u)dJ_u - \psi_{\Delta J_{t_k}|\mathcal{F}_{t_{k-1}}}\left(-i\tilde{\theta}(\cdot); T_{t_{k-1}}\right)\right) \\
\psi_{\Delta J_t|\mathcal{F}_{t_n}}\left(\tilde{\theta}(\cdot); T_{t_n}\right) &= \ln \mathbb{E}\left[\exp\left(i\int_{t_n}^t \tilde{\theta}(s)dJ_s\right)\middle|\mathcal{F}_{t_n}\right], \text{ for } t_{n-1} < t \leq t_n, \quad n = 1, \ldots, \bar{n}.
\end{aligned}$$

Assuming that suitable integrability conditions hold, the process $Z^{\boldsymbol{\theta}} = \{Z_t^{\boldsymbol{\theta}}, t \geq 0\}$ is a positive $\mathbb{P}$-martingale with $Z_0^{\boldsymbol{\theta}} = 1$ (see A.3 in the Appendix). Hence (3.1) defines the change of measure

$$\left.\frac{d\mathbb{Q}^{\boldsymbol{\theta}}}{d\mathbb{P}}\right| \mathcal{F}_t = Z_t^{\boldsymbol{\theta}},$$

where $\mathbb{Q}^{\boldsymbol{\theta}} \sim \mathbb{P}$ is the no arbitrage pricing measure. As a consequence, the dynamics of the gas price process changes as follows. First, $d\hat{B}_t = dB_t - \hat{\theta}(t)dt$ is a standard Brownian motion under $\mathbb{Q}^{\boldsymbol{\theta}}$, since the Esscher transform (3.1) includes the Girsanov transform as a special case. Second, J is a pure jump process with $\mathcal{F}_t^{\lambda}$-conditional characteristic function

$$\mathbb{E}^{\boldsymbol{\theta}}\left[e^{i\omega J_t}|\mathcal{F}_t^{\lambda}\right] = \exp\left(\int_0^t (\phi_G(\omega - i\tilde{\theta}(s)) - \phi_G(-i\tilde{\theta}(s)))\lambda_s ds\right). \tag{3.3}$$

Then, the log-price Y_t (2.3) under $\mathbb{Q}^{\boldsymbol{\theta}}$ satisfies the SDE

$$dY_t = \kappa\left(\mu + \frac{\sigma}{\kappa}\hat{\theta}(t) - Y_t\right)dt + \sigma d\hat{B}_t + d\tilde{J}_t,\ Y_0 = \ln s_0, \tag{3.4}$$

and reads for $u \leq t$

$$Y_t = Y_u e^{-\kappa(t-u)} + \mu(1 - e^{-\kappa(t-u)}) + \sigma\int_u^t e^{-\kappa(t-s)}\hat{\theta}(s)ds + \sigma\int_u^t e^{-\kappa(t-s)}d\hat{B}_s + \int_u^t e^{-\kappa(t-s)}d\tilde{J}_s. \tag{3.5}$$

As previously noticed by [Benth and Koekebakker, 2008], $\hat{\theta}$ and $\tilde{\theta}$ can be interpreted as market prices of risk, where $\hat{\theta}$ accounts for the risk coming from normal variations of the gas price, while $\tilde{\theta}$ accounts for the jump risk. We assume that temperature does not bear any risk premium, and so the distribution of the temperature process under $\mathbb{Q}^{\boldsymbol{\theta}}$ and $\mathbb{P}$ coincides.

In order to gain intuition on the effect of the change of measure on the jump part of the process (2.3), we set $\tilde{\theta}$ as a constant function

$$\tilde{\theta}(t) = \tilde{\theta}^c < +\infty,\ t \geq 0, \tag{3.6}$$

and we observe that in this case the jump process under $\mathbb{Q}^{\boldsymbol{\theta}}$ has the following $\mathcal{F}_{\tilde{t}}^{\lambda}$-conditional characteristic function

$$\mathbb{E}^{\boldsymbol{\theta}}\left[e^{i\omega J_t}|\mathcal{F}_{\tilde{t}}^{\lambda}\right] = \exp\left((\tilde{\phi}_G(\omega) - 1)\int_0^t \tilde{\lambda}_s ds\right),\ t \leq \tilde{t},$$

where $\tilde{\phi}_G(\cdot)$ and $\tilde{\lambda}_s$ are respectively the characteristic function of the jump size and the stochastic intensity under $\mathbb{Q}^{\boldsymbol{\theta}}$

$$\begin{aligned}\tilde{\phi}_G(\omega) &= \tilde{\varsigma}\frac{\tilde{\upsilon}_+}{\tilde{\upsilon}_+ - i\omega} + (1 - \tilde{\varsigma})\frac{\tilde{\upsilon}_-}{\tilde{\upsilon}_- + i\omega},\\ \tilde{\lambda}_s &= \phi_G(-i\tilde{\theta}^c)\lambda_s,\end{aligned}$$

and where the jump size has a double exponential distribution as in (2.2) with new parameters

$$\begin{aligned}\tilde{\upsilon}_+ &= \upsilon_+ - \tilde{\theta}^c,\ \tilde{\upsilon}_+ > 1\\ \tilde{\upsilon}_- &= \upsilon_- + \tilde{\theta}^c,\ \tilde{\upsilon}_+ > 0\\ \tilde{\varsigma} &= \varsigma\frac{\upsilon_+}{\phi_G(-i\tilde{\theta}^c)\tilde{\upsilon}_+}.\end{aligned}$$

We conclude that conditional on $\mathcal{F}_{\tilde{t}}^{\lambda}$, the process $J = \{J_t, t \leq \tilde{t}\}$ with the specification (3.6) is under $\mathbb{Q}^{\boldsymbol{\theta}}$ a compound Poisson process (see A.5 in the Appendix).

3.2.2 Calibration

The Esscher transform (3.1) turns out to be a very flexible tool when it comes to the calibration procedure, since it introduces an infinite number of degrees of freedom in the $\mathbb{Q}^{\boldsymbol{\theta}}$-dynamics of the gas price by the market price of risk (3.2).

Here we propose to find the market price of risk for regular variation $\hat{\theta}$ by matching model implied and market futures prices that are quoted at the moment of the calibration, an approach that is similar in the spirit to the one proposed by [Benth et al., 2003] and [Cartea and Figueroa, 2005]. This approach is particularly convenient in our framework, since it provides a term structure of market prices of risk.

As notice by [Benth and Koekebakker, 2008] and [Benth and Sgarra, 2012], the Esscher transform is a flexible change of measure that allows to change the distribution of a jump process. In this work we have also proved that for a constant specification for the market price of risk (3.6) the Esscher transform changes both the intensity and the size distribution of a compound Poisson process with double exponential distributed jumps (see A.5 in the Appendix). Furthermore, in this special case we can see the effect of the Esscher transform on the jump size distribution by looking at the sign of the market price of risk. When $\tilde{\theta}^c > 0$, the intensity gives more importance to positive jumps, which in turns becomes larger on average and more dispersed, increasing in the end the skewness of the distribution. Viceversa, when $\tilde{\theta}^c < 0$ the skewness decreases.

3.2.3 Arbitrage free spot-futures model

By definition of futures price we have the following no arbitrage relationship with the gas spot price

$$F_u^{\boldsymbol{\theta}}(t) = \mathbb{E}^{\boldsymbol{\theta}}[S_t|\mathcal{F}_u],\ 0 \leq u \leq t. \tag{3.7}$$

We stress that in our model futures and forward contracts have the same value, since the instantaneous interest rate r is assumed constant, and therefore we can use the two terms interchangeably. As we have already pointed out, in order to derive the expression of the market price of risk $\hat{\theta}$ we do not need to impose the usual no arbitrage condition

$$\mathbb{E}^{\boldsymbol{\theta}}[S_t|\mathcal{F}_u] = S_u e^{r(t-u)}. \tag{3.8}$$

To be precise, the no arbitrage relation (3.8) does not hold in the gas spot market because of limitations on trading the physical commodity and the cost of storage it (the so-called *cost of carry*). Actually, the following spot-futures relation holds

$$F_u(t) = S_u e^{(r+q-c)(t-u)},$$

where $q > 0$ represents the cost of storage in yield percentage term and $c \in \mathbb{R}$ is the so called convenience yield, namely the compensation for holding the physical asset rather than the futures.

Furthermore, as highlighted by [Benth and Sgarra, 2012], there is no way to find an expression for $\hat{\theta}$ that satisfies (3.8) when the log-price $Y_t = \ln S_t$ has a mean reverting dynamics as in (3.4). Similarly as in [Benth et al., 2003], we simply let the market choosing $\hat{\theta}$ by imposing that the futures prices implied by the model at time $u = 0$ equals the current value of the $\bar{j} \in \mathbb{N}$ futures that are currently traded in the market $\{F_0^{mkt}(t_j^*)\}_{j=1}^{\bar{j}}$ with maturities $\mathcal{T}^* = \{t_j^*\}_{j=1}^{\bar{j}}$, i.e.

$$F_0^{\boldsymbol{\theta}}(t_j^*) = F_0^{mkt}(t_j^*), \quad \forall t_j^* \in \mathcal{T}^*. \tag{3.9}$$

This approach is standard in the literature on short rate models for pricing interest rate derivatives (see e.g. [Björk, 2009]).

From the expression for the model implied futures pricing formula (see A.6 in the Appendix) we notice that the calibration of the market price of risk for regular variations $\hat{\theta}$ depends in general on the value assumed by the market price of jump risk $\tilde{\theta}$, and therefore the calibration procedure of both market prices of risk must be performed jointly. However, here we assume that $\tilde{\theta}$ has a fixed value (e.g. equal to zero), so that we can calibrate $\hat{\theta}$ separately. Notably, the procedure works as follows. Starting from the first futures maturity $t_1^\star$, we look for a constant market price of risk

$$\hat{\theta}(t) = \hat{\theta}_1, \quad t \in [0, t_1^\star],$$

that satisfies

$$F_0^{\boldsymbol{\theta}}(t_1^*) = F_0^{mkt}(t_1^*).$$

Then, we look for another constant market price of risk, $\hat{\theta}_2$, such that

$$\hat{\theta}(t) = \begin{cases} \hat{\theta}_1, & t \in [0, t_1^\star], \\ \hat{\theta}_2, & t \in (t_1^\star, t_2^\star], \end{cases}$$

by imposing that

$$\begin{aligned} F_0^{\boldsymbol{\theta}}(t_1^*) &= F_0^{mkt}(t_1^*) \\ F_0^{\boldsymbol{\theta}}(t_2^*) &= F_0^{mkt}(t_2^*). \end{aligned}$$

By proceeding recursively forward in time, we come up with a piece-wise function of time for the market price of risk

$$\hat{\theta}(t) = \begin{cases} \hat{\theta}_1, & t \in [0, t_1^\star], \\ \hat{\theta}_2, & t \in (t_1^\star, t_2^\star], \\ \quad \vdots & \\ \hat{\theta}_{\bar{n}}, & t \in (t_{n-1}^\star, t_{\bar{n}}^\star], \end{cases} \tag{3.10}$$

that satisfies

$$\begin{aligned} F_0^{\boldsymbol{\theta}}(t_1^*) &= F_0^{mkt}(t_1^*) \\ F_0^{\boldsymbol{\theta}}(t_2^*) &= F_0^{mkt}(t_2^*) \\ &\vdots \\ F_0^{\boldsymbol{\theta}}(t_{\bar{n}}^*) &= F_0^{mkt}(t_{\bar{n}}^*). \end{aligned}$$

Given the piece-wise specification and the expression of the model implied futures pricing formula (see A.6 in the Appendix) as a function of the market price of risk (3.10), the calibration procedure amounts to solve a system of linear equations, which can be accomplished in an exact way. We stress that in the general case where the market price of jump risk $\tilde{\theta}$ must be calibrated using a target function that depends on the market price of risk $\hat{\theta}$, this recursive procedure must be implemented numerically by minimizing a suitable distance between model implied and actual market futures prices.

3.2.4 Jump risk calibration

The Esscher transform (3.1) affects the pure jump process J (and the relative integral in the solution of the gas log-price) by introducing a new time dependent parameter $\tilde{\theta}$ that can be interpreted as market price of jump risk.

As highlighted e.g. by [Cont and Tankov, 2003], jump-diffusion models are able to reproduce the volatility smile that characterizes short maturity options, namely high implied volatilities for deep in/out-of-the-money options and low implied volatilities for near at-the-money ones. We recall that the volatility smile accounts for the non normality of the density of the option's underlying implied by option prices.

The liquidity of the market of options on gas futures is typically low compared to liquid options markets (stock, FX, and fixed-income markets to name a few), in that there are few liquid prices across both strike and expiry dimensions (to have a rough idea of the number of quoted options for a fixed maturity, have a look at the relative implied volatilities displayed in Figures 4.4-4.5-4.6). For this reason, despite the fact that traders prefers to relate the value of the contract to the cost of hedging, the classical approach of calibrating all the parameters of the model by minimizing the distance between quoted and model prices of options might not be as meaningful as for a liquid option market. On the other hand, the volatility smile observed for different options' maturities (see Figure 1.2b) could embed information about the market prices of jump risk.

In this section we will try to extract the information contained in options prices in order to gain some intuition about the calibration procedure of the market price of jump risk. The key concept that will be presented is a method to extract the no arbitrage density of futures prices consistent with the volatility surface observed in the market of options on futures (see Figure 1.2b).

Let us introduce the pricing function of a call option with expiry u, written on a t-maturity futures price ($u < t$) with strike price k, as

$$\begin{aligned} c(k,u) &= e^{-ru}\mathbb{E}^{\boldsymbol{\theta}}[(F_u(t)-k)^+] \\ &= e^{-ru}\int_{\ln(k/F_0(t))}^{+\infty}(F_0(t)e^z-k)p^{\boldsymbol{\theta}}_{Z_u(t)}(z)dz, \end{aligned} \tag{3.11}$$

where in the last passage we defined the true futures price by means of a suitable unobservable random factor $Z_u(t)$ as

$$F_u(t) = F_0(t)e^{Z_u(t)}.$$

We assume that $p^{\boldsymbol{\theta}}_{Z_u(t)}(\cdot)$ represents the true density of $Z_u(t)$ under the pricing measure $\mathbb{Q}^{\boldsymbol{\theta}}$.

Our proposal is to "interpolate" the true density function $p^{\boldsymbol{\theta}}_{Z_u(t)}(\cdot)$ by means of another distribution, which approximates it, in a way that is consistent with the observed volatility surface. In particular, consider the case where the true density is approximated by a finite mixture of $\bar{m} \in \mathbb{N}$ shifted kernel functions

$$p^{Ker}_{Z_u(t)}(z;\varrho) = \frac{1}{\bar{m}}\sum\nolimits_{m=1}^{\bar{m}} K_{\epsilon_m}(z-\upsilon_m) \simeq p^{\boldsymbol{\theta}}_{Z_u(t)}(z), \tag{3.12}$$

where $\varrho = (\upsilon_1, \epsilon_1, \ldots, \upsilon_{\bar{m}}, \epsilon_{\bar{m}})$ represent the vector of parameters of the kernel functions, with $\upsilon_m \in \mathbb{R}$ as location parameter of the m-th kernel and $\epsilon_m > 0$ as its width. Many kernel functions can be used to perform this task, see e.g. [Benko, 2007].

The approximate call pricing function, which depends on the choice of the kernel, then reads

$$\tilde{c}(k,u;\varrho) = \frac{1}{\bar{m}} \sum\nolimits_{m=1}^{\bar{m}} e^{-ru} \int_{\ln(k/F_0(t))}^{+\infty} (F_0(t)e^z - k) K_{\epsilon_m}(z - \upsilon_m) dz \simeq c(k,u). \tag{3.13}$$

In order to preserve the analytical tractability, we use the Gaussian kernel functions

$$K_{\epsilon_m}(z - \upsilon_m) = \frac{1}{\sqrt{2\pi}\epsilon_m} \exp\left(-\frac{(z-\upsilon_m)^2}{2\epsilon_m^2} \right), \; m = 1, \ldots, \bar{m},$$

which implies the following closed-form expression for the approximate call pricing function

$$\tilde{c}(k,u;\varrho) = \frac{1}{\bar{m}} \sum\nolimits_{m=1}^{\bar{m}} e^{-ru} \left(F_0(t) e^{\upsilon_m + \frac{\epsilon_m^2}{2}} F_{\mathcal{N}(0,1)}\left(d_1(\upsilon_m, \epsilon_m)\right) - k F_{\mathcal{N}(0,1)}\left(d_2(\upsilon_m, \epsilon_m)\right) \right), \tag{3.14}$$

where

$$\begin{aligned} d_1(\upsilon_m, \epsilon_m) &= \frac{\ln\left(F_0(t)/k\right) + (\upsilon_m + \epsilon_m^2)}{\epsilon_m}, \\ d_2(\upsilon_m, \epsilon_m) &= d_1(\upsilon_m, \epsilon_m) - \epsilon_m, \end{aligned}$$

and where $F_{\mathcal{N}(0,1)}(\cdot)$ is the cumulative distribution function of a standard normal random variable (see A.9 in the Appendix). The approximate pricing function is an average of Black-Scholes-like pricing functions [Black and Scholes, 1973], one for each element of the normal mixture density.

This modelling approach is not original per se. Actually, [Melick and Thomas, 1997] proposed a conceptually identical approach to fit the terminal distribution of oil futures prices implicit in quoted options, while [Brigo and Mercurio, 2002] generalized it to a continuous time stochastic process for derivatives pricing purpose. Nevertheless, to our knowledge this approach has never been applied to the gas option market.

Now let us assume that the market quotes $\bar{j} \in \mathbb{N}$ futures contracts with different maturities $\{F_0^{mkt}(t_j^*),\}_{j=1}^{\bar{j}}$. For each maturity, there are (let us say $\bar{\imath} \in \mathbb{N}$) options with different strike prices but the same expiry (usually one business day before the futures maturity) $\{\hat{c}(k_i, u_j^*)\}_{i=1}^{\bar{\imath}}$. The interpolated pricing density of the futures, implicit in the option quotes, can be recovered for each futures maturity t_j^*, $j = 1, \ldots, \bar{j}$, by solving for ϱ_j the following optimization problem

$$\begin{aligned} \varrho_j^* &= \text{argmin}_{\varrho_j} \sum\nolimits_{i=1}^{\bar{\imath}} \left(\frac{\tilde{c}(k_i, u_j^*; \varrho_j) - \hat{c}(k_i, u_j^*)}{\hat{c}(k_i, u_j^*)} \right)^2 \\ &\text{subject to} \begin{cases} \epsilon_m > 0, \; m = 1, \ldots, \bar{m} \\ \mathbb{E}^{\boldsymbol{\theta}}[e^{Z_{u_j^*}(t_j^*)}] = 1 \\ F_0(t_j^*) = F_0^{mkt}(t_j^*) \end{cases} . \end{aligned} \tag{3.15}$$

The optimal parameters (3.15) allows one to recover the finite set of interpolated futures prices densities $\{p^{Ker}_{Z_{u_j^*}(t_j^*)}(z;\varrho_j)\}_{j=1}^{\bar{j}}$ and the "Black 76" volatilities implied in the interpolated prices (3.14) for each maturity, that can be directly compared with the market

implied "Black 76" volatilities like the ones displayed in Figure 1.2b. The results of this fitting procedure to actual options and futures data is given in Section 4.1.2.

The described procedure allows one to use the interpolated futures price densities to fit a deterministic time dependent market price of risk parameter $\tilde{\theta}$ for each option expiry u_j^*, $j = 1, \ldots, \bar{j}$. For example, a term structure of market prices of risk for both $\hat{\theta}$ and $\tilde{\theta}$ can be obtained by a suitable moment-matching procedure, which extends the one for the calibration of $\hat{\theta}$ for a given value of $\tilde{\theta}$ presented in section 3.2.3. This approach is in principle feasible in the proposed framework, since we can obtain by Monte Carlo simulations the distribution of a futures contract using the relative pricing function (see A.6 in the Appendix). However, matching moments in a satisfactory way with just one parameter for each option expiry at out disposal can be a very challenging task.

3.3 Gas storage contract/facility payoff

Consider the set of decision dates $\mathcal{T} = \{t_n\}_{n=1}^{\bar{n}}$. We recall that $\mathcal{T}$ is also the partition (2.9) of the time interval $[0, \tau]$. At each decision date $t_n \in \mathcal{T}$ the gas storage contract has the following payoff

$$- S_{t_n} \times \Delta q_{t_n}, \tag{3.16}$$

where the gas volume change is

$$\Delta q_{t_n} = \begin{cases} \Delta q_{t_n} > 0 & \text{(injection)} \\ \Delta q_{t_n} = 0 & \text{(no action)} \\ \Delta q_{t_n} < 0 & \text{(withdrawal)} \end{cases} .$$

For each $t_n \in \mathcal{T}$, we distinguish three possible cash-flows depending on the sign of the gas volume change Δq_{t_n} (also called injection/withdrawal rate):

payoff < 0	if $\Delta q_{t_n} > 0$
payoff $= 0$	if $\Delta q_{t_n} = 0$
payoff > 0	if $\Delta q_{t_n} < 0$

The payoff (3.16) can be interpreted as the payoff of a strip of $\bar{n}$ European long/short call options written on the gas price S_t with expiries $\{t_n\}_{n=1}^{\bar{n}}$ and zero strike price, where the optionality regards the choice of the quantity of options to be bought or sold at each time t_n. Furthermore, if we make the substitution $S_{t_n} \to \max(S_{t_n} - k, 0)$ in (3.16), with $k > 0$, we can recover the payoff of a swing option written on S_t with $\bar{m} \leq \bar{n}$ exercise rights, strike k, and

$$\Delta q_{t_n} = \begin{cases} 0 & \text{no exercise} \\ -1 & \text{exercise} \end{cases} \quad \text{if } - \sum\nolimits_{k=1}^{n-1} \Delta q_{t_k} < \bar{m}, n = 1, \ldots, \bar{n}.$$

Furthermore, when $\bar{m} = 1$ we recover the payoff of a discretely monitored American call option as a special case of the swing option payoff.

Notice that for easy of explanation we assumed zero costs for injecting and withdrawing gas, zero bid-ask spread, and no penalty function in the definition of the payoff. Nevertheless, for the physical facility case the payoff (3.16) must include at least a penalty function at final time, e.g. the one suggested by [Edoli et al., 2016]

$$- c(S_{t_{\bar{n}}}) \times (\bar{q} - q_{t_{\bar{n}+1}})^+, \tag{3.17}$$

where $c(\cdot)$ is a positive valued function of the final gas price and $\bar{q} > 0$ is the amount of gas that should be contained at time $t_{\bar{n}+1}$, i.e. one period after the last time of the contract/facility life cycle. The penalty (3.17) can have a drammatic effect on the value of the gas storage facility and thus cannot be neglected. In particular, such a penalty function can cause the value to become negative.

At each time $t_n \in \mathcal{T}$ the amount of gas Δq_{t_n} to be injected or withdrawn is subject to the constraints determined by the contract or the facility. A classical constraint is a capacity constraint

$$q^l_{t_n} \leq q_{t_n} \leq q^u_{t_n},$$

where $q^u_{t_n} > 0$ and $q^l_{t_n} \geq 0$ are the maximum and the minimum amount of storable gas, and $q_{t_n} = q_0 + \sum_{k=1}^{n} \Delta q_{t_k}$ is the amount of gas stored at time t_n, which depends on the initial amount of gas $q_0 \geq 0$ and the history of injections/withdrawals from time t_0 to time t_n. Usually a storage contract (facility) has constraints on starting and ending level of gas volume to be respected by the holder of the contract (owner of the facility), and this explains why the maximum and the minimum level of gas can be time dependent. Other constraints can be imposed, e.g. a constraint on the volume of gas injected/withdrawn

$$\Delta q^l_{t_n} \leq \Delta q_{t_n} \leq \Delta q^u_{t_n},$$

where $\Delta q^u_{t_n} > 0$ and $\Delta q^l_{t_n} < 0$ are the upper and lower bounds on the volume change.

We assumed for simplicity no costs of injection/withdrawal, but in principle such costs can be function of the other variables like the gas price S_{t_n}, the size of $|\Delta q_{t_n}|$, the gas level q_{t_n}, etc. The same reasoning holds for the gas changes Δq_{t_n}, see e.g. [Edoli and Vargiolu, 2013]. For example, in the physical storage case injecting gas can be subject to a cost $c_1 > 0$ that is proportional to $S_{t_n} \times \Delta q_{t_n}$, thus changing the payoff (3.16) as

$$\begin{array}{rl} -S_{t_n} \times \Delta q_{t_n} & \text{if} \quad \Delta q_{t_n} \leq 0 \\ -S_{t_n} \times \Delta q_{t_n} \times (1 + c_1) & \text{if} \quad \Delta q_{t_n} > 0. \end{array}$$

Furthermore, the volume change can depend on the physics of gases, an for this reason it can be subject to the following physical constraints

$$\begin{aligned} \Delta q^l_{t_n} &= -k_1 \times \sqrt{q_{t_n}} \\ \Delta q^u_{t_n} &= k_2 \times \sqrt{\frac{1}{q_{t_n} + q_b} + k_3}, \end{aligned}$$

where $k_1, k_2, k_3, q_b > 0$ are suitable constants, see [Edoli et al., 2016].

Given the premises, as in [Edoli and Vargiolu, 2013] for each time $t_n \in \mathcal{T}$ we can define the space of admissible volume changes as

$$\begin{aligned} \mathcal{A}(t_n, q_{t_n}, [q^l_{t_{\bar{n}+1}}, q^u_{t_{\bar{n}+1}}]) = \big\{ & \Delta q_{t_n} \in [\Delta q^l_{t_n}, \Delta q^u_{t_n}] : \\ & q_{t_n} + \Delta q_{t_n} \in [r_{\min}(t_n, q^l_{t_{\bar{n}+1}}), r_{\max}(t_n, q^u_{t_{\bar{n}+1}})] \cap [q^l_{t_n}, q^u_{t_n}] \big\}, \end{aligned}$$

where

$$\begin{aligned} r_{\min}(t_n, q^l_{t_{\bar{n}+1}}) &= \max\{\Delta q^l_{t_n} n,\, q^l_{t_{\bar{n}+1}} - \Delta q^u_{t_n}(\bar{n} - n)\}; \\ r_{\max}(t_n, q^u_{t_{\bar{n}+1}}) &= \min\{\Delta q^u_{t_n} n,\, q^u_{t_{\bar{n}+1}} - \Delta q^l_{t_n}(\bar{n} - n)\}. \end{aligned}$$

Clearly, if at time t_n the level of gas is below $q^l_{t_{\bar{n}+1}} - \Delta q^u_{t_n}(\bar{n}-n)$, then it would not be possible to inject enough gas up to time $t_{\bar{n}}$ in order to reach $q^l_{t_{\bar{n}+1}}$, as well as at time t_n one cannot have withdrawn more than $\Delta q^l_{t_n} n$. Conversely, if at time t_n the level of gas is above $q^u_{t_{\bar{n}+1}} - \Delta q^l_{t_n}(\bar{n}-n)$, then it would not be possible to withdraw enough gas up to time $t_{\bar{n}}$ in order to reach $q^u_{t_{\bar{n}}+1}$, as well as at time t_n one cannot have injected more than $\Delta q^u_{t_n} n$. Furthermore, in the gas storage contract case one must also enforce the constraint that $q_{t_n} + \Delta q_{t_n} \in [q^l_{t_n}, q^u_{t_n}]$ for each $n = 1, \dots, \bar{n}+1$, since one cannot withdraw if the storage is empty and cannot inject if the storage is full.

3.4 Dynamic programming algorithm

Computing the value of a gas storage contract/facility amounts to maximize the expected present value of the intertemporal cash-flows

$$g(t_n, Y_{t_n}, \Delta q_{t_n}) = -e^{Y_{t_n}} \cdot \Delta q_{t_n} \tag{3.18}$$

under the pricing measure $\mathbb{Q}^{\boldsymbol{\theta}}$ with respect to the admissible control policies $\Delta q = \{\Delta q_{t_n}\}_{n=1}^{\bar{n}} \in \mathcal{A}$, i.e.

$$v(t_0, y_0, c_0, q_0) = \sup_{\Delta q \in \mathcal{A}} \sum_{n=0}^{\bar{n}-1} \mathbb{E}^{\boldsymbol{\theta}}[e^{-rt_{n+1}} g(t_{n+1}, Y_{t_{n+1}}, \Delta q_{t_{n+1}}) + e^{-rt_{\bar{n}}} p(Y_{t_{\bar{n}}}, q_{t_{\bar{n}+1}})], \tag{3.19}$$

where the penalty function $p(\cdot,\cdot)$ is defined in (3.17) and the space of admissible controls is defined as

$$\mathcal{A} = \{\{\Delta q_{t_n}\}_{n=1}^{\bar{n}} \ \mathbb{F}\text{-adapted and s.t. } \Delta q_{t_n} \in \mathcal{A}(t_n, q_{t_n}, [q^l_{t_{\bar{n}+1}}, q^u_{t_{\bar{n}+1}}]) \cap [q^l_{t_n}, q^u_{t_n}]\}.$$

This maximization problem can be solved by dynamic programming (see e.g. [Bertsekas et al., 1995], [Bertsekas and Shreve, 1978]). Indeed, we define for each $t_n \in \mathcal{T}$ the deterministic function

$$\begin{aligned} v(t_n, y_n, c_n, q_n) \;=\; & \sup_{\Delta q_{t_n} \in \mathcal{A}(t_n, q_{t_n}, [q^l_{t_{\bar{n}+1}}, q^u_{t_{\bar{n}+1}}])} g(t_n, y_n, \Delta q_{t_n}) 1_{\{t_n > t_0\}}(t_n) \\ & + p(y_{\bar{n}}, q_{t_{\bar{n}}} + \Delta q_{t_{\bar{n}}}) 1_{\{t_{\bar{n}}\}}(t_n) + e^{-r(t_{n+1}-t_n)} f(t_n, y_n, c_n, q_n + \Delta q_{t_n}) 1_{\{t_n < t_{\bar{n}}\}}(t_n), \end{aligned} \tag{3.20}$$

where

$$f(t_n, y_n, c_n, q_n + \Delta q_{t_n}) \;=\; \mathbb{E}^{\boldsymbol{\theta}}[v(t_{n+1}, Y_{t_{n+1}}, T_{t_{n+1}}, q_n + \Delta q_{t_n}) | Y_{t_n} = y_n, T_{t_n} = c_n] \tag{3.21}$$

$$p(y_{\bar{n}}, q_{t_{\bar{n}}} + \Delta q_{t_{\bar{n}}}) \;=\; -c(e^{y_{\bar{n}}}) \times (\bar{q} - q_{t_{\bar{n}}} - \Delta q_{t_{\bar{n}}})^+. \tag{3.22}$$

Then, as proved in [Edoli and Vargiolu, 2013]:

- the functions (3.20)-(3.21)-(3.22) are such that $v(t_0, y_0, c_0, q_0)$ coincides with the value of the gas storage contract (3.19);
- there exists an optimal Markovian policy $\Delta q^* = \{\Delta q^*_{t_n} = \mathfrak{a}(t_n, y_n, c_n, q_n)\}_{n=1}^{\bar{n}}$, where $\mathfrak{a}(\cdot,\cdot,\cdot,\cdot)$ is obtained by the dynamic programming equation (3.20);

- given the specification of the payoff (3.18), the optimal policy $\Delta q^*_{t_n}$ is of bang-bang type for each $t_n \in \mathcal{T}$, meaning that given the constraints on the maximum and minimum volume change, it can takes on values zero, maximum ($\Delta q^u_{t_n}$) or minimum ($\Delta q^l_{t_n}$) only, and therefore the admissible payoff simplifies as:

$$\boxed{\begin{array}{lll} g(t_n, Y_{t_n}, \Delta q_{t_n}) < 0 & \text{if } \Delta q_{t_n} = \Delta q^u_{t_n} & \text{(injection)} \\ g(t_n, Y_{t_n}, \Delta q_{t_n}) = 0 & \text{if } \Delta q_{t_n} = 0 & \text{(no action)} \\ g(t_n, Y_{t_n}, \Delta q_{t_n}) > 0 & \text{if } \Delta q_{t_n} = \Delta q^l_{t_n} & \text{(withdrawal)} \end{array}} \tag{3.23}$$

We observe that at final time $t_{\bar{n}}$ the solution of the problem is trivial, since it is always convenient to withdraw the maximum amount of gas that we are allowed to do, namely $|\Delta q^l_{t_n}|$ or zero. For the other times $t_n \in \mathcal{T}$, the action Δq_{t_n} taken at time t_n influences the expectation (3.21), e.g. withdrawing gas at time t_n at a price S_{t_n} results in a positive cash-flow $g(t_n, Y_n, \Delta q_{t_n}) > 0$, but given the constraints in $\mathcal{A}$ it negatively affects the possibility of withdrawing gas at times $\{t_m\}_{m=n+1}^{\bar{n}}$ if $S_{t_m} > S_{t_n}$ for $n < m \leq \bar{n}$.

3.5 A FFT-based implementation of the dynamic programming algorithm

To our knowledge there is no closed-form expression for the value function satisfying the dynamic programming equations (3.20)-(3.21)-(3.22), and a numerical approximation technique must be used in order to obtain the value of the storage contract $v(t_0, y_0, c_0, q_0)$ under the presented framework.

A variety of different numerical methods have been proposed to compute the continuation value of a dynamic programming algorithm for pricing gas storage contracts. [Bäuerle and Riess, 2016], [Bjerksund et al., 2008], [Boogert and De Jong, 2008] and [Carmona and Ludkovski, 2010] among others employed the Least Square Monte Carlo method pioneered by [Longstaff and Schwartz, 2001] to price the continuation value of an American option. [Bäuerle and Riess, 2016], [Edoli and Vargiolu, 2013] and [Felix and Weber, 2012] discretize the dynamics of the underlying processes by using recombining trees. [Chen and Forsyth, 2007] and [Thompson et al., 2009] formulate the problem as a stochastic optimal control in continuous time and then compute the gas storage value by discretization of the relative partial integro differential equation.

Here we take a FFT-based approach as in [Kiely et al., 2015], which in turns is conceptually equivalent to the approach that [Jaimungal and Surkov, 2011] proposed for pricing Bermudan-style derivatives in a mean reverting Levy framework. This approach relies on the knowledge of the closed form expression for the $\mathcal{F}_{t_n}$-conditional characteristic functions of both the log-gas price process under $\mathbb{Q}^{\boldsymbol{\theta}}$ (3.5) and the temperature process (2.8) at time t_{n+1} for each $n = 0, \ldots, \bar{n} - 1$. For each time $t_n \in \mathcal{T}$, and setting for easy of notation $\Delta t = t_{n+1} - t_n$, we can compute the conditional expectation (3.21) as

$$\begin{aligned} f(t_n, y_n, c_n, q_{n+1}) &= \frac{1}{2\pi} \int_{i\tau-\infty}^{i\tau+\infty} e^{-i\varpi c_n} \mathfrak{F}[v_T(ze^{-a\Delta t}; t_{n+1}, y_n, c_n, q_{n+1})](\varpi) \times \\ &\quad \phi_{T_{t_{n+1}}|\mathcal{F}_{t_n}}(-\varpi e^{a\Delta t}; 0) d\varpi,\ \varpi = l + i\tau,\ l, \tau \in \mathbb{R}, \end{aligned} \tag{3.24}$$

where

$$v_T(z;t_{n+1},y_n,c_n,q_{n+1}) = \frac{1}{2\pi}\int_{i\xi-\infty}^{i\xi+\infty} e^{-i\omega y_n}\mathfrak{F}[v(t_{n+1},ue^{-\kappa\Delta t},z,q_{n+1})](\omega)\times \phi^{\boldsymbol{\theta}}_{Y_{t_{n+1}}|\mathcal{F}_{t_n}}(-\omega e^{\kappa\Delta t};0,c_n)d\omega,\ \omega=d+i\xi,\ \xi,d\in\mathbb{R}, \quad (3.25)$$

and $\mathfrak{F}[g]:\mathbb{C}\to\mathbb{C}$ is the complex Fourier transform of the integrable function $g:\mathbb{R}\to\mathbb{R}$

$$\mathfrak{F}[g](\omega)=\int_{-\infty}^{+\infty} e^{i\omega x}g(x)dx,\ \omega\in\mathbb{C},$$

(see Appendix A.7).

The two integrals (3.24)-(3.25) are discretized and implemented by a FFT-based algorithm, similar to the CONV algorithm for Bermudan options proposed by [Lord et al., 2008]. To be precise, for each $t_n\in\mathcal{T}$ we first truncate the range of $(Y_{t_{n+1}},T_{t_{n+1}})$ to $[-r_Y/2,r_Y/2]\times[-r_T/2,r_T/2]\subset\mathbb{R}^2$, for a suitable choice of the constants $r_Y>0$ and $r_T>0$, and the real part of the complex Fourier domain to $[-\bar{k}\pi/r_Y,(\bar{k}-2)\pi/r_Y]\times[-\bar{k}\pi/r_T,(\bar{k}-2)\pi/r_T]\subset\mathbb{R}^2$, and then we discretize the truncated domains by the uniform $\bar{k}-$points grids

$$\{\tilde{y}_m=\tilde{y}_0+m\Delta y\}_{m=0}^{\bar{k}-1},\quad \{\tilde{l}_h=\tilde{l}_0+h\Delta\varpi\}_{h=0}^{\bar{k}-1} \quad (3.26)$$

$$\{\tilde{c}_p=\tilde{c}_0+p\Delta c\}_{p=0}^{\bar{k}-1},\quad \{\tilde{d}_h=\tilde{d}_0+h\Delta\omega\}_{h=0}^{\bar{k}-1}, \quad (3.27)$$

choosing the number of points as $\bar{k}=2^{\tilde{n}}$, where $\tilde{n}$ is a sufficiently large positive integer, $\tilde{y}_0=-r_Y/2$, $\tilde{c}_0=-r_T/2$, $\tilde{l}_0=-\bar{k}\pi/r_Y$, $\tilde{d}_0=-\bar{k}\pi/r_T$, and the step size of the grids satisfies the Nyquist relation

$$\Delta y\cdot\Delta\omega=\Delta c\cdot\Delta\varpi=\frac{2\pi}{\bar{k}}. \quad (3.28)$$

Then the integrals (3.24)-(3.25) can be approximated by the finite sums

$$\tilde{f}(t_n,\tilde{y}_m,\tilde{c}_p,q_{n+1}) = \frac{(-)^p e^{\tau p\Delta c}}{\bar{k}}\sum_{h=0}^{\bar{k}-1} e^{-i2\pi hm/\bar{k}}\left(\phi_{T_{t_{n+1}}|\mathcal{F}_{t_n}}(-e^{a\Delta t}(\tilde{l}_0+i\tau+h\Delta\varpi);0)\right) \times\sum_{j=0}^{\bar{k}-1} e^{i2\pi hj/\bar{k}}\left((-)^j e^{-\tau j\Delta c}\ \tilde{v}_T^{int}(e^{-a\Delta t}\tilde{c}_j;\tilde{y}_m,\tilde{c}_p,q_{n+1})w_j\right) \quad (3.29)$$

and

$$\tilde{v}_T(\tilde{c}_j;t_{n+1},\tilde{y}_m,\tilde{c}_p,q_{n+1}) = \frac{(-)^m e^{\xi m\Delta y}}{\bar{k}}\sum_{h=0}^{\bar{k}-1} e^{-i2\pi hm/\bar{k}}\left(\phi^{\boldsymbol{\theta}}_{Y_{t_{n+1}}|\mathcal{F}_{t_n}}(-e^{\kappa\Delta t}(\tilde{d}_0+i\xi+h\Delta\omega);0,\tilde{c}_p)\right) \times\sum_{k=0}^{\bar{k}-1} e^{i2\pi hk/\bar{k}}\left((-)^k e^{-\xi k\Delta y}\tilde{v}^{int}(t_n,e^{-\kappa\Delta t}\tilde{y}_k,\tilde{c}_j,q_{n+1})\ w_k\right), \quad (3.30)$$

where $\{\tilde{v}_T^{int}(e^{-a\Delta t}\tilde{c}_j;\tilde{y}_m,\tilde{c}_p,q_{n+1})\}_{j=0}^{\bar{k}-1}$ and $\{\tilde{v}^{int}(e^{-\kappa\Delta t}\tilde{y}_k,\tilde{c}_j,q_{n+1})\}_{k=0}^{\bar{k}-1}$ are obtained by interpolating $\{\tilde{v}_T(\tilde{c}_j;\tilde{y}_m,\tilde{c}_p,q_{n+1})\}_{j=0}^{\bar{k}-1}$ and $\{\tilde{v}(t_n,\tilde{y}_k,\tilde{c}_j,q_{n+1})\}_{k=0}^{\bar{k}-1}$ on the rescaled grids

$$\{e^{-\kappa\Delta t}\tilde{y}_m\}_{m=0}^{\bar{k}-1} \quad (3.31)$$

$$\{e^{-a\Delta t}\tilde{c}_p\}_{p=0}^{\bar{k}-1}. \quad (3.32)$$

The summations in (3.29)-(3.30) can be computed using the Fast Fourier Transform (FFT) algorithm and its inverse (IFFT) proposed by [Cooley and Tukey, 1965]. Both (3.30) and (3.29) are generalizations of the CONV method developed by [Lord et al., 2008] for pricing Bermudan options in a Levy process framework, as previously acknowledged by [Kiely et al., 2015], who developed similar formulas for Lévy-driven mean reverting processes with closed-form characteristic function.

In order to implement in practice the dynamic programming algorithm (3.20)-(3.21)-(3.22), for each $t_n \in \mathcal{T}$ we transform the continuous range of the gas volume q_n into a discrete grid of $\bar{r} \in \mathbb{N}$ levels of gas volume

$$\{\tilde{q}_n^r\}_{r=1}^{\bar{r}}, \text{ such that } \tilde{q}_n^{r+1} > \tilde{q}_n^r,\ r = 1, \dots, \bar{r} - 1,$$

and then for each $r = 1, \dots, \bar{r}$ we maximize with respect to the admissible action $\Delta q_{t_n} \in \mathcal{A}(t_n, \tilde{q}_n^r, [q_{\bar{n}+1}^l, q_{\bar{n}+1}^u])$, thus obtaining another discrete grid of optimal levels of gas volume

$$\{\tilde{q}_{n+1}^{r;*} = \tilde{q}_n^r + \Delta q_{t_n}^*\},\ r = 1, \dots, \bar{r} - 1.$$

It follows that the computation of the summations (3.29)-(3.30) must be repeated for each admissible level of gas volume $\tilde{q}_n^l$ and each admissible control $\Delta q_{t_n} \in \mathcal{A}(t_n, \tilde{q}_n^r, [q_{\bar{n}+1}^l, q_{\bar{n}+1}^u])$.

Here we present a sketch of the dynamic programming algorithm:

1. Set $n \to \bar{n}$;
2. For $k, j = 0, \dots, \bar{k} - 1$, $r = 0, \dots, \bar{r} - 1$, compute the discretized value function
$$\tilde{v}(t_n, \tilde{y}_k, \tilde{c}_j, \tilde{q}_{\bar{n}}^r + \Delta q_{t_{\bar{n}}}^*); \tag{3.33}$$
3. Set $n \to n - 1$;
4. For $k, j = 0, \dots, \bar{k} - 1$, $r = 0, \dots, \bar{r} - 1$, interpolate the value function computed at time t_{n+1} on the re-scaled grid (3.31) and compute
$$(-)^k e^{-\xi k \Delta y} \tilde{v}^{int}(t_n, e^{-\kappa \Delta t} \tilde{y}_k, \tilde{c}_j, \tilde{q}_{\bar{n}}^r + \Delta q_{t_n}); \tag{3.34}$$
5. Using the $\mathcal{F}_{t_n}$-conditional characteristic function of $Y_{t_{n+1}}$, compute for $h, p = 0, \dots, \bar{k} - 1$
$$\phi^{\boldsymbol{\theta}}_{Y_{t_{n+1}}|\mathcal{F}_{t_n}}(-(\tilde{d}_0 + i\xi + h\Delta\omega)e^{\kappa\Delta t}; 0, \tilde{c}_p); \tag{3.35}$$
6. Compute (3.30) by first computing the FFT of (3.34), and then by computing the IFFT of the convolution between (3.35) and the previously computed FFT, thus getting for $m, j, p = 0, \dots, \bar{k} - 1$, $r = 0, \dots, \bar{r} - 1$
$$\tilde{v}_T(\tilde{c}_j; t_{n+1}, \tilde{y}_m, \tilde{c}_p, \tilde{q}_{\bar{n}}^r + \Delta q_{t_n}); \tag{3.36}$$
7. For $m, j, p = 0, \dots, \bar{k} - 1$, $r = 0, \dots, \bar{r} - 1$ interpolate (3.36) on the re-scaled grid (3.32) in order to obtain
$$(-)^j e^{-\tau j \Delta c} \tilde{v}_T^{int}(e^{-a\Delta t}\tilde{c}_j; \tilde{y}_m, \tilde{c}_p, \tilde{q}_{\bar{n}}^r + \Delta q_{t_n}); \tag{3.37}$$
8. Using the $\mathcal{F}_{t_n}$-conditional characteristic function (2.12) of $T_{t_{n+1}}$, compute for $h = 0, \dots, \bar{k} - 1$
$$\phi_{T_{t_{n+1}}|\mathcal{F}_{t_n}}(-e^{a\Delta t}(\tilde{l}_0 + i\tau + h\Delta\varpi); 0); \tag{3.38}$$

9. Compute (3.29) by first computing the FFT of (3.37), and then by computing the IFFT of the convolution between (3.38) and the previously computed FFT, thus getting for $m, p = 0, \dots, \bar{k} - 1$, $r = 0, \dots, \bar{r} - 1$

$$\tilde{f}(t_n, \tilde{y}_m, \tilde{c}_p, \tilde{q}^r_{n+1}); \tag{3.39}$$

10. if $n \neq 0$

    - For $m, p = 0, \dots, \bar{k} - 1$, $r = 0, \dots, \bar{r} - 1$, optimize with respect to Δq_{t_n} to obtain the discretized value function

    $$\tilde{v}(t_n, \tilde{y}_m, \tilde{c}_p, \tilde{q}^r_n + \Delta q_{t_n}) = g(t_n, \tilde{y}_m, \Delta q^*_{t_n}) 1_{\{t_n > t_0\}} + e^{-r\Delta t} \tilde{f}(t_n, \tilde{y}_m, \tilde{c}_p, \tilde{q}^r_{\bar{n}} + \Delta q^*_{t_n}).$$

    otherwise

    - For $m, p = 0, \dots, \bar{k}-1$, $r = 0, \dots, \bar{r}-1$, compute the discretized value function

    $$\tilde{v}(t_n, \tilde{y}_m, \tilde{c}_p, \tilde{q}^r_{n+1}) = e^{-r\Delta t} \tilde{f}(t_n, \tilde{y}_m, \tilde{c}_p, \tilde{q}^r_{\bar{n}+1}).$$

11. If $n = 0$ stop, otherwise go to Step 3.

The algorithm turns out to be quite efficient for the computation of the continuation value. Indeed, for each $n = 1, \dots, \bar{n}$, steps 6-9 costs $O\left(\bar{k} \log_2\left(\bar{k}\right)\right)$ operations each one. The use of a two-dimensional FFT approach would have required to perform the same computations an overall cost of $O\left(\bar{k}^2 \log_2\left(\bar{k}^2\right)\right)$ operations for each $n = 1, \dots, \bar{n}$, resulting in a less efficient algorithm.

An alternative simulation-based approach to the above algorithm is the following:

1. Simulate $\bar{s} \in \mathbb{N}$ paths of the temperature process (2.8);
2. Conditioning on each path, compute the continuation value by means of a one-dimensional FFT approach, adapting the algorithm proposed by [Kiely et al., 2015] to an Ornstein-Uhlenbeck process driven by a non-homogeneous Lévy process;
3. Obtain the value of the contract by averaging over the simulated paths.

However, this approach is suboptimal from a computational point of view, since it would cost $O(\bar{k} \log_2\left(\bar{k}\right))$ operations for each $n = 1, \dots, \bar{n}$ to compute one price along one simulated path, with $\bar{s} \gg 0$ in order to guarantee the same precision of the presented algorithm based on the FFT.

An error analysis for the computation of the expectations in steps 6-9 and the grid interpolation is provided in [Lord et al., 2008] and [Kiely et al., 2015] respectively.

We finally remark that the grids for the discretization of the support of gas log-price and temperature distribution do not need to have the same size, i.e. if $\bar{k}^Y$ is the size for the gas log-price grid and $\bar{k}^T$ the one for the temperature grid, we can set $\bar{k}^Y \neq \bar{k}^T$. This would not be possible when using the two-dimensional FFT algorithm.

Chapter 4

Numerical results

Here we present the numerical results of the calibration procedures and a toy example of pricing of a gas storage contract.

4.1 Calibration and simulation study

In this section we show the numerical outputs of the calibration procedure and an illustrative simulation study.

4.1.1 Maximum Likelihood Estimation

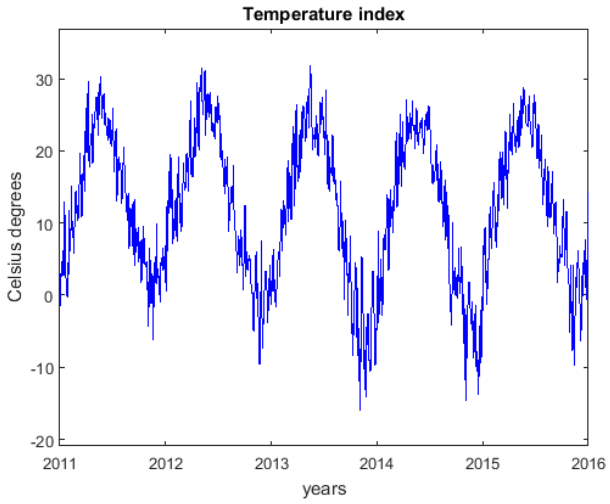

(a)

Figure 4.1: time series of the arithmetic average of the mean daily temperatures recorded in New York and Chicago over the period March 2, 2011 - March 9, 2016; (source: academic.udayton.edu/kissock/http/Weather/citylistUS.htm.).

We estimate the parameters of the gas log-price and the temperature index using the daily observations of the HH spot price and the temperature recorded in New York and Chicago during the period March 2, 2011 - March 9, 2016. The temperature index is obtained as the arithmetic average of the temperatures recorded in New York and Chicago (see Figure 4.1). The data of the HH spot price is provided by Bloomberg,

while the data of the temperatures can be freely downloaded from the website academic.udayton.edu/kissock/http/Weather/citylistUS.htm..

The estimation procedure is divided into two steps. In the first step, we estimate *separately* the parameters of gas and the temperature process by maximizing the likelihood of the marginal processes; in the last step, we use the outputs of the first step as a starting point of the true MLE, that is implemented using the joint likelihood function (2.14).

As for the calibration of the time dependent drift function (2.7) of the temperature, we use the Matlab function `nlinfit` as suggested by [Benth and Koekebakker, 2008]. Furthermore, in order to avoid overfitting, we arbitrarily choose to set the temperature thresholds of the intensity process (2.10) as $\alpha^1 = 5$ and $\alpha^2 = 20$, $\lambda^1 = \lambda^3 = 0$, $\vartheta = 2\pi$. We stress that all such parameters can be obtained by MLE as well. Finally, the initial values for the HH gas price and temperature index are respectively $s_0 = 1.3312$ and $c_0 = 2.7778$.

Gas price estimated parameters							
κ	μ	σ	ς	η_+	η_-	λ^2	λ^4
1.5848	1.1253	0.2463	0.3482	13.3250	19.4945	14.6199	0.4221

Table 4.1: MLE parameters of the gas price process, obtained using the time series of daily observations of the HH gas price and the temperature index, built as the arithmetic average of temperatures measured in New York and Chicago, over the period March 2, 2011 - March 9, 2016; data for the HH gas price provided by Bloomberg; data for the temperature provided by the website academic.udayton.edu/kissock/http/Weather/citylistUS.htm.

The estimated parameters of the gas price process are reported in Table 4.1, which we can use to write explicitly the calibrated $\mathbb{P}$-dynamics

$$\begin{aligned} dY_t &= 1.5848 \times (1.1253 - Y_t)dt + 0.2463 \times dB_t + dJ_t,\ Y_0 = \ln 1.3312 \\ p_G(y) &= 0.3482 \times 13.3250\ e^{-13.3250\ y}\ 1_{\{y>0\}}(y) + 0.6518 \times 19.4945\ e^{-19.4945\ |y|}\ 1_{\{y<0\}}(y) \\ \lambda_t &= 14.6199 \times (5 - h(t, T_{t_n}))^+ \times 1_{\mathbb{H}}(t) + 0.4221 \times (h(t, T_{t_n}) - 20)^+) \times 1_{\mathbb{C}}(t). \end{aligned}$$

As expected from the graphical inspection of the gas log-price time series, the mean reversion speed parameter $\kappa = 1.5848$ is not large. Notice also that $\lambda^2 = 14.6199 \gg \lambda^1 = 0.4221$, which highlights the different influence of large temperature deviations during winter and summer period, and seems to be consistent with the historical pattern displayed in Figure 1.5: large deviations of the temperature do not cause spikes in the HH gas price during the summer.

Temperature index estimated parameters					
a	η	δ	β	γ	ϱ
88.2588	52.6069	12.8014	-0.2856	-13.1280	-198.8193

Table 4.2: MLE parameters of the temperature index obtained using the time series of daily observations of the HH gas price and the temperature index, built as the arithmetic average of temperatures measured in New York and Chicago, over the period March 2, 2011 - March 9, 2016; data provided by the website academic.udayton.edu/kissock/http/Weather/citylistUS.htm; the parameters of the time dependent drift of the temperature are obtained using the Matlab function `nlinfit`.

The estimated parameters of the temperature index are displayed in Table 4.2, and the calibrate $\mathbb{P}$-dynamics is

$$\begin{aligned} dT_t &= \left(\frac{dT_t^m}{dt} + 88.2588 \times (T_t^m - T_t)\right) dt + 52.6069 \times d\check{B}_t,\ T_0 = 2.7778 \\ T_t^m &= 12.8014 - 0.2856 \times t - 13.1280 \times \sin(2\pi t - 198.8193). \end{aligned}$$

Beyond the typical strong seasonal effect, we notice that the inclusion of the temperature recorded in Chicago has a negative effect on the long term constant mean level $\delta = 12.8014$, which is quite low, and also on the linear drift parameter $\beta = -0.2856$, which is negative but negligible in the short run. According to the literature on temperature modelling the linear drift coefficient should account for the "global warming/urban heating effect" (see e.g. [Alaton et al., 2002]), and thus its value should be positive. However, since we used only five years of data to estimate the temperature parameters, we prefer to set it to zero when it comes to pricing.

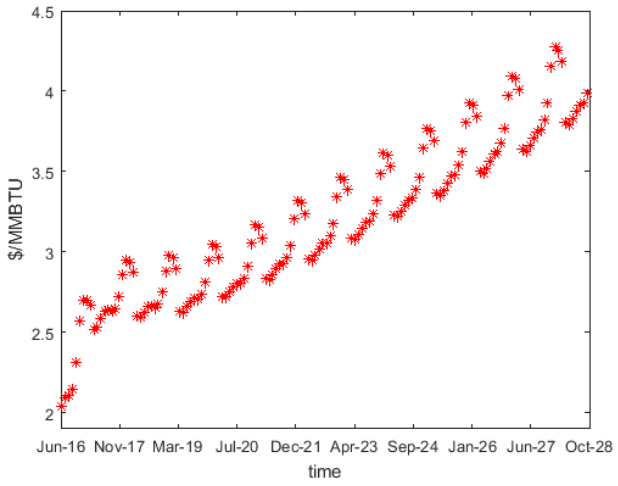

Figure 4.2: term structure of futures prices quoted on March 9, 2016.

4.1.2 Market price of risk calibration

The calibration of the market price of risk (see Section 3.2.2) forces the initial model-implied futures prices to perfectly fit the term structure of futures prices, which is displayed in Figure 4.2.

In Figure 4.3a we compare the calibrated piece-wise term structure of market prices of risk and the term structure of futures prices (see Table 4.3) of the first 13 maturities available as of March 9, 2016. The latter inherit the seasonality in the futures market. In Figure 4.3b, instead, we compare the calibrated piece-wise term structure of market prices of risk and the term structure of market risk premia $F_0^{mkt}(t) - \mathbb{E}[S_t]$ (see Table 4.3). We notice that depending on market conditions both term structures can become negative.

To our knowledge, the calibration of the market price of jump risk is a problem that has not yet been addressed in a satisfactory way in the literature of commodity modelling, and especially in the literature on natural gas. An heuristic analysis is provided for the electricity market by [Benth and Sgarra, 2012].

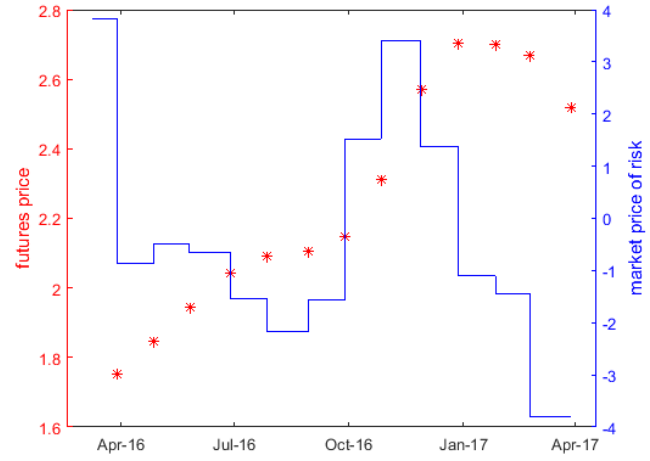

(a)

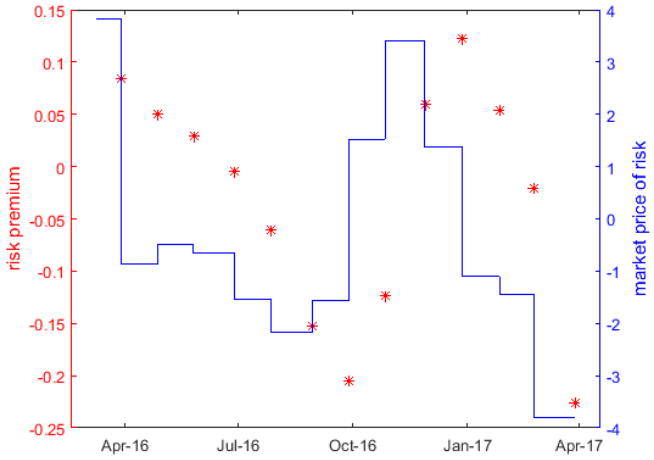

(b)

Figure 4.3: term structure of market futures prices quoted on March 9, 2016 (red stars) and relative market prices of risk (blue line) (4.3a); term structure of market risk premia quoted on March 9, 2016 (red stars) and relative market prices of risk (blue line) (4.3b).

In Figures 4.4-4.5-4.6-4.7 we graphically show the results of the interpolation procedure of the terminal density of the futures prices implicit in the quoted option prices. Since we chose to interpolate the true density with a mixture of two normal distributions ($\bar{m} = 2$ in (3.12)), we have fitted four different parameters for each of the thirteen futures maturity considered, see Table 4.5. By means of this procedure we can first observe that the terminal distribution of futures prices implicit in the quoted option prices is far from being normal for all the expiries considered, see Table 4.4. This empirical fact is in principle consistent with our pricing formula for futures (see A.6 in the Appendix). Whether the model-implied futures distribution can *in practice* match the market-implied one or not is questionable. In principle, by assuming a piece-wise constant market price of jump risk for each option expiry, we can try to calibrate it by matching the model-implied moments with the empirical ones displayed in Table 4.4, thus obtaining a term structure of market prices of risk, similarly to the one displayed in Figures 4.3a-4.3b.

Maturity (t=days)	$F_0^{mkt}(t)$	$F_0^{mkt}(t) - \mathbb{E}[S_t]$	$\hat{\theta}$
20	1.7520	0.0845	3.8211
49	1.8460	0.0505	−0.8619
78	1.9460	0.0298	−0.4895
111	2.0410	−0.0046	−0.6553
140	2.0910	−0.0607	−1.5455
173	2.1060	−0.2046	−2.1731
203	2.1470	−0.1238	−1.5611
232	2.3110	0.0597	1.5249
264	2.5720	0.1231	3.4169
294	2.7030	0.0533	1.3687
324	2.7000	0.0533	−1.1040
352	2.6700	−0.0213	−1.4388
385	2.5170	−0.2257	−3.8059

Table 4.3: calibrated market prices of risk on March 9, 2016.

However, since the distribution of the model-implied futures price distribution can be recovered only numerically through Monte Carlo simulations, this approach turns out to be computationally burdensome. For this reason, we do not perform any calibration procedure, and set the market price of jump risks $\tilde{\theta}$ equal to zero for all options maturities in order to price the storage contract.

Expiry (days)	Std dev.	Skewness	Kurtosis
19	0.1359	−0.1985	3.7815
48	0.1908	−0.2190	3.7076
77	0.2198	−0.2525	3.6225
110	0.2425	−0.3652	3.7840
139	0.2591	−0.2691	3.6065
170	0.2819	−0.3141	3.7585
202	0.3017	−0.3104	3.8869
231	0.3193	−0.3956	4.2950
261	0.3316	−0.2353	4.4411
293	0.3692	−0.1569	4.7586
323	0.4074	−0.2691	4.9061
351	0.4298	−0.2630	4.9447

Table 4.4: moments of the interpolated terminal distribution of futures prices consistent with the implied volatilities of quoted options on March 9, 2016.

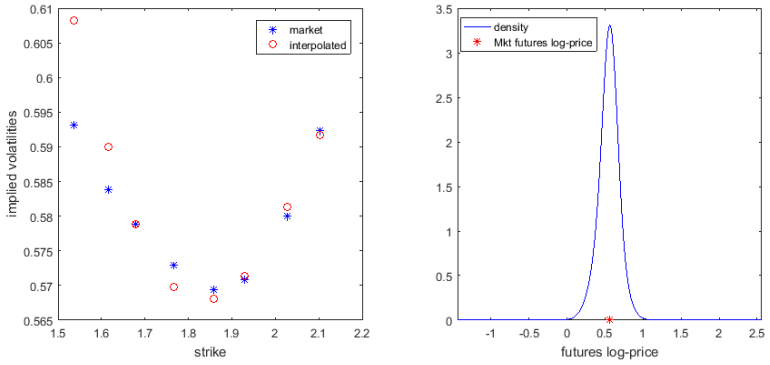

(a)

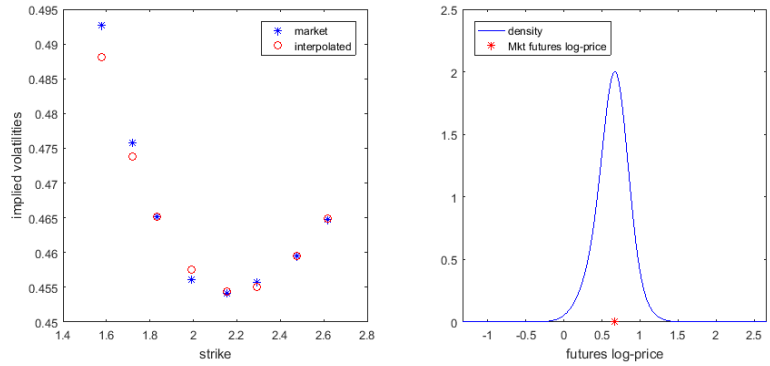

(b)

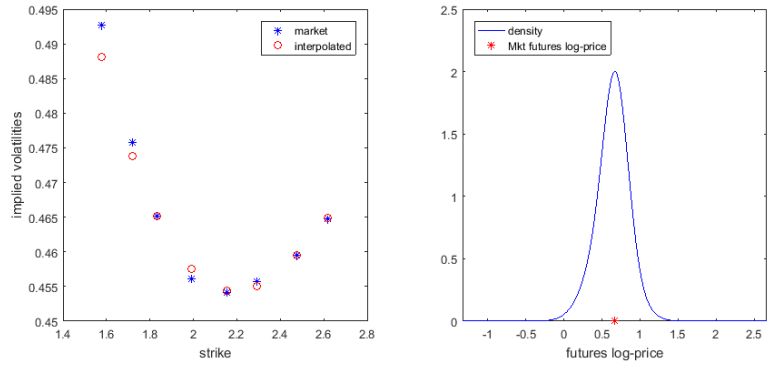

(c)

Figure 4.4: market versus interpolated implied volatilities for expiries 19 (a), 48 (b), 77 (c) days (left plots); interpolated terminal density function of futures prices consistent with the interpolated implied volatilities for expiries.

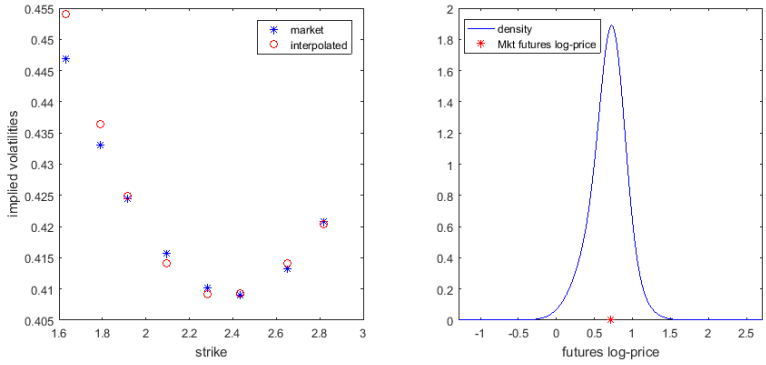

(a)

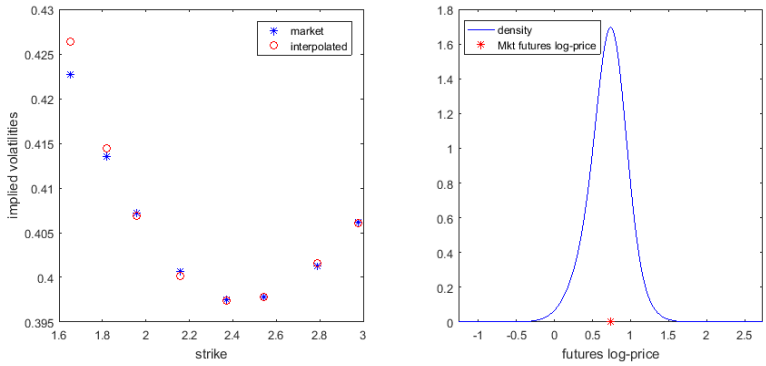

(b)

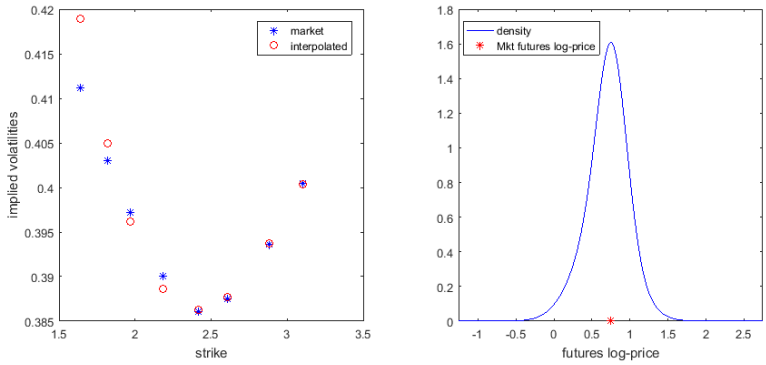

(c)

Figure 4.5: market versus interpolated implied volatilities for expiries 110 (a), 139 (b), 170 (c) days (left plots); interpolated terminal density function of futures prices consistent with the interpolated implied volatilities for expiries.

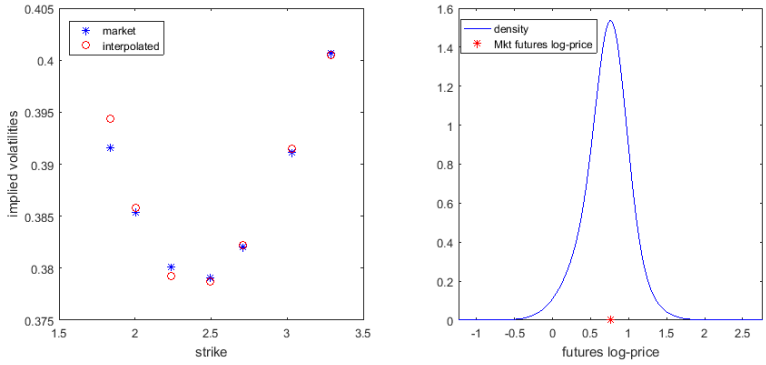

(a)

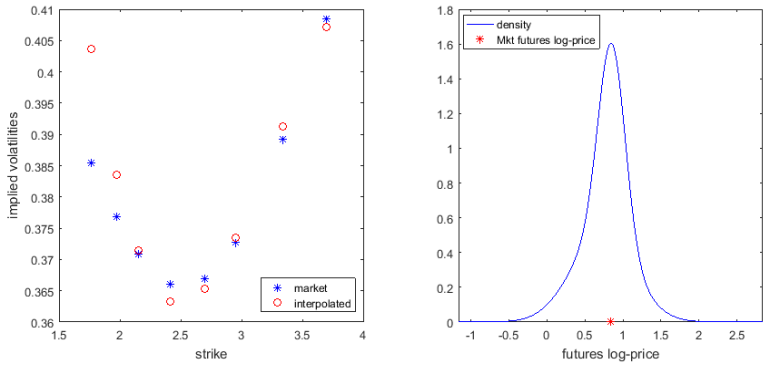

(b)

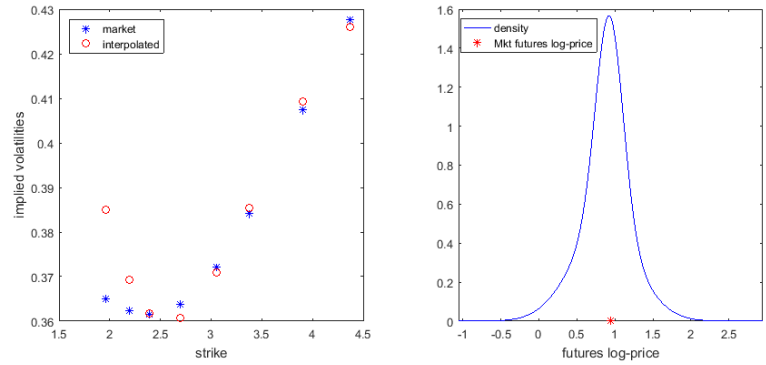

(c)

Figure 4.6: market versus interpolated implied volatilities for expiries 202 (a), 231 (b), 261 (c) days (left plots); interpolated terminal density function of futures prices consistent with the interpolated implied volatilities for expiries.

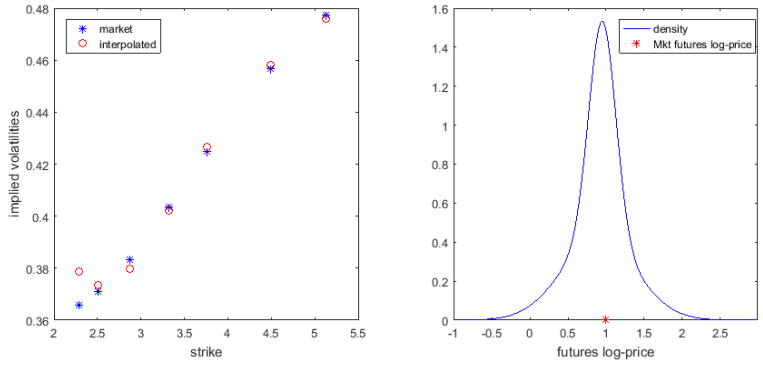

(a)

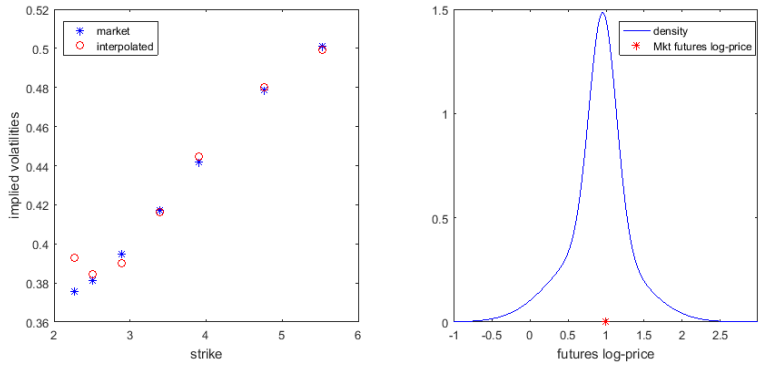

(b)

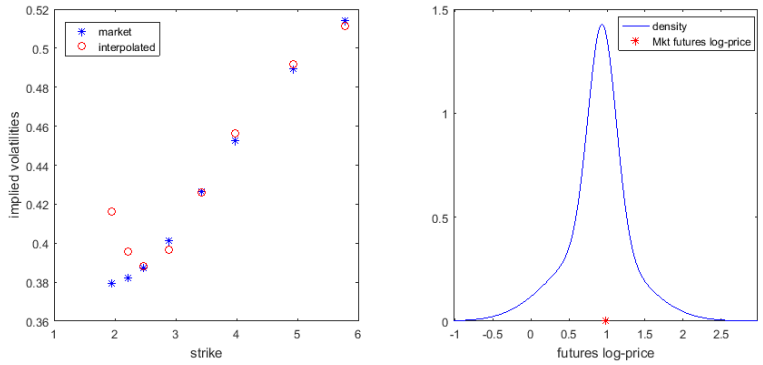

(c)

Figure 4.7: market versus interpolated implied volatilities for expiries 293 (a), 323 (b), 351 (c) days (left plots); interpolated terminal density function of futures prices consistent with the interpolated implied volatilities for expiries.

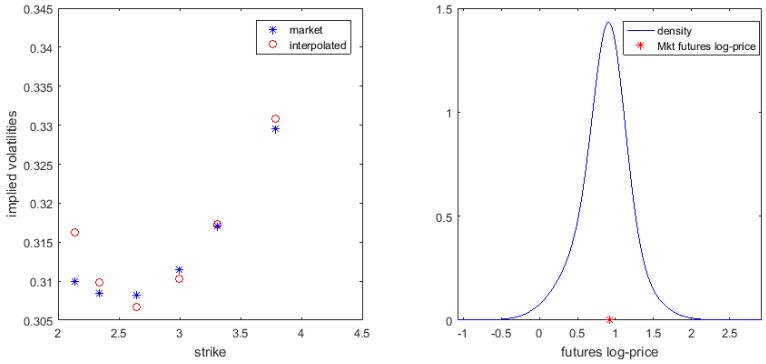

Figure 4.8: market versus interpolated implied volatilities for expiry 384 days (left plot); interpolated terminal density function of futures prices consistent with the interpolated implied volatilities for expiries.

Expiry (days)	υ_1	υ_2	ϵ_1	ϵ_2	RMSE
19	0.0084	-0.0267	0.0934	0.1661	0.0167
48	0.0106	-0.0466	0.1337	0.2308	0.0050
77	0.0167	-0.0643	0.1569	0.2621	0.0052
110	$0,0288$	-0.0862	0.1591	0.2928	0.0082
139	0.0186	-0.0844	0.1849	0.3078	0.0038
170	0.0198	-0.0973	0.1897	0.3407	0.0081
202	$0,0129$	-0.1017	0.1954	0.3706	0.0030
231	0.0146	-0.1134	0.1755	0.4062	0.0198
261	-0.0167	-0.0918	0.1798	0.4298	0.0214
293	-0.0429	-0.0934	0.1769	0.4899	0.0139
323	-0.0362	-0.1280	0.1776	0.5442	0.0187
351	-0.0448	-0.1385	0.1838	0.5756	0.0400
384	-0.1083	-0.0043	0.4281	0.2038	0.0069

Table 4.5: fitted parameters of the interpolated terminal distribution of futures prices consistent with the implied volatilities of options quoted on March 9, 2016 (RMSE = Root Mean Square Error).

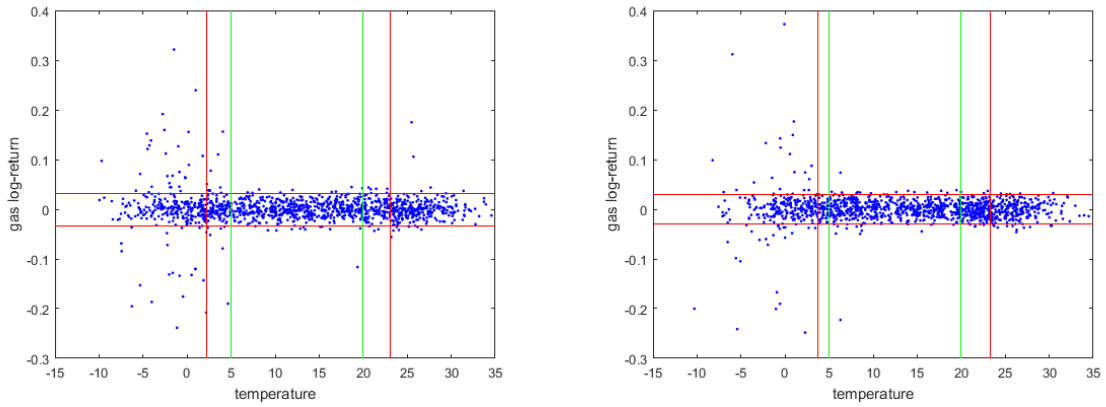

Figure 4.9: scatterplots of HH gas log-return versus the arithmetic average of the mean daily temperature recorded in New York and Chicago, obtained by simulation; the red bands represent the empirical standard deviation around the empirical mean of the simulated samples, while the green lines represent the threshold levels of the stochastic intensity.

4.1.3 A simulation study

In this section we use the calibrated parameters to show some graphical results obtained by simulating some paths of the temperature index and the gas price.

As shown in Figures 4.9-4.10-4.11, the simulation study seems to confirm that our model is able to grasp the essential features of the time series of gas and temperature, as well as the rather strong dependence of gas log-returns to temperature during the winter period, i.e. when the temperature is low.

In Figure 4.9 we replicate by Monte Carlo simulation the scatterplot of historical observations of log-returns and temperature displayed in Figure 1.5. We observe that the model capture reasonably well the two regimes of gas log-returns with respect to the temperature level, namely high dispersion of log-returns for low temperatures and low log-returns dispersion otherwise, but also that the it is not capable to replicate the very (few) large deviations of gas when the temperature is extremely low. We will further investigate this issue in our future research. A possible remedy is to use fat tails distributions to model the temperature index.

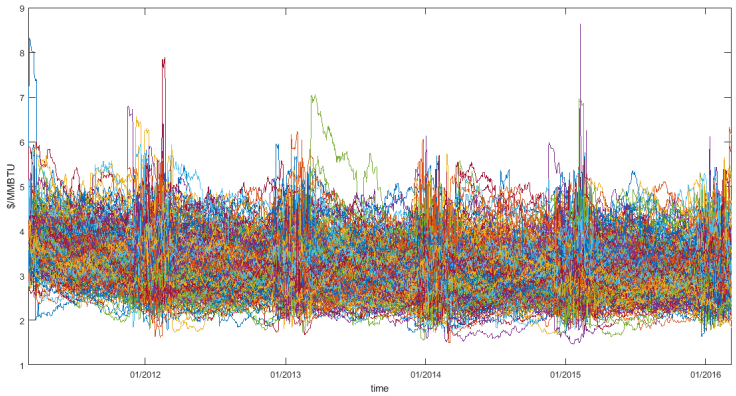

Figure 4.10: Monte Carlo paths of the HH gas price process.

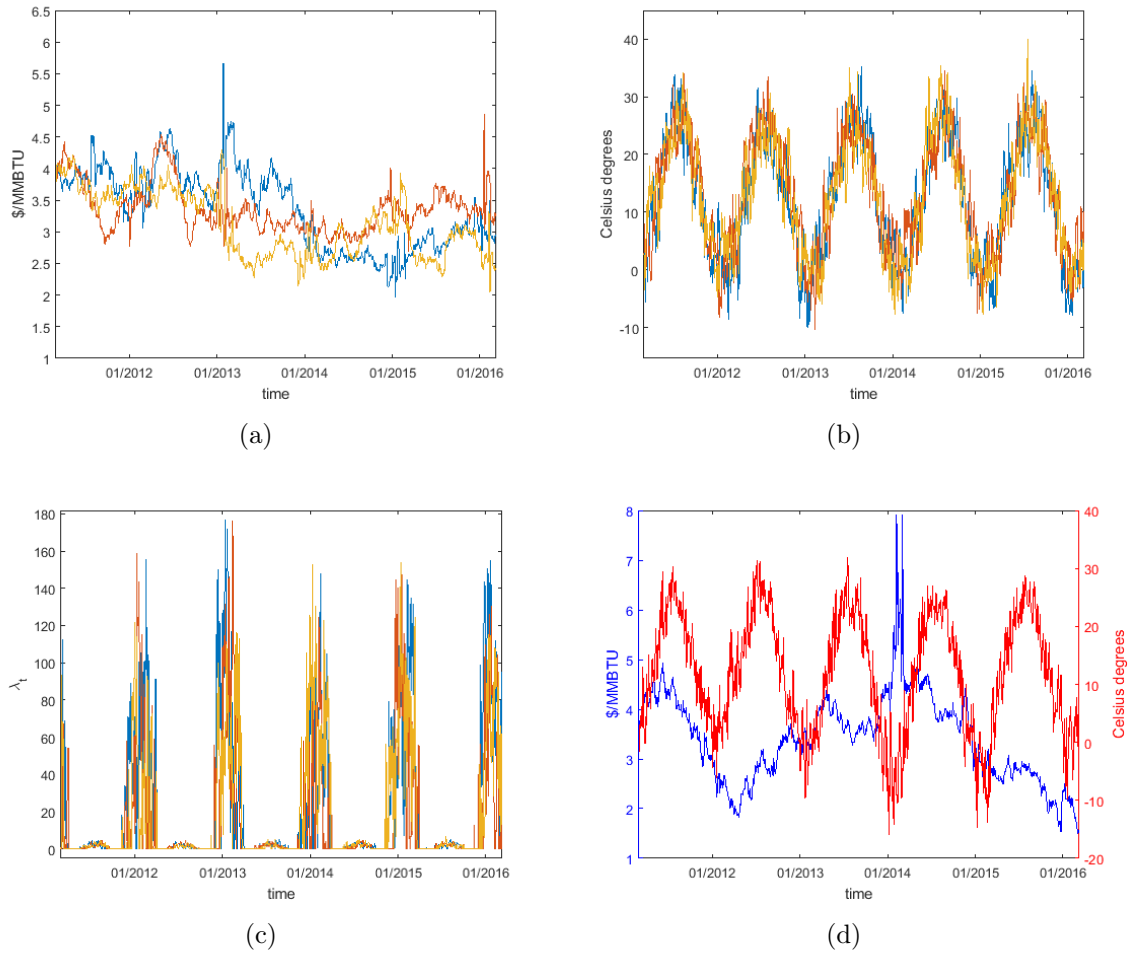

Figure 4.11: three simulated paths of the gas price (a), temperature index (b) and stochastic jump intensity (c), obtained using the estimated parameters in Tables 4.1-4.2; time series of the HH gas price over the period March 2, 2011 - March 9, 2016 (d) (source: Bloomberg).

4.2 Gas storage pricing

In this section we provide a numerical example of pricing of a gas storage contract, with particular emphasis on the difference between virtual storage contracts and storage contracts with penalty.

4.2.1 Virtual storage contract

In this toy example we consider a contract that starts on March 10, 2016 and ends on March 9, 2017. The maximum gas capacity is 100,000 MMBTU, with a daily maximum withdrawal and injection rates both equal to 5,000 MMBTU. We price this contract using both our calibrated model and an intrinsic approach based on trading futures contracts quoted at the end of March 9, 2016 with maturity less or equal than the maturity of the storage contract. We used the Eonia as the instantaneous risk-free interest rate, which

on March 9, 2016 was $r = -0.0024$. As for the FFT algorithm settings, we set $\bar{k}^Y = 2^7$ and $\bar{k}^T = 2^6$.

Approach	Value ($)	Unitary value ($/MMBTU)	% diff.
Extrinsic	109,770	1.0977	-
Extrinsic (no jumps)	131,760	1.3176	+20.03
Intrinsic	95,100	0.95000	-13.36

Table 4.6: comparison between contract values obtained by intrinsic and extrinsic approaches.

The intrinsic approach can account only for a portion (approximately the 86%) of the value obtained using the extrinsic approach under the model with temperature dependent jumps (see Table 4.6).

In order to evaluate the impact of the temperature, we computed the contract value using a classical Gaussian mean-reverting process obtained from (2.1) by "switching off" the jump part (see A.1 in the Appendix for the estimated parameters of the Gaussian model). Our model returns a lower value with respect to the Gaussian model, which is basically consistent with an overall lower volatility of the gas price, especially during the summer. Indeed, the volatility parameter estimated using the Gaussian model ($\sigma = 0.5827$) is much larger than the one obtained using a temperature dependent gas price model ($\sigma = 0.2463$), and jumps cannot compensate for the difference.

In Figure 4.12 we show an example of optimal action at a given time of the life of the contract as a function of gas price and temperature index for a fixed level of gas volume. Furthermore, we display the evolution of the value function of the dynamic programming algorithm (3.20) as a function of:

- Gas price and temperature index, for a fixed level of gas volume (Figures 4.13-4.16-4.19-4.22);
- Gas price and gas volume, for a fixed level of temperature index (Figures 4.14-4.17-4.20-4.23);
- Temperature and gas volume, for a fixed level of gas price (Figures 4.15-4.18-4.21-4.24).

As expected, the temperature affects the value function mostly during the winter period, which lasts from October to March, compare Figures 4.13-4.22 with Figures 4.16-4.19. In the two former figures it is clearly visible the impact of low temperatures on the value, while in the latter figures the impact of high temperatures is almost absent. In particular, in Figure 4.13 we notice that low temperatures (for approximately $T_{t_2} \leq 0$ Celsius degrees) have a detrimental effect on value, except for small values of the gas spot price (for approximately $S_{t_2} \leq 2$ $/MMBTU). This asymmetry can be explained by the fact that a downward (upward) jump can attract the price process towards its long term mean when it is higher (lower), thus having a negative (positive) effect on the continuation value.

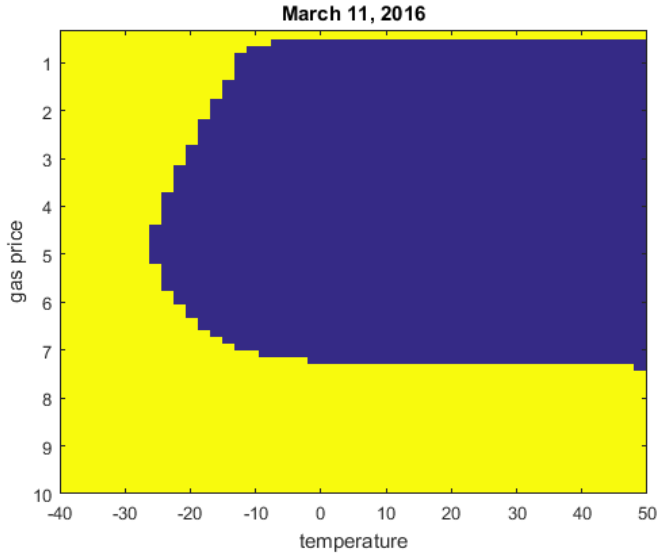

Figure 4.12: Optimal action as a function of gas price and temperature index on the first day of life of the contract after inception ($n = 2$) for the level of gas $q_{t_2} = 0$. In yellow the regions where is optimal to inject, in violet the regions where it is optimal to do nothing.

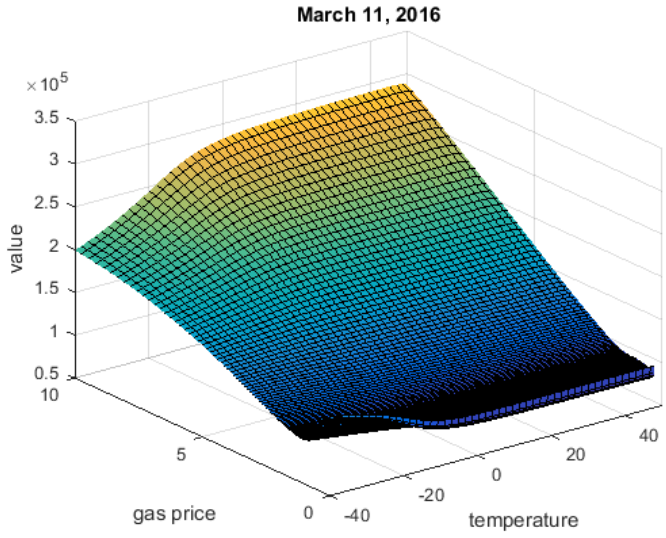

Figure 4.13: Storage value as a function of gas price and temperature index on the first day of life of the contract after the inception ($n = 2$) for the level of gas $q_{t_2} = 0$.

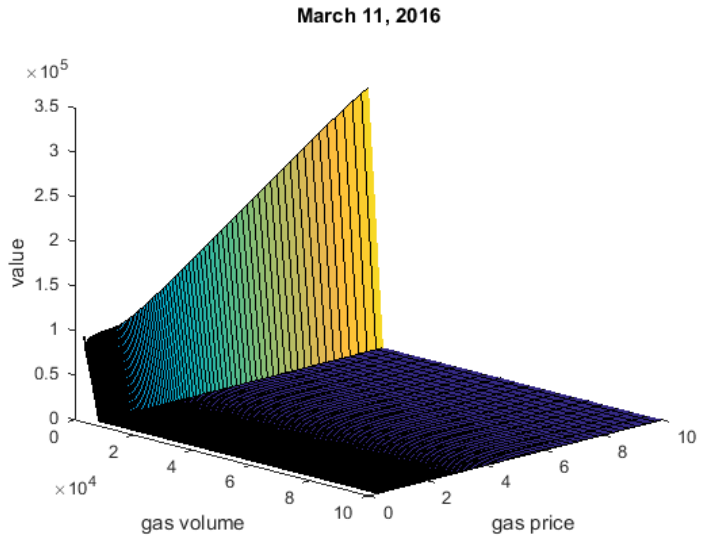

Figure 4.14: Storage value as a function of gas price and gas volume on the first day of life of the contract after the inception ($n = 2$) for a temperature index level equal to the initial value $T_0 = 14.1944$.

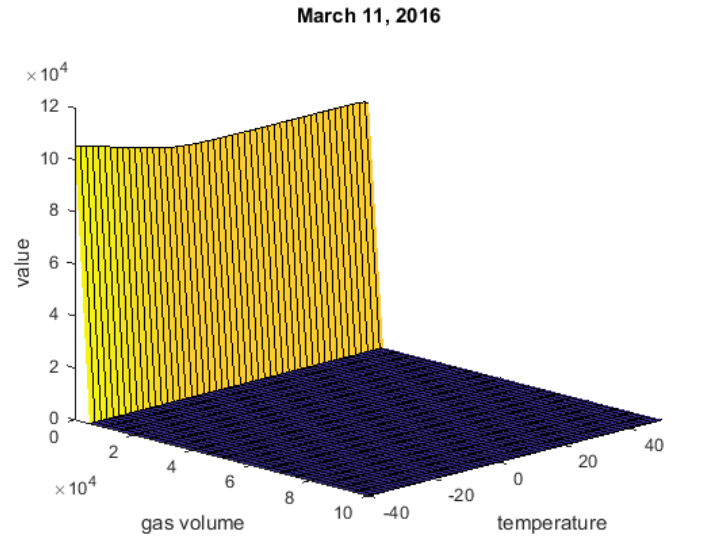

Figure 4.15: Storage value as a function of temperature index and gas volume on the first day of life of the contract after the inception ($n = 2$) for a gas price value equal to the initial value $S_0 = 1.5734$.

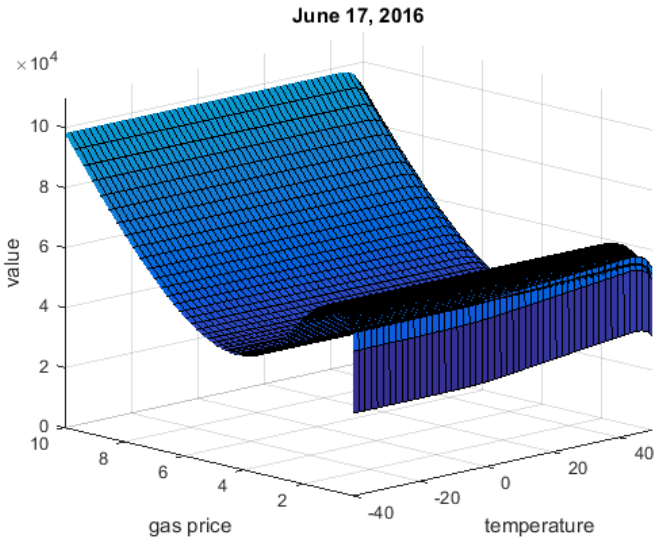

Figure 4.16: Storage value as a function of gas price and temperature index on the 100-th day of life of the contract ($n = 100$) for the level of gas $q_{t_{100}} = 0$.

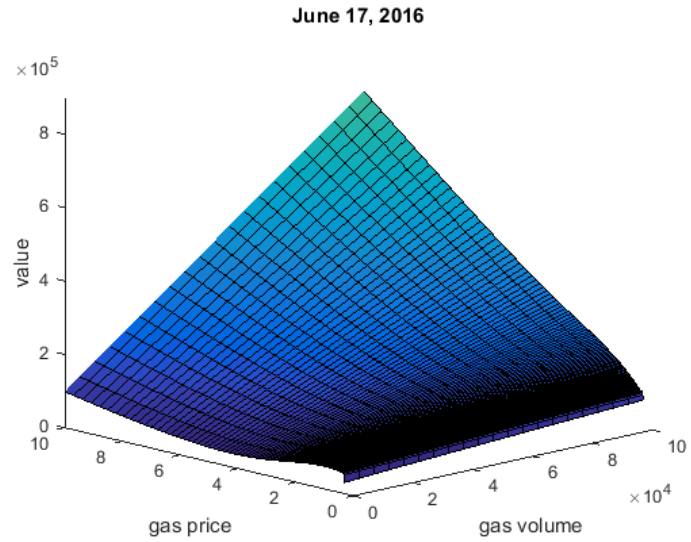

Figure 4.17: Storage value as a function of gas price and gas volume on the 100-th day of life of the contract ($n = 100$) for a temperature index level equal to the initial value $T_0 = 14.1944$.

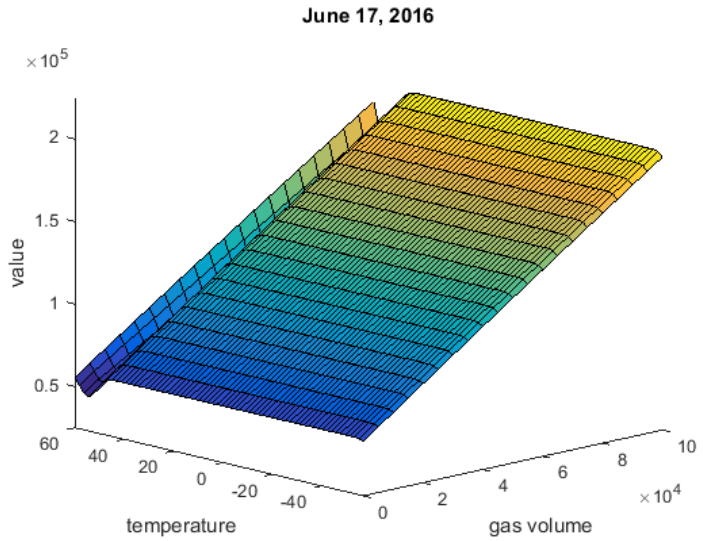

Figure 4.18: Storage value as a function of temperature index and gas volume on the 100-th day of life of the contract ($n = 100$) for a gas price value equal to the initial value $S_0 = 1.5734$.

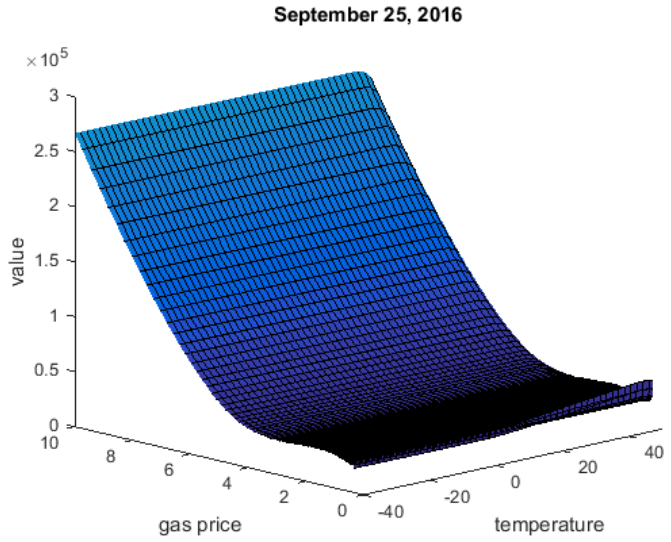

Figure 4.19: Storage value as a function of gas price and temperature index on the 200-th day of life of the contract ($n = 200$) for the level of gas $q_{t_{200}} = 0$.

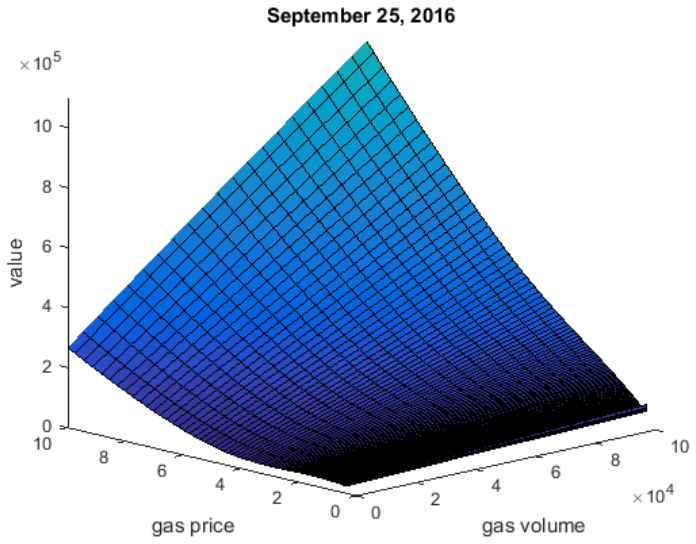

Figure 4.20: Storage value as a function of gas price and gas volume on the 200-th day of life of the contract ($n = 200$) for a temperature index level equal to the initial value $T_0 = 14.1944$.

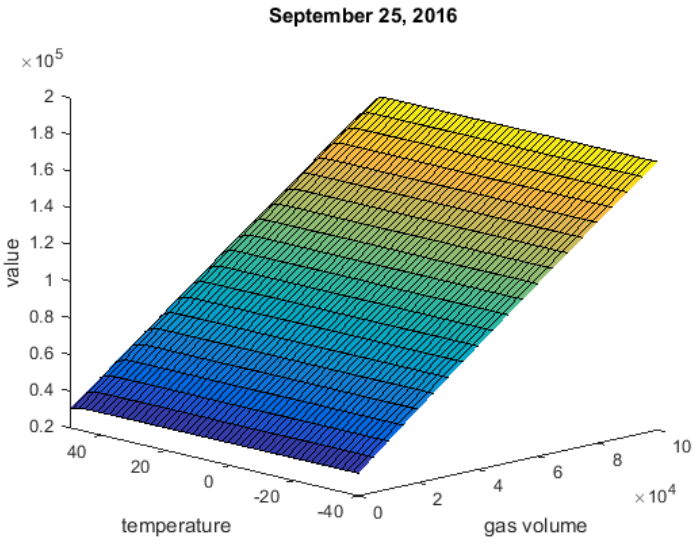

Figure 4.21: Storage value as a function of temperature index and gas volume on the 200-th day of life of the contract ($n = 200$) for a gas price value equal to the initial value $S_0 = 1.5734$.

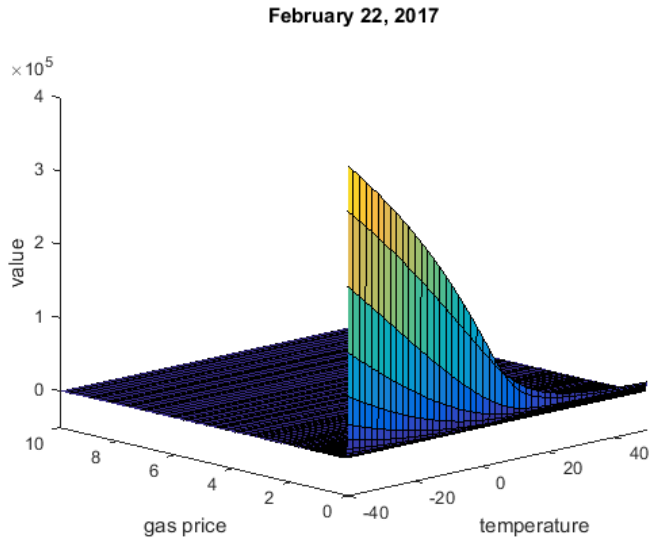

Figure 4.22: Storage value as a function of gas price and temperature index on the 350-th day of life of the contract ($n = 350$) for the level of gas $q_{t_{350}} = 0$.

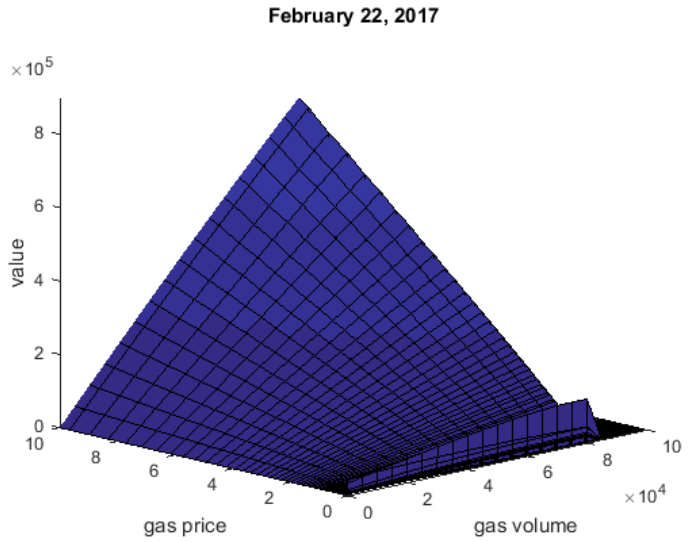

Figure 4.23: Storage value as a function of gas price and gas volume on the 350-th day of life of the contract ($n = 350$) for a temperature index level equal to the initial value $T_0 = 14.1944$.

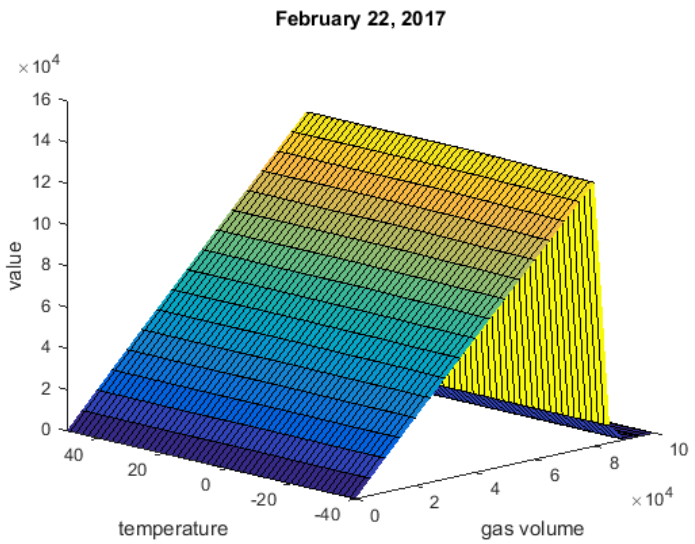

Figure 4.24: Storage value as a function of temperature index and gas volume on the 350-th day of life of the contract ($n = 350$) for a gas price value equal to the initial value $S_0 = 1.5734$.

4.2.2 Storage contract with penalty

Now we compare the values obtained using the extrinsic approach in Table 4.6 with the values of a contract with the same features of the previous one but adding a penalty (3.17) on the final volume, with

$$c(S_{t_{\bar{n}}}) = 0.1 \times S_{t_{\bar{n}}}. \tag{4.1}$$

It is necessary to introduce such a penalty in order to evaluate a realistic contract for using a physical storage facility. Indeed, the toy example presented before should be intended as a simplified example of virtual gas storage contract.

Approach	Value ($)	Unitary value ($/MMBTU)	% diff.
Extrinsic + penalty	$87,6931$	0.876931	-
Extrinsic + penalty (no jumps)	$106,9183$	1.069183	+21.92

Table 4.7: comparison between contract values obtained by the extrinsic approach using two different models.

By comparing Table 4.7 with Table 4.6 we notice that the penalty (3.17)-(4.1) has a non negligible negative effect on the value of the contract. In particular, there is a reduction in value of about 20% using the temperature dependent model, while in the Gaussian case the reduction is about 18% with respect to the no penalty case. Figure 4.25 allows us to visualize the impact of the penalty on the value function with respect to the no penalty case represented in Figure 4.22. The penalty function makes the value a decreasing function of the gas price, and makes it even negative in the region where in the no penalty case was equal to zero. We do not show the value surface for other time periods since its shape does not change dramatically from a qualitative point of view with respect to the no penalty case. Indeed, the impact of the penalty tends to vanish when the maturity of the contract increases.

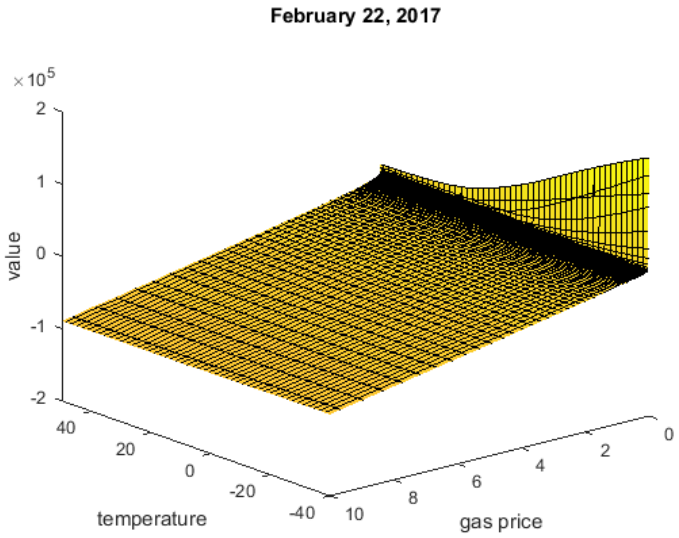

Figure 4.25: Storage value as a function of gas price and temperature index on the 350-th day of life of the contract ($n = 350$) for the level of gas $q_{t_{350}} = 0$, accounting for the penalty function (3.17)-(4.1).

Conclusions and future work

We proposed a framework for computing the value of gas storage facilities/contracts using a gas price model that explicitly depends on the temperature. Indeed, we found a nonlinear relationship between gas price and temperature: jumps in gas price happen more often when the temperature is low. Our model is able to grasp this and the other essential features of the Henry Hub gas price, except the very few large deviations of the price when the temperature is extremely low.

We first specified the model under the real world measure. Then, by a suitable change of measure, we derived an equivalent no arbitrage pricing measure. The model can be calibrated under both measures.

In order to compute the value function of the gas storage, we proposed a new FFT-based dynamic programming algorithm.

We priced a hypothetical gas storage contract using our model, that we calibrated on the actual data of the Henry Hub gas price, futures and a suitable temperature index built as an average of the temperatures recorded in New York and Chicago. In particular, we found that temperature dependent jumps can have a non negligible effect on the value.

We think that our work can be improved in several directions. First, we plan to better investigate the effect of the temperature on the valuation of gas storage contracts/facilities. Second, we plan to study an effective calibration procedure of the market price of jump risk, so that we can provide a comprehensive analysis of the market prices of risk in the Henry Hub market. Third, we plan to do a comparative analysis of our pricing algorithm with other methods that represent the standard for pricing this kind of contracts, namely recombining trees and Least Square Monte Carlo methods. Finally, it would be interesting to test the model on other gas markets, e.g. on the European markets.

Bibliography

[Alaton et al., 2002] Alaton, P., Djehiche, B., and Stillberger, D. (2002). On modelling and pricing weather derivatives. *Applied Mathematical Finance*, 9(1):1–20.

[Bäuerle and Riess, 2016] Bäuerle, N. and Riess, V. (2016). Gas storage valuation with regime switching. *Energy Systems*, 7(3):499–528.

[Baviera and Mainetti, 2016] Baviera, R. and Mainetti, T. F. (2016). A joint model for temperature and natural gas with an application to the us market. *Quantitative Finance*, pages 1–15.

[Benko, 2007] Benko, M. (2007). *Functional data analysis with applications in finance*. PhD thesis, Humboldt-Universität zu Berlin, Wirtschaftswissenschaftliche Fakultät.

[Benth et al., 2003] Benth, F. E., Ekeland, L., Hauge, R., and Nielsen, B. R. F. (2003). A note on arbitrage-free pricing of forward contracts in energy markets. *Applied Mathematical Finance*, 10(4):325–336.

[Benth and Šaltytė-Benth, 2005] Benth, F. E. and Šaltytė-Benth, J. (2005). Stochastic modelling of temperature variations with a view towards weather derivatives. *Applied Mathematical Finance*, 12(1):53–85.

[Benth and Sgarra, 2012] Benth, F. E. and Sgarra, C. (2012). The risk premium and the esscher transform in power markets. *Stochastic Analysis and Applications*, 30(1):20–43.

[Benth and Koekebakker, 2008] Benth, J. S. and Koekebakker, S. (2008). *Stochastic modeling of electricity and related markets. Advanced Series on Statistical Science and Applied Probability*. World Scientific.

[Bertsekas et al., 1995] Bertsekas, D. P., Bertsekas, D. P., Bertsekas, D. P., and Bertsekas, D. P. (1995). *Dynamic programming and optimal control*, volume 1. Athena Scientific Belmont, MA.

[Bertsekas and Shreve, 1978] Bertsekas, D. P. and Shreve, S. E. (1978). *Stochastic optimal control: The discrete time case*, volume 23. Academic Press New York.

[Bjerksund et al., 2008] Bjerksund, P., Stensland, G., and Vagstad, F. (2008). Gas storage valuation: Price modelling v. optimization methods. *Optimization Methods (October 17, 2008). NHH Dept. of Finance & Management Science Discussion Paper*, (2008/20).

[Björk, 2009] Björk, T. (2009). *Arbitrage theory in continuous time*. Oxford university press.

[Black, 1976] Black, F. (1976). The pricing of commodity contracts. *Journal of financial economics*, 3(1):167–179.

[Black and Scholes, 1973] Black, F. and Scholes, M. (1973). The pricing of options and corporate liabilities. *The journal of political economy*, pages 637–654.

[Bollerslev, 1986] Bollerslev, T. (1986). Generalized autoregressive conditional heteroskedasticity. *Journal of econometrics*, 31(3):307–327.

[Boogert and De Jong, 2008] Boogert, A. and De Jong, C. (2008). Gas storage valuation using a monte carlo method. *The journal of derivatives*, 15(3):81–98.

[Borovkova and Geman, 2006] Borovkova, S. and Geman, H. (2006). Seasonal and stochastic effects in commodity forward curves. *Review of Derivatives Research*, 9(2):167–186.

[Brennan and Schwartz, 1985] Brennan, M. J. and Schwartz, E. S. (1985). Evaluating natural resource investments. *Journal of business*, pages 135–157.

[Breslin et al., 2008] Breslin, J., Clewlow, L., Elbert, T., Kwok, C., and Strickland, C. (2008). Gas storage: Overview & static valuation. *Lacima Group*.

[Breslin et al., 2009] Breslin, J., Clewlow, L., Elbert, T., Kwok, C., Strickland, C., and van der Zee, D. (2009). Gas storage: Rolling instrinsic valuation. *Energy Risk, January*, pages 61–65.

[Brigo and Mercurio, 2002] Brigo, D. and Mercurio, F. (2002). Lognormal-mixture dynamics and calibration to market volatility smiles. *International Journal of Theoretical and Applied Finance*, 5(04):427–446.

[Brody et al., 2002] Brody, D. C., Syroka, J., Zervos, M., et al. (2002). Dynamical pricing of weather derivatives. *Quantitative Finance*, 2(3):189–198.

[Brown and Yücel, 2008] Brown, S. P. and Yücel, M. K. (2008). What drives natural gas prices? *The Energy Journal*, pages 45–60.

[Bühlmann et al., 1996] Bühlmann, H., Delbaen, F., Embrechts, P., and Shiryaev, A. N. (1996). No-arbitrage, change of measure and conditional esscher transforms. *CWI quarterly*, 9(4):291–317.

[Campbell and Diebold, 2011] Campbell, S. D. and Diebold, F. X. (2011). Weather forecasting for weather derivatives. *Journal of the American Statistical Association*.

[Carmona and Ludkovski, 2010] Carmona, R. and Ludkovski, M. (2010). Valuation of energy storage: an optimal switching approach. *Quantitative Finance*, 10(4):359–374.

[Cartea et al., 2014] Cartea, Á., Cheeseman, J., and Jaimungal, S. (2014). How to value a gas storage facility. *Available at SSRN 2377781*.

[Cartea and Figueroa, 2005] Cartea, A. and Figueroa, M. G. (2005). Pricing in electricity markets: a mean reverting jump diffusion model with seasonality. *Applied Mathematical Finance*, 12(4):313–335.

[Cartea and Williams, 2008] Cartea, A. and Williams, T. (2008). Uk gas markets: The market price of risk and applications to multiple interruptible supply contracts. *Energy Economics*, 30(3):829–846.

[Chen and Forsyth, 2007] Chen, Z. and Forsyth, P. A. (2007). A semi-lagrangian approach for natural gas storage valuation and optimal operation. *SIAM Journal on Scientific Computing*, 30(1):339–368.

[Chen and Forsyth, 2010] Chen, Z. and Forsyth, P. A. (2010). Implications of a regime-switching model on natural gas storage valuation and optimal operation. *Quantitative Finance*, 10(2):159–176.

[Cont and Tankov, 2003] Cont, R. and Tankov, P. (2003). *Financial modelling with jump processes*, volume 2. CRC press.

[Cooley and Tukey, 1965] Cooley, J. W. and Tukey, J. W. (1965). An algorithm for the machine calculation of complex fourier series. *Mathematics of computation*, 19(90):297–301.

[Cox and Isham, 1980] Cox, D. R. and Isham, V. (1980). *Point processes*, volume 12. CRC Press.

[De Jong, 2016] De Jong, C. (2016). Gas storage pricing and hedging. *Managing Energy Price Risk, 4th ed., Risk Books. London, England, UK*, pages 479–503.

[Dornier and Queruel, 2000] Dornier, F. and Queruel, M. (2000). Caution to the wind. *Energy & power risk management*, 13(8):30–32.

[Edoli et al., 2016] Edoli, E., Fiorenzani, S., and Vargiolu, T. (2016). *Optimization Methods for Gas and Power Markets: Theory and Cases.* Springer.

[Edoli and Vargiolu, 2013] Edoli, E. and Vargiolu, T. (2013). Stochastic optimization for the pricing of structured contracts in energy markets. *Argo Magazine 2, 27 - 36.*

[Esscher, 1932] Esscher, F. (1932). On the probability function in the collective theory of risk. *Skandinavisk Aktuarietidskrift*, 15:175–195.

[Eydeland and Wolyniec, 2003] Eydeland, A. and Wolyniec, K. (2003). *Energy and power risk management: New developments in modeling, pricing, and hedging*, volume 206. John Wiley & Sons.

[Felix and Weber, 2012] Felix, B. J. and Weber, C. (2012). Gas storage valuation applying numerically constructed recombining trees. *European Journal of Operational Research*, 216(1):178–187.

[Geman, 2007] Geman, H. (2007). Mean reversion versus random walk in oil and natural gas prices. In *Advances in Mathematical finance*, pages 219–228. Springer.

[Gerber et al., 1994] Gerber, H. U., Shiu, E. S., et al. (1994). Option pricing by esscher transforms. *Transactions of the Society of Actuaries*, 46(99):140.

[Goia et al., 2010] Goia, A., May, C., and Fusai, G. (2010). Functional clustering and linear regression for peak load forecasting. *International Journal of Forecasting*, 26(4):700–711.

[Gray and Khandelwal, 2004] Gray, J. and Khandelwal, P. (2004). Towards a realistic gas storage model. *Commodities Now*, (June):1–4.

[Henaff et al., 2013] Henaff, P., Laachir, I., and Russo, F. (2013). Gas storage valuation and hedging. a quantification of the model risk. *arXiv preprint arXiv:1312.3789*.

[Jaimungal and Surkov, 2011] Jaimungal, S. and Surkov, V. (2011). Lévy-based cross-commodity models and derivative valuation. *SIAM Journal on Financial Mathematics*, 2(1):464–487.

[Kallsen and Shiryaev, 2002] Kallsen, J. and Shiryaev, A. N. (2002). The cumulant process and esscher's change of measure. *Finance and Stochastics*, 6(4):397–428.

[Kiely et al., 2015] Kiely, G., Murphy, B., and Cummins, M. (2015). Gas storage valuation under lévy processes using the fast fourier transform. *Available at SSRN 2561864*.

[Kou, 2002] Kou, S. G. (2002). A jump-diffusion model for option pricing. *Management science*, 48(8):1086–1101.

[Lai et al., 2010] Lai, G., Margot, F., and Secomandi, N. (2010). An approximate dynamic programming approach to benchmark practice-based heuristics for natural gas storage valuation. *Operations research*, 58(3):564–582.

[Löhndorf and Wozabal, 2015] Löhndorf, N. and Wozabal, D. (2015). Optimal gas storage valuation and futures trading under a high-dimensional price process.

[Longstaff and Schwartz, 2001] Longstaff, F. A. and Schwartz, E. S. (2001). Valuing american options by simulation: a simple least-squares approach. *Review of Financial studies*, 14(1):113–147.

[Lord et al., 2008] Lord, R., Fang, F., Bervoets, F., and Oosterlee, C. W. (2008). A fast and accurate fft-based method for pricing early-exercise options under lévy processes. *SIAM Journal on Scientific Computing*, 30(4):1678–1705.

[Melick and Thomas, 1997] Melick, W. R. and Thomas, C. P. (1997). Recovering an asset's implied pdf from option prices: an application to crude oil during the gulf crisis. *Journal of Financial and Quantitative Analysis*, 32(01):91–115.

[Mu, 2007] Mu, X. (2007). Weather, storage, and natural gas price dynamics: Fundamentals and volatility. *Energy Economics*, 29(1):46–63.

[Müller et al., 2015] Müller, J., Hirsch, G., and Müller, A. (2015). Modeling the price of natural gas with temperature and oil price as exogenous factors. In *Innovations in Quantitative Risk Management*, pages 109–128. Springer.

[Roncoroni et al., 2015] Roncoroni, A., Fusai, G., and Cummins, M. (2015). *Handbook of multi-commodity markets and products: Structuring, trading and risk management*. John Wiley & Sons.

[Schwartz and Smith, 2000] Schwartz, E. and Smith, J. E. (2000). Short-term variations and long-term dynamics in commodity prices. *Management Science*, 46(7):893–911.

[Stoll and Wiebauer, 2010] Stoll, S.-O. and Wiebauer, K. (2010). A spot price model for natural gas considering temperature as an exogenous factor with applications. *J. Energy Mark*, 3(3):113–128.

[Thompson et al., 2009] Thompson, M., Davison, M., and Rasmussen, H. (2009). Natural gas storage valuation and optimization: A real options application. *Naval Research Logistics (NRL)*, 56(3):226–238.

Appendix A

Tables and proofs

A.1 Gaussian model calibration

The maximum likelihood estimation for the Gaussian model returned the following parameters:

κ	μ	σ
1.6594	1.1890	0.5827

Table A.1: MLE parameters of the gas price process using a Gaussian model, obtained using the time series of daily observations of the HH gas price over the period March 2, 2011 - March 9, 2016; data for the HH gas price provided by Bloomberg.

Here we report the calibrated market price of risk for the Gaussian model:

Maturity (t=days)	$F_0^{mkt}(t)$	$F_0^{mkt}(t) - \mathbb{E}[S_t]$	$\hat{\theta}$
20	1.7520	0.0620	1.1795
49	1.8460	−0.0070	−0.8147
78	1.9460	−0.0606	−0.6301
111	2.0410	−0.1318	−0.7000
140	2.0910	−0.2170	−1.0517
173	2.1060	−0.3322	−1.2561
203	2.1470	−0.4149	−1.0922
232	2.3110	−0.3585	0.2452
264	2.5720	−0.1903	1.1211
294	2.7030	−0.1312	0.3322
324	2.7000	−0.2098	−0.7477
352	2.6700	−0.2922	−0.9046
385	2.5170	−0.5061	−1.9173

Table A.2: calibrated market prices of risk on March 9, 2016.

A.2 Gas consumption 2014-2016

2014	Residential	Commercial	Industrial	Electric power	Other	Total
Jan	1,037	572	722	663	160	3,204
Feb	853	490	659	551	188	2,741
Mar	700	421	681	561	195	2,558
Apr	356	251	628	549	178	1,962
May	203	177	606	647	177	1,810
Jun	126	141	586	721	171	1,745
Jul	113	138	605	843	182	1,881
Aug	105	137	609	898	184	1,933
Sep	122	149	591	771	176	1,809
Oct	212	202	610	703	186	1,913
Nov	544	362	660	600	89	2,358
Dec	717	427	690	639	206	2,679

Table A.3: monthly consumption of billion cubic feet of gas for type of consumer in the US during the 2014; source: www.eia.gov/naturalgas/monthly)

2015	Residential	Commercial	Industrial	Electric power	Other	Total
Jan	937	532	720	714	213	3,116
Feb	902	517	661	651	196	2,927
Mar	633	385	663	709	202	2,592
Apr	319	232	609	668	36	2,013
May	177	160	604	739	183	1,863
Jun	124	135	576	893	180	1,908
Jul	108	134	593	1,054	188	2,077
Aug	103	135	601	1,035	187	2,061
Sep	108	138	580	902	181	1,909
Oct	201	195	614	798	186	1,994
Nov	406	283	639	737	190	2,255
Dec	591	352	675	771	202	2,591

Table A.4: monthly consumption of billion cubic feet of gas for type of consumer in the US during the 2015; source: www.eia.gov/naturalgas/monthly)

A.3 Change of measure

First, for the mutual independence between the Brownian motion of the gas log-price B and the pure jump process of the log-price J, we have

$$\mathbb{E}\left[Z_t^{\boldsymbol{\theta}}\right] = \mathbb{E}\left[\hat{Z}_t\right] \times \mathbb{E}\left[\tilde{Z}_t\right].$$

Then, under suitable integrability conditions, $\hat{Z}_t$ is a $\mathbb{P}$-martingale, since for any $s \leq t$

2016	Residential	Commercial	Industrial	Electric power	Other	Total
Jan	889	507	722	777	212	3,107
Feb	698	416	666	692	195	2,667
Mar	457	299	669	740	195	2,360
Apr	330	234	624	726	183	2,097
May	196	172	619	807	184	1,978
Jun	123	139	596	977	180	2,015
Jul	108	136	624	1,148	188	2,204

Table A.5: monthly consumption of billion cubic feet of gas for type of consumer in the US during the 2016; source: www.eia.gov/naturalgas/monthly)

we have

$$\begin{aligned}
\mathbb{E}\left[\hat{Z}_t|\mathcal{F}_s\right] &= \hat{Z}_s \times \mathbb{E}\left[\frac{\hat{Z}_t}{\hat{Z}_s}\middle|\mathcal{F}_s\right] \\
&= \hat{Z}_s \times \mathbb{E}\left[\exp\left(\int_s^t \hat{\theta}(u)dB_u - \frac{1}{2}\int_s^t \hat{\theta}^2(u)du\right)\middle|\mathcal{F}_s\right] \\
&= \hat{Z}_s \times \mathbb{E}\left[\exp\left(\int_s^t \hat{\theta}(u)dB_u\right)\middle|\mathcal{F}_s\right] \times \exp\left(-\frac{1}{2}\int_s^t \hat{\theta}^2(u)du\right) = \hat{Z}_s,
\end{aligned}$$

from which follows that $\mathbb{E}\left[\hat{Z}_t\right] = \hat{Z}_0 = 1$.

Similarly, $\tilde{Z}_t$ is, under suitable integrability conditions, a $\mathbb{P}$-martingale. Indeed, for $n = \bar{n}$ and $t_{\bar{n}-1} \le s \le t \le t_{\bar{n}}$ we have

$$\begin{aligned}
\mathbb{E}\left[\tilde{Z}_t|\mathcal{F}_s\right] &= \tilde{Z}_s \times \mathbb{E}\left[\frac{\tilde{Z}_t}{\tilde{Z}_s}\middle|\mathcal{F}_s\right] \\
&= \tilde{Z}_s \times \mathbb{E}\left[\frac{\exp\left(\int_{t_{\bar{n}-1}}^t \tilde{\theta}(u)dJ_u\right)}{\mathbb{E}\left[\exp\left(\int_{t_{\bar{n}-1}}^t \tilde{\theta}(u)dJ_u\right)\middle|\mathcal{F}_{t_{n-1}}\right]} \times \frac{\mathbb{E}\left[\exp\left(\int_{t_{\bar{n}-1}}^s \tilde{\theta}(u)dJ_u\right)\middle|\mathcal{F}_{t_{n-1}}\right]}{\exp\left(\int_{t_{\bar{n}-1}}^s \tilde{\theta}(u)dJ_u\right)}\middle|\mathcal{F}_s\right] \\
&= \tilde{Z}_s \times \mathbb{E}\left[\exp\left(\int_s^t \tilde{\theta}(u)dJ_u\right) \times \frac{\exp\left(\int_{t_{\bar{n}-1}}^s \left(\phi_G(-i\tilde{\theta}(u)) - 1\right)\lambda_u du\right)}{\exp\left(\int_{t_{\bar{n}-1}}^t \left(\phi_G(-i\tilde{\theta}(u)) - 1\right)\lambda_u du\right)}\middle|\mathcal{F}_s\right] \\
&= \tilde{Z}_s \times \mathbb{E}\left[\exp\left(\int_s^t \tilde{\theta}(u)dJ_u\right)\middle|\mathcal{F}_s\right] \times \exp\left(-\int_s^t \left(\phi_G(-i\tilde{\theta}(u)) - 1\right)\lambda_u du\right) = \tilde{Z}_s
\end{aligned}$$

By iterating the same argument for all $n < \bar{n}$ it follows that $\mathbb{E}\left[\tilde{Z}_t\right] = \tilde{Z}_0 = 1$.

A.4 Gas log-price $\mathbb{Q}^{\boldsymbol{\theta}}$-dynamics

Re-write the solution of the SDE of the gas log-price (2.3) under $\mathbb{P}$ as

$$Y_t = Y_t^D + Y_t^J, \tag{A.1}$$

where

$$\begin{aligned} Y_t^D &= Y_u e^{-\kappa(t-u)} + \mu(1-e^{-\kappa(t-u)}) + \sigma \int_u^t e^{-\kappa(t-s)} dB_s \\ Y_t^J &= \int_u^t e^{-\kappa(t-s)} dJ_s. \end{aligned}$$

The $\mathcal{F}_u$-conditional characteristic function of Y_t^D under $\mathbb{Q}^{\boldsymbol{\theta}}$ then reads for $u \leq t$

$$\begin{aligned} \mathbb{E}^{\boldsymbol{\theta}}\left[e^{i\omega Y_t^D} \middle| \mathcal{F}_u \right] &= \mathbb{E}\left[e^{i\omega Y_t^D} \cdot \frac{\hat{Z}_t}{\hat{Z}_u} \middle| \mathcal{F}_u \right] \\ &= \mathbb{E}\left[\exp\left(i\omega \left(Y_u e^{-\kappa(t-u)} + \mu(1-e^{-\kappa(t-u)}) + \sigma \int_u^t e^{-\kappa(t-s)} dB_s \right) \right) \times \right. \\ &\quad \left. \exp\left(\int_u^t \hat{\theta}(s) dB_s - \frac{1}{2} \int_u^t \hat{\theta}^2(s) ds \right) | \mathcal{F}_u \right] \\ &= \exp\left(i\omega \left(Y_u e^{-\kappa(t-u)} + \mu(1-e^{-\kappa(t-u)}) \right) \right) \times \\ &\quad \mathbb{E}\left[\exp\left(i\omega\sigma \int_u^t \left(e^{-\kappa(t-s)} - i\frac{\hat{\theta}(s)}{\omega\sigma} \right) dB_s \right) \right] \exp\left(-\frac{1}{2} \int_u^t \hat{\theta}^2(s) ds \right) \\ &= \exp\left(i\omega \left(Y_u e^{-\kappa(t-u)} + \mu(1-e^{-\kappa(t-u)}) \right) \right) \times \\ &\quad \exp\left(-\frac{\omega^2\sigma^2}{2} \int_u^t \left(e^{-\kappa(t-s)} - i\frac{\hat{\theta}(s)}{\omega\sigma} \right)^2 ds \right) \exp\left(-\frac{1}{2} \int_u^t \hat{\theta}^2(s) ds \right) \\ &= \exp(i\omega \left(Y_u e^{-\kappa(t-u)} + \mu(1-e^{-\kappa(t-u)}) \right)) \times \\ &\quad \exp\left(-\frac{\omega^2\sigma^2}{2} \int_u^t \left(e^{-2\kappa(t-s)} - \left(\frac{\hat{\theta}(s)}{\omega\sigma} \right)^2 - i2e^{-\kappa(t-s)} \frac{\hat{\theta}(s)}{\omega\sigma} \right) ds \right) \times \\ &\quad \exp\left(-\frac{1}{2} \int_u^t \hat{\theta}^2(s) ds \right) \\ &= \exp(i\omega \left(Y_u e^{-\kappa(t-u)} + \mu(1-e^{-\kappa(t-u)}) \right)) \times \\ &\quad \exp\left(-\frac{\omega^2\sigma^2}{2} \int_u^t \left(e^{-2\kappa(t-s)} - i2e^{-\kappa(t-s)} \frac{\hat{\theta}(s)}{\omega\sigma} \right) ds \right) \\ &= \exp\left(i\omega Y_u e^{-\kappa(t-u)} + i\omega\mu(1-e^{-\kappa(t-u)}) + i\omega\sigma \int_u^t e^{-\kappa(t-s)} \hat{\theta}(s) ds - \right. \\ &\quad \left. \frac{\omega^2\sigma^2}{2} \int_u^t e^{-2\kappa(t-s)} ds \right) \\ &= \exp\left(i\omega Y_u e^{-\kappa(t-u)} + i\omega\mu(1-e^{-\kappa(t-u)}) + i\omega\sigma \int_u^t e^{-\kappa(t-s)} \hat{\theta}(s) ds - \right. \\ &\quad \left. \frac{\omega^2\sigma^2}{4\kappa} (1-e^{-2\kappa(t-u)}) \right), \end{aligned}$$

from which follows that the diffusion part of the solution under $\mathbb{Q}^{\boldsymbol{\theta}}$ is

$$Y_t^D = Y_u e^{-\kappa(t-u)} + \mu(1-e^{-\kappa(t-u)}) + \sigma \int_u^t e^{-\kappa(t-s)} \hat{\theta}(s) ds + \sigma \int_u^t e^{-\kappa(t-s)} d\tilde{B}_s.$$

Similarly, we derive the $\mathcal{F}_u \vee \mathcal{F}_t^\lambda$-conditional characteristic function of Y_t^D under $\mathbb{Q}^{\boldsymbol{\theta}}$ for $u \leq t$:

$$\begin{aligned}
\mathbb{E}^{\boldsymbol{\theta}}\left[e^{i\omega Y_t^J}\middle|\mathcal{F}_u \vee \mathcal{F}_t^\lambda\right] &= \mathbb{E}\left[e^{i\omega Y_t^D} \times \frac{\hat{Z}_t}{\hat{Z}_u}\middle|\mathcal{F}_u \vee \mathcal{F}_t^\lambda\right] \\
&= \mathbb{E}\left[\exp\left(i\omega\int_u^t e^{-\kappa(t-s)}dJ_s\right) \times \frac{\hat{Z}_t}{\hat{Z}_u}\middle|\mathcal{F}_u \vee \mathcal{F}_t^\lambda\right] \\
&= \mathbb{E}\left[\exp\left(i\omega\int_u^t e^{-\kappa(t-s)}dJ_s\right)\exp\left(\int_u^t \tilde{\theta}(s)dJ_s\right)\middle|\mathcal{F}_u \vee \mathcal{F}_t^\lambda\right] \times \\
&\quad \exp\left(-\int_u^t \left(\phi_G(-i\tilde{\theta}(s)) - 1\right)\lambda_s ds\right) \\
&= \mathbb{E}\left[\exp\left(i\omega\int_u^t e^{-\kappa(t-s)}dJ_s\right)\exp\left(\int_u^t \tilde{\theta}(s)dJ_s\right)\middle|\mathcal{F}_u \vee \mathcal{F}_t^\lambda\right] \times \\
&\quad \exp\left(-\int_u^t \left(\phi_G(-i\tilde{\theta}(s)) - 1\right)\lambda_s ds\right) \\
&= \mathbb{E}\left[\exp\left(i\int_u^t (\omega e^{-\kappa(t-s)} - i\tilde{\theta}(s))dJ_s\right)\middle|\mathcal{F}_u \vee \mathcal{F}_t^\lambda\right] \times \\
&\quad \exp\left(-\int_u^t \left(\phi_G(-i\tilde{\theta}(s)) - 1\right)\lambda_s ds\right) \\
&= \mathbb{E}\left[\exp\left(i\int_u^t (\omega e^{-\kappa(t-s)} - i\tilde{\theta}(s))dJ_s\right)\middle|\mathcal{F}_u \vee \mathcal{F}_t^\lambda\right] \times \\
&\quad \exp\left(-\int_u^t \left(\phi_G(-i\tilde{\theta}(s)) - 1\right)\lambda_s ds\right) \\
&= \exp\left(\int_u^t (\phi_G(\omega e^{-\kappa(t-s)} - i\tilde{\theta}(s)) - \phi_G(-i\tilde{\theta}(s)))\lambda_s ds\right),
\end{aligned}$$

where the last passage follows from Lemma 15.1 in [Cont and Tankov, 2003]. Then the $\mathcal{F}_u$-conditional characteristic function of Y_t^J is

$$\mathbb{E}^{\boldsymbol{\theta}}\left[e^{i\omega Y_t^J}\middle|\mathcal{F}_u\right] = \mathbb{E}^{\boldsymbol{\theta}}\left[\exp\left(\int_u^t (\phi_G(\omega e^{-\kappa(t-s)} - i\tilde{\theta}(s)) - \phi_G(-i\tilde{\theta}(s)))\lambda_s ds\right)\middle|\mathcal{F}_u\right],$$

i.e. we have to integrate with respect to the distribution of the temperature in order to obtain the unconditional characteristic function.

A.5 Jump process $\mathbb{Q}^{\boldsymbol{\theta}}$-dynamics: constant market price of risk

The $\mathcal{F}_t^\lambda$-conditional characteristic function of the jump process $J = \{J_u, u \leq t\}$ under $\mathbb{Q}^{\boldsymbol{\theta}}$ reads

$$\begin{aligned}
\mathbb{E}^{\boldsymbol{\theta}}\left[e^{i\omega J_t}\middle|\mathcal{F}_t^\lambda\right] &= \mathbb{E}\left[e^{i\omega J_t}\cdot\hat{Z}_t\middle|\mathcal{F}_t^\lambda\right] \\
&= \exp\left(\int_u^t (\phi_G(\omega - i\tilde{\theta}(s)) - \phi_G(-i\tilde{\theta}(s)))\lambda_s ds\right).
\end{aligned}$$

When the market price of jump risk is constant (3.6), the integrand function in the exponent can be factorized as

$$\int_0^t (\phi_G(\omega - i\tilde{\theta}^c) - \phi_G(-i\tilde{\theta}^c))\lambda_s ds = (\phi_G(\omega - i\tilde{\theta}^c) - \phi_G(-i\tilde{\theta}^c)) \int_0^t \lambda_s ds$$

where

$$\begin{aligned}
\phi_G(\omega - i\tilde{\theta}^c) - \phi_G(-i\tilde{\theta}^c) &= \varsigma \frac{\upsilon_+}{\upsilon_+ - i(\omega - i\tilde{\theta}^c)} + (1-\varsigma)\frac{\upsilon_-}{\upsilon_- + i(\omega - i\tilde{\theta}^c)} - \\
&\quad \left(\varsigma \frac{\upsilon_+}{\upsilon_+ - \tilde{\theta}^c} + (1-\varsigma)\frac{\upsilon_-}{\upsilon_- + \tilde{\theta}^c}\right) \\
&= \tilde{\varsigma}\frac{\tilde{\upsilon}_+}{\tilde{\upsilon}_+ - i\omega} + (1-\tilde{\varsigma})\frac{\tilde{\upsilon}_-}{\tilde{\upsilon}_- + i\omega} - 1 \\
&= \tilde{\phi}_G(\omega) - 1
\end{aligned}$$

and

$$\begin{aligned}
\tilde{\upsilon}_+ &= \upsilon_+ - \tilde{\theta}^c \\
\tilde{\upsilon}_- &= \upsilon_- + \tilde{\theta}^c \\
\tilde{\varsigma} &= \varsigma \frac{\upsilon_+}{\phi_G(-i\tilde{\theta}^c)\tilde{\upsilon}_+}.
\end{aligned}$$

We conclude that conditioning on $\mathcal{F}_t^{\lambda}$, $J = \{J_u, u \le t\}$ is a compound Poisson process with jump size distribution and intensity given by

$$\begin{aligned}
\tilde{p}_G(y) &= \frac{e^{\tilde{\theta}^c y} p_G(y)}{\phi_G(-i\tilde{\theta}^c)} = \tilde{\varsigma}\tilde{\upsilon}_+ \exp(-\tilde{\upsilon}_+ y)1_{y>0} + (1-\tilde{\varsigma})\tilde{\upsilon}_- \exp(-\tilde{\upsilon}_- |y|)1_{y<0} \\
\tilde{\lambda}_t &= \phi_G(-i\tilde{\theta}^c)\lambda_t.
\end{aligned}$$

A.6 Futures pricing formula

From the definition of futures price (3.7) and the results in (A.4), the pricing formula for a futures is

$$F_u^{\boldsymbol{\theta}}(t) = \exp\left(\hat{\psi}_{Y_t^D|\mathcal{F}_u}(-i; Y_u) + \tilde{\psi}_{Y_t^J|\mathcal{F}_u}(-i; T_{t_n})\right),\ t_n \le u \le t \le t_{\bar{n}},\ n = 0, \ldots, \bar{n} - 1,$$

where

$$\begin{aligned}
\hat{\psi}_{Y_t^D|\mathcal{F}_u}(\omega; Y_u) &= \left(i\omega Y_u e^{-\kappa(t-u)} + i\omega\mu(1 - e^{-\kappa(t-u)}) + i\omega\sigma \int_u^t e^{-\kappa(t-s)}\hat{\theta}(s)ds \right. \\
&\quad \left. -\frac{\omega^2\sigma^2}{4\kappa}(1 - e^{-2\kappa(t-u)})\right) \\
\tilde{\psi}_{Y_t^J|\mathcal{F}_u}(\omega; T_{t_n}) &= \ln\left(\mathbb{E}^{\boldsymbol{\theta}}\left[\exp\left(\int_u^t (\phi_G(\omega e^{-\kappa(t-s)} - i\tilde{\theta}(s)) - \phi_G(-i\tilde{\theta}(s)))\lambda_s ds\right)\middle| \mathcal{F}_u\right]\right).
\end{aligned}$$

A.7 Continuation value

Consider the continuation value

$$\begin{aligned} f(t_n, y_n, c_n, q_{n+1}) &= \mathbb{E}^{\boldsymbol{\theta}}[v(t_{n+1}, Y_{t_{n+1}}, T_{t_{n+1}}, q_{n+1})|Y_{t_n} = y_n, T_{t_n} = c_n] \\ &= \int_{\mathbb{R}^2} v(t_{n+1}, u, z, q_{n+1}) \cdot p^{\boldsymbol{\theta}}_{Y_{t_{n+1}}, T_{t_{n+1}}|\mathcal{F}_{t_n}}(u, z|y_n, c_n)dudz,\ n = 0, \ldots, \bar{n} - 1. \end{aligned} \tag{A.2}$$

From the $\mathcal{F}_{t_n}$-conditional independence property we can factorize the joint density inside the double integral as

$$\begin{aligned} \int_{\mathbb{R}^2} v(t_{n+1}, u, z, q_{n+1}) \times p^{\boldsymbol{\theta}}_{Y_{t_{n+1}}, T_{t_{n+1}}|\mathcal{F}_{t_n}}(u, z|y_n, c_n)dudz &= \\ \int_{\mathbb{R}}\int_{\mathbb{R}} v(t_{n+1}, u, z, q_{n+1}) p^{\boldsymbol{\theta}}_{Y_{t_{n+1}}|\mathcal{F}_{t_n}}(u|y_n, c_n)du\ p^{\boldsymbol{\theta}}_{T_{t_{n+1}}|\mathcal{F}_{t_n}}(z|c_n)dz. \end{aligned}$$

Now define the inner integral as

$$v_T(z; t_{n+1}, y_n, c_n, q_{n+1}) = \int_{\mathbb{R}} v(t_{n+1}, u, z, q_{n+1}) \times p^{\boldsymbol{\theta}}_{Y_{t_{n+1}}|\mathcal{F}_{t_n}}(u|y_n, c_n)du. \tag{A.3}$$

Furthermore, assuming that it exists, we define the complex Fourier transform of the value function as

$$\begin{aligned} \mathfrak{v}_{Y_{t_{n+1}}}(\omega; t_{n+1}, z, q_{n+1}) &= \mathfrak{F}[v(t_{n+1}, u, z, q_{n+1})](\omega) \\ &= \int_{i\xi-\infty}^{i\xi+\infty} e^{i\omega u} v(t_{n+1}, u, z, q_{n+1})du,\ \omega = d + i\xi,\ d, \xi \in \mathbb{R}. \end{aligned}$$

Then we can re-write the value function as

$$v(t_{n+1}, u, z, q_{n+1}) = \mathfrak{F}^{-1}[\mathfrak{v}_Y(\omega; t_{n+1}, z, q_{n+1})](u) \tag{A.4}$$

$$= \frac{1}{2\pi}\int_{i\xi-\infty}^{i\xi+\infty} e^{-i\omega u}\mathfrak{v}_Y(\omega; t_{n+1}, z, q_{n+1})d\omega. \tag{A.5}$$

Now define the extended version of the $\mathcal{F}_{t_n}$-conditional characteristic function of as $Y_{t_{n+1}}$

$$\begin{aligned} \phi^{\boldsymbol{\theta}}_{Y_{t_{n+1}}|\mathcal{F}_{t_n}}(\omega; y_n, c_n) &= \mathfrak{F}[p^{\boldsymbol{\theta}}_{Y_{t_{n+1}}}(u|y_n, c_n)](\omega) \\ &= \int_{i\xi-\infty}^{i\xi+\infty} e^{i\omega u} p^{\boldsymbol{\theta}}_{Y_{t_{n+1}}|\mathcal{F}_{t_n}}(u|y_n, c_n)du. \end{aligned}$$

By direct substitution we get

$$v_T(z; t_{n+1}, x_n, c_n, q_{n+1}) = \frac{1}{2\pi}\int_{i\xi-\infty}^{i\xi+\infty} \mathfrak{v}_Y(\omega; t_{n+1}, z, q_{n+1})\phi^{\boldsymbol{\theta}}_{Y_{t_{n+1}}|\mathcal{F}_{t_n}}(-\omega; y_n, c_n)d\omega. \tag{A.6}$$

Now define the change of variables $\tilde{\omega} = \omega e^{-\kappa(t_{n+1}-t_n)}$. By exploiting the scaling property of the Fourier transform we can write

$$\begin{aligned} \mathfrak{v}_Y(\tilde{\omega}e^{\kappa(t_{n+1}-t_n)}; t_{n+1}, z, q_{n+1}) &= e^{-\kappa(t_{n+1}-t_n)}\mathfrak{F}[v(t_{n+1}, ue^{-\kappa(t_{n+1}-t_n)}, z, q_{n+1})](\tilde{\omega}) \\ \phi^{\boldsymbol{\theta}}_{Y_{t_{n+1}}|\mathcal{F}_{t_n}}(\tilde{\omega}e^{\kappa(t_{n+1}-t_n)}; y_n, c_n) &= e^{i\tilde{\omega}y_n}\phi^{\boldsymbol{\theta}}_{Y_{t_{n+1}}|\mathcal{F}_{t_n}}(\tilde{\omega}e^{\kappa(t_{n+1}-t_n)}; 0, c_n), \end{aligned}$$

and by substituting in (A.6) we finally get

$$\begin{aligned} v_T(z;t_{n+1},y_n,c_n,q_{n+1}) &= \frac{e^{\kappa(t_{n+1}-t_n)}}{2\pi}\int_{i\xi-\infty}^{i\xi+\infty} e^{-i\tilde{\omega}y_n}\mathfrak{v}_Y(\tilde{\omega}e^{\kappa(t_{n+1}-t_n)};t_{n+1},z,q_{n+1}) \quad \text{(A.7)} \\ &\quad \phi^{\boldsymbol{\theta}}_{Y_{t_{n+1}}|\mathcal{F}_{t_n}}(-\tilde{\omega}e^{\kappa(t_{n+1}-t_n)};0,c_n)d\tilde{\omega} \\ &= \frac{1}{2\pi}\int_{i\xi-\infty}^{i\xi+\infty} e^{-i\tilde{\omega}y_n}\mathfrak{F}[v(t_{n+1},ue^{-\kappa(t_{n+1}-t_n)},z,q_{n+1})](\tilde{\omega})\times \\ &\quad \phi^{\boldsymbol{\theta}}_{Y_{t_{n+1}}|\mathcal{F}_{t_n}}(-\tilde{\omega}e^{\kappa(t_{n+1}-t_n)};0,c_n)d\tilde{\omega}. \quad \text{(A.8)} \end{aligned}$$

Now we repeat the same procedure by integrating (A.8) (assuming that it is an integrable function) with respect to the temperature as

$$f(t_n,y_n,c_n,q_{n+1}) = \int_{\mathbb{R}} v_T(z;t_{n+1},y_n,c_n,q_{n+1})p_{T_{t_{n+1}}|\mathcal{F}_{t_n}}(z|c_n)dz.$$

To do so, assuming that it exists, we define the complex Fourier transform of (A.8) as

$$\begin{aligned} \mathfrak{v}_T(\varpi;t_{n+1},y_n,c_n,q_{n+1}) &= \mathfrak{F}[v_T(z;t_{n+1},y_n,c_n,q_{n+1})](\varpi) \\ &= \int_{i\tau-\infty}^{i\tau+\infty} e^{i\varpi z}v_T(z;t_{n+1},y_n,c_n,q_{n+1})dz,\ \varpi = l+i\tau,\ l,\tau\in\mathbb{R}, \end{aligned}$$

and we re-write the integrand as

$$\begin{aligned} v_T(z;t_{n+1},y_n,c_n,q_{n+1}) &= \mathfrak{F}^{-1}[\mathfrak{v}_T(\varpi;t_{n+1},y_n,c_n,q_{n+1})](z) \\ &= \frac{1}{2\pi}\int_{i\tau-\infty}^{i\tau+\infty} e^{-i\varpi z}\mathfrak{v}_T(\varpi;t_{n+1},y_n,c_n,q_{n+1})d\varpi. \end{aligned}$$

Now define the extended version of the $\mathcal{F}_{t_n}$-conditional characteristic function of $T_{t_{n+1}}$ as

$$\begin{aligned} \phi_{T_{t_{n+1}}|\mathcal{F}_{t_n}}(\varpi;c_n) &= \mathfrak{F}[p^{\boldsymbol{\theta}}_{T_{t_{n+1}}}(z|c_n)](\omega) \\ &= \int_{i\xi-\infty}^{i\xi+\infty}\exp(i\omega u)p_{T_{t_{n+1}}|\mathcal{F}_{t_n}}(z|c_n)dz. \end{aligned}$$

By a direct substitution we get

$$\begin{aligned} f(t_n,y_n,c_n,q_{n+1}) &= \int_{\mathbb{R}} v_T(z;t_{n+1},y_n,c_n,q_{n+1})\times p_{T_{t_{n+1}}}(z|c_n)dz \\ &= \frac{1}{2\pi}\int_{i\tau-\infty}^{i\tau+\infty}\mathfrak{v}_T(\varpi;t_{n+1},y_n,c_n,q_{n+1})\ \phi_{T_{t_{n+1}}|\mathcal{F}_{t_n}}(-\varpi;c_n)d\varpi. \end{aligned}$$

Define the change of variables $\varpi = \tilde{\omega}e^{-a(t_{n+1}-t_n)}$. By exploiting the scaling property of the Fourier transform we can write

$$\begin{aligned} \mathfrak{v}_T(\varpi e^{a(t_{n+1}-t_n)};t_{n+1},x_n,c_n,q_{n+1}) &= e^{-a(t_{n+1}-t_n)}\ \mathfrak{F}[v_T(ze^{-a(t_{n+1}-t_n)}|t_{n+1},x_n,c_n,q_{n+1})](\varpi); \\ \phi_{T_{t_{n+1}}|\mathcal{F}_{t_n}}(\varpi e^{a(t_{n+1}-t_n)};c_n) &= e^{i\varpi c_n}\ \phi_{T_{t_{n+1}}|\mathcal{F}_{t_n}}(\varpi e^{a(t_{n+1}-t_n)};0). \end{aligned}$$

As a consequence, the continuation value reads

$$\begin{aligned} f(t_n,x_n,c_n,q_{n+1}) &= \frac{e^{a(t_{n+1}-t_n)}}{2\pi}\int_{i\tau-\infty}^{i\tau+\infty}\mathfrak{v}_T(\varpi;t_{n+1},x_n,c_n,q_{n+1})\ \phi_{T_{t_{n+1}}|\mathcal{F}_{t_n}}(-\varpi;c_n)d\varpi \\ &= \frac{1}{2\pi}\int_{i\tau-\infty}^{i\tau+\infty} e^{-i\varpi c_n}\mathfrak{F}[v_T(ze^{-a(t_{n+1}-t_n)}|t_{n+1},x_n,c_n,q_{n+1})](\varpi)\times \\ &\quad \phi_{T_{t_{n+1}}|\mathcal{F}_{t_n}}(-\varpi e^{a(t_{n+1}-t_n)};0)d\varpi. \quad \text{(A.9)} \end{aligned}$$

A.8 Discrete Fourier Transform

First, for each time $t_n \in \mathcal{T}$ and for $j, m, p = 0, \dots, \bar{k}-1$, we discretize the integral (A.8) with respect to the grids (3.26)-(3.27) as

$$\begin{aligned}
\tilde{v}_T(c_j; t_{n+1}, y_m, c_p, q_{n+1}) &= \frac{\Delta\tilde{\omega}}{2\pi} \sum_{h=0}^{\bar{k}-1} e^{-i\tilde{\omega}_h y_m}\ \mathfrak{F}[\tilde{v}^{int}(e^{-\kappa(t_{n+1}-t_n)}\ y_k, c_j, q_{n+1})](\tilde{\omega}_h)\ \times \\
&\quad \phi^{\boldsymbol{\theta}}_{Y_{t_{n+1}}|\mathcal{F}_{t_n}}(-\tilde{\omega}_h e^{\kappa(t_{n+1}-t_n)}; 0, c_p) \\
&= \frac{\Delta y \Delta\tilde{\omega}}{2\pi} \sum_{h=0}^{\bar{k}-1} e^{-i\tilde{\omega}_h y_m} \phi^{\boldsymbol{\theta}}_{Y_{t_{n+1}}|\mathcal{F}_{t_n}}(-\tilde{\omega}_h e^{\kappa(t_{n+1}-t_n)}; 0, c_p) \times \\
&\quad \sum_{k=0}^{\bar{k}-1} e^{i\tilde{\omega}_h y_k} \tilde{v}^{int}(e^{-\kappa(t_{n+1}-t_n)} y_k, c_j, q_{n+1}) w_k \\
&= \frac{\Delta y \Delta\tilde{\omega}}{2\pi} \sum_{h=0}^{\bar{k}-1} e^{-i(\tilde{\omega}_0 + h\Delta\tilde{\omega})(y_0 + m\Delta y)} \times \\
&\quad \phi^{\boldsymbol{\theta}}_{Y_{t_{n+1}}|\mathcal{F}_{t_n}}(-(\tilde{\omega}_0 + h\Delta\tilde{\omega}) e^{\kappa(t_{n+1}-t_n)}; 0, c_p) \times \\
&\quad \sum_{k=0}^{\bar{k}-1} e^{i(\tilde{\omega}_0 + h\Delta\tilde{\omega})(y_0 + k\Delta y)} \tilde{v}^{int}(e^{-\kappa(t_{n+1}-t_n)} y_k, c_j, q_{n+1}) w_k,
\end{aligned}$$

where $\tilde{v}^{int}(e^{-\kappa(t_{n+1}-t_n)}\ y_k, c_j, q_{n+1})$ can be obtained by first computing the vector of values $\{\tilde{v}^{int}(\ y_k, c_j, q_{n+1})\}_{k=0}^{\bar{k}-1}$, and then interpolating with respect to the rescaled vector $\{e^{-\kappa(t_{n+1}-t_n)} y_k\}_{k=0}^{\bar{k}-1}$, and where w_j's are the weights of the summation chosen according to the trapezoidal rule, i.e. $w_0 = w_{\bar{k}-1} = 1/2$ and $w_k = 1$ for $k = 1, \dots, \bar{k}-2$.

Using the Nyquist relation (3.28) we can write

$$(\tilde{\omega}_0 + h\Delta\tilde{\omega})(y_0 + k\Delta y) = \tilde{\omega}_0 y_0 + \tilde{\omega}_0 k \Delta y + h\Delta\tilde{\omega} y_0 + 2\pi hk/\bar{k},$$

and since $\tilde{\omega}_h = d_h + i\xi$, $d_0 = -\bar{k}\pi/r_Y$, $\tilde{\omega}_0 \Delta y = -\pi$, $e^{i\pi} = -1$, after some trivial computations we finally obtain

$$\begin{aligned}
&\tilde{v}_T(c_j; t_{n+1}, y_m, c_p, q_{n+1}) = \\
&(-)^m e^{\xi m \Delta y} \frac{1}{\bar{k}} \sum_{h=0}^{\bar{k}-1} e^{-i2\pi hm/\bar{k}} \left(\phi^{\boldsymbol{\theta}}_{Y_{t_{n+1}}|\mathcal{F}_{t_n}}(-(d_0 + i\xi + h\Delta\tilde{\omega}) e^{\kappa(t_{n+1}-t_n)}; 0, c_p) \right) \\
&\times \sum_{k=0}^{\bar{k}-1} e^{i2\pi hk/\bar{k}} \left((-)^k e^{-\xi k \Delta y} \tilde{v}^{int}(e^{-\kappa(t_{n+1}-t_n)} y_k, c_j, q_{n+1})\ w_k \right).
\end{aligned}$$

By an identical reasoning, we discretize the integral (A.9) with respect to the grids (3.26)-(3.27) as

$$\begin{aligned}
\tilde{f}(t_n, y_m, c_p, \tilde{q}) &= (-1)^p e^{\tau p \Delta c} \frac{1}{\bar{k}} \sum_{h=0}^{\bar{k}-1} e^{-i2\pi hm/\bar{k}} \left(\phi_{T_{t_{n+1}}|\mathcal{F}_{t_n}}(-e^{a(t_{n+1}-t_n)}(l_0 + i\tau + h\Delta\varpi); 0) \right) \\
&\quad \times \sum_{j=0}^{\bar{k}-1} e^{i2\pi hj/\bar{k}} \left((-)^j e^{-\tau j \Delta c} \tilde{v}^{int}_T(e^{-a(t_{n+1}-t_n)} c_j; x_m, c_p, q_{n+1}) w_j \right).
\end{aligned}$$

The two summations can be computed by the FFT algorithm.

A.9 Kernel density pricing function

By substituting the approximate kernel density (3.12) into the approximate pricing function (3.13) we obtain

$$\begin{aligned}
\tilde{c}(k;\varrho) &= \frac{1}{\bar{m}}\sum\nolimits_{m=1}^{\bar{m}} e^{-ru}\int_{\ln(k/F_0(h))}^{+\infty}(F_0(h)e^z-k)K_{\epsilon_m}(z-\upsilon_m)dz \\
&= \frac{1}{\bar{m}}\sum\nolimits_{m=1}^{\bar{m}} e^{-ru}\int_{\ln(k/F_0(h))}^{+\infty}(F_0(h)e^z-k)\frac{1}{\sqrt{2\pi}\epsilon_m}\exp(-\frac{(z-\upsilon_m)^2}{2\epsilon_m^2})dz \\
&= \frac{e^{-ru}}{\bar{m}}\sum\nolimits_{m=1}^{\bar{m}}\frac{1}{\sqrt{2\pi}\epsilon_m}\left(\int_{\ln(k/F_0(h))}^{+\infty}F_0(h)\exp\left(z-\frac{(z-\upsilon_m)^2}{2\epsilon_m^2}\right)dz\right. \\
&\quad \left.-k\int_{\ln(k/F_0(h))}^{+\infty}\exp\left(-\frac{(z-\upsilon_m)^2}{2\epsilon_m^2}\right)dz\right).
\end{aligned}$$

By defining the change of variables $y=(z-\upsilon_m)/\epsilon_m$, we can write the m-th term of the sum as

$$\begin{aligned}
&\frac{1}{\sqrt{2\pi}\epsilon_m}\left(\int_{\ln(k/F_0(h))}^{+\infty}F_0(h)e^{z-\frac{(z-\upsilon_m)^2}{2\epsilon_m^2}}dz-k\int_{\ln(k/F_0(h))}^{+\infty}e^{-\frac{(z-\upsilon_m)^2}{2\epsilon_m^2}}dz\right) \\
= &\frac{1}{\sqrt{2\pi}\epsilon_m}\left(F_0(h)\int_{\frac{\ln(k/F_0(h))-\upsilon_m}{\epsilon_m}}^{+\infty}e^{y\epsilon_m+\upsilon_m-\frac{y^2}{2}}dy-k\int_{\frac{\ln(k/F_0(h))-\upsilon_m}{\epsilon_m}}^{+\infty}e^{-\frac{y^2}{2}}dy\right) \\
= &\frac{1}{\sqrt{2\pi}\epsilon_m}\left(F_0(h)e^{\upsilon_m+\frac{1}{2}\epsilon_m^2}\int_{\frac{\ln(k/F_0(h))-\upsilon_m}{\epsilon_m}}^{+\infty}e^{-\frac{1}{2}(y-\epsilon_m)^2}dy-k\int_{\frac{\ln(k/F_0(h))-\upsilon_m}{\epsilon_m}}^{+\infty}e^{-\frac{y^2}{2}}dy\right) \\
= &\frac{1}{\sqrt{2\pi}\epsilon_m}\left(F_0(h)e^{\upsilon_m+\frac{1}{2}\epsilon_m^2}\int_{\frac{\ln(k/F_0(h))-\upsilon_m}{\epsilon_m}-\epsilon_m}^{+\infty}e^{-\frac{y^2}{2}}dy-k\int_{\frac{\ln(k/F_0(h))-\upsilon_m}{\epsilon_m}}^{+\infty}e^{-\frac{y^2}{2}}dy\right) \\
= &F_0(h)e^{\upsilon_m+\frac{1}{2}\epsilon_m^2}F_{\mathcal{N}(0,1)}\left(-\frac{\ln(k/F_0(h))-(\upsilon_m+\epsilon_m^2)}{\epsilon_m}\right)-kF_{\mathcal{N}(0,1)}\left(-\frac{\ln(k/F_0(h))-\upsilon_m}{\epsilon_m}\right) \\
= &F_0(h)e^{\upsilon_m+\frac{1}{2}\epsilon_m^2}F_{\mathcal{N}(0,1)}\left(-\frac{\ln(k/F_0(h))-(\upsilon_m+\epsilon_m^2)}{\epsilon_m}\right)-kF_{\mathcal{N}(0,1)}\left(-\frac{\ln(k/F_0(h))-\upsilon_m}{\epsilon_m}\right).
\end{aligned}$$

Thus defining

$$\begin{aligned}
d_1(\upsilon_m,\epsilon_m) &= \frac{\ln(F_0(h)/k)+(\upsilon_m+\epsilon_m^2)}{\epsilon_m} \\
d_2(\upsilon_m,\epsilon_m) &= c_1(\upsilon_m,\epsilon_m)-\epsilon_m,
\end{aligned}$$

we obtain the m-th term of the sum (3.14).